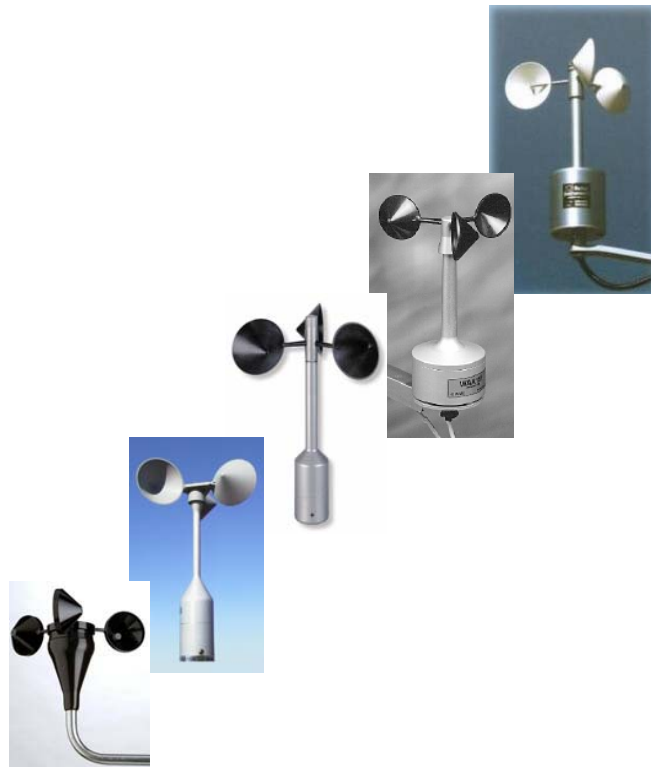


ACCUWIND - Classification of Five Cup Anemometers According to IEC61400-12-1

T.F. Pedersen, J.-Å. Dahlberg,
Peter Busche



Abstract The characteristics of five cup anemometers were investigated in detail, and data are presented in figures and tables. The characteristics include: normal wind tunnel calibrations; angular response measurements at 5, 8 and 11m/s; torque coefficient curve measurements from combined tilt and ramp-gust tests, torque coefficient curve measurements for non-tilted conditions; rotor inertia measurements and measurements of friction of bearings at temperatures -10°C to 40°C. The characteristics are fitted to two different time domain cup anemometer models, and simulations of the cup anemometers are made with artificial wind generators to make classifications according to annex I and J of the standard IEC 61400-12-1 on power performance measurements. Results of classification are shown in graphs of systematic deviations and class index tables.

ISBN 87-550-3516-7

Contents

Preface 4

1 Introduction 5

2 Cup Anemometer Type Descriptions 5

3 Wind Tunnel and Laboratory Test Results 6

3.1 Normal WT calibrations 6

3.1.1 Linear regression results 6

3.1.2 Typical time traces from the calibrations 8

3.2 Angular response measurements by tilt tests at FOI 10

3.3 Angular response measurements by tilt tests at DEWI 13

3.4 Torque coefficient curves from combined tilt and ramp-gust tests 15

3.4.3 Torque coefficient curves for horizontal flow conditions. 18

3.4.4 Comparison of angular response from steady and dynamic measurements 20

3.5 Measurement of Rotor Inertia 22

3.6 Measurement of Friction Characteristics 22

4 Classification 25

4.1 Classification Ranges 25

4.2 Cup Anemometer Models and Fitting 26

4.3 Wind Generation Model 27

4.4 Classification with Inclined-Flow-Torque-Coefficient Model (IFTC) 27

4.4.5 Classification of NRG cup anemometer 27

4.4.6 Classification of Risø cup anemometer 29

4.4.7 Classification of Thies FC cup anemometer 31

4.4.8 Classification of Vaisala cup anemometer 33

4.4.9 Classification of Vector cup anemometer 35

4.5 Classification with Tilt-Response & Torque-Coefficient Model (TRTC) 37

4.5.10 Classification of NRG cup anemometer 37

4.5.11 Classification of Risø cup anemometer 40

4.5.12 Classification of Thies FC cup anemometer 43

4.5.13 Classification of Vaisala cup anemometer 46

4.5.14 Classification of Vector cup anemometer 49

4.6 Classification with Tilt-Response & Torque-Coefficient Model (TRTC) without friction 52

4.6.15 Classification of NRG cup anemometer without influence of friction 52

4.6.16 Classification of Risø cup anemometer without influence of friction 55

4.6.17 Classification of Thies FC cup anemometer without influence of friction 58

4.6.18 Classification of Vaisala cup anemometer without influence of friction 61

4.6.19 Classification of Vector cup anemometer without influence of friction 64

4.7 Comparison of Data 67

5 Conclusions 69

6 References 69

Preface

This report presents results of a European research project ACCUWIND on improvement of evaluation and classification methods of cup and sonic anemometry. The report presents results of task 1 on cup anemometry. The six ACCUWIND project partners are:

- *Risø National Laboratory, RISØ, Denmark*
- *Deutsches Windenergie Institut GmbH, DEWI, Germany*
- *Swedish Defence Research Agency, FOI, Sweden*
- *Centre for Renewable Energy Sources, CRES, Greece*
- *Energy Research Centre of the Netherlands, ECN, the Netherlands*
- *Universidad Politecnica de Madrid, UPM, Spain*

The work was made under contract with the European Commission, project number NNE5-2001-00831. Additional support to this part of the project was given by Risø (Risø National Laboratory, DK) and FOI (Swedish Defence Research Agency, SE)

1 Introduction

The present report is an investigation of the characteristics of five commercial cup anemometers being used in wind energy. All calibrations and tests are made under wind tunnel and laboratory conditions following the procedures outlined in the general report [1]. The measured characteristics are fitted to time domain cup anemometer models, in order for the models to simulate time domain 3D wind conditions. The models are used to calculate deviations from normal calibration conditions to realistic atmospheric operational conditions by the input of time domain 3D wind, generated by artificial wind generators [2]. The calculations are used to classify the cup anemometers according to the annex I of the IEC 61400-12-1 power performance measurement standard [3]. This report does on the other hand not represent full evaluation and classification of individual types of cup anemometers as the IEC standard requires at least two cup anemometers of a type to be tested and evaluated.

2 Cup Anemometer Type Descriptions

The cup anemometers used in the investigations are shown in Figure 2-1. The cup anemometers have been chosen from their use in wind energy, and they represent ranges of design and characteristics that should be appropriate for evaluation of the procedures described in [1,3]. The cup anemometers all have three conical plastic cups, which are in details different. Four of the cup anemometers have quite slender shafts, but with hub parts that differ significantly. The details of the cup, rotor, shaft, bearing and body designs influence the angular and dynamic characteristics as shown in the CLASSCUP project [4]. Details will not be presented here, but the main dimensions that are incorporated in measurements and cup anemometer models are outlined in Table 2-1.






				
NRG Maximum 40 (NRG)	Risø P2546 (RIS)	Thies First Class (THF)	Vaisala WAA151 (VAI)	Vector L100K (VEC)

Figure 2-1 Cup anemometer types being used in the evaluation and classification. Acronyms in parenthesis are used in the report in figures and graphs to identify the types.

Table 2-1 Main cup anemometer data being used in the analysis

	NRG	RIS	THF	VAI	VEC
Cup diameter (mm)	51	70	80	54	51
Projected cup area A (mm ²)	2000	3850	5030	2290	2040
Rotor diameter (mm)	191	186	240	184	155
Radius to cup centre R (mm)	70	58	80	65	52
Pulses/rev	2	12 ^{*)}	37	14	25

*) special purpose tooth wheel while normally being 2

3 Wind Tunnel and Laboratory Test Results

The characteristics of the cup anemometers have been investigated in the LT5 wind tunnel at FOI, partly in the Oldenburg wind tunnel (DEWI), and in climate chamber and in laboratory at RISØ. The investigations follow the procedures described in [1], and the following chapters describe the results of each test.

3.1 Normal WT calibrations

All tests are preceded by a normal calibration of the anemometer together with the four light propeller anemometers. The propeller anemometers are used to measure the instantaneous wind speed during gust tests. The calibration procedure follows in principal an ordinary calibration [3]. Each data point is acquired during 125 seconds. The measurement sequence starts and ends with a zero reading with the tunnel shut down. The first point is 5 m/s then 7, 9 etc. up to 15 m/s. On the way down the even wind speeds are measured. The analogue volt values from the WT pressure transducer and tilt angle sensor are sampled at 100 Hz. The pulses from the anemometer and the propellers are clocked with a 100 kHz timer. The evaluation procedure involves; counting of pulses, conversion of pressure signals to wind speeds and linear regression fitting.

3.1.1 Linear regression results

The normal calibrations of the five cup anemometers in the LT5 wind tunnel are presented in Figure 3-1 to Figure 3-5.

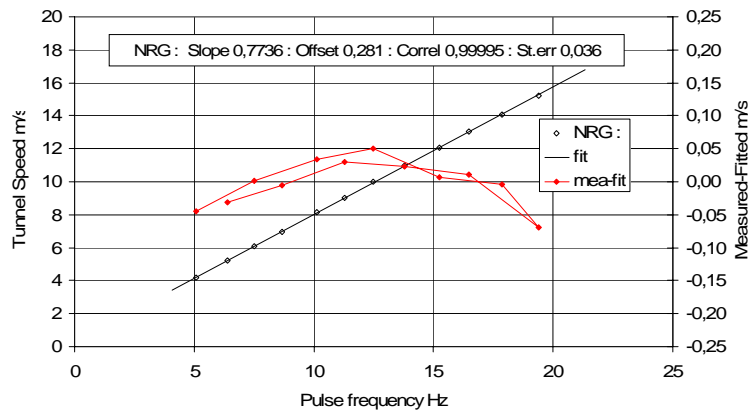


Figure 3-1 Linear regression results for the NRG cup anemometer.

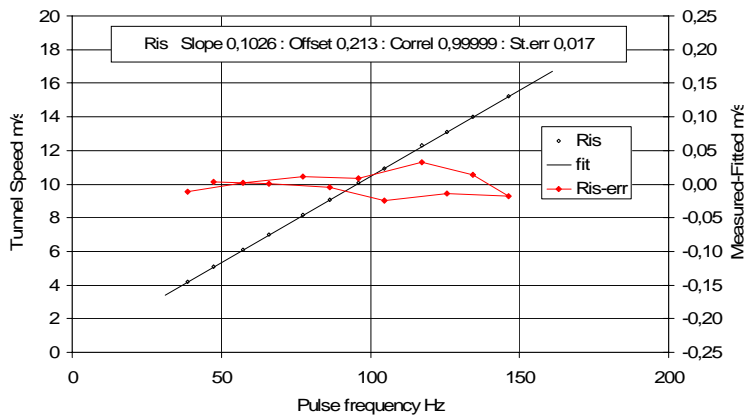


Figure 3-2 Linear regression results for the RIS cup anemometer.

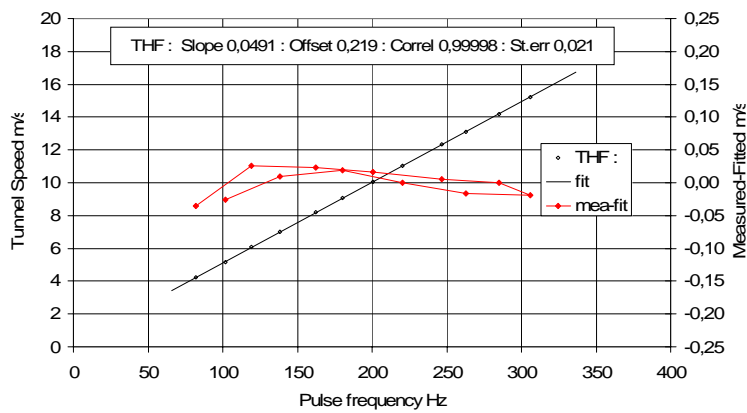


Figure 3-3 Linear regression results for the THF cup anemometer.

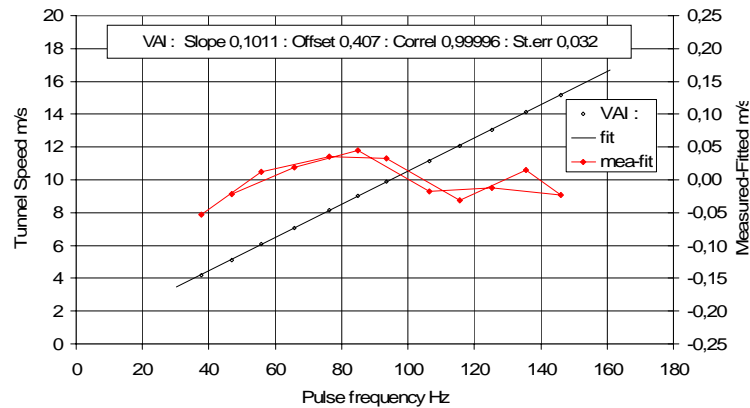


Figure 3-4 Linear regression results for the VAI cup anemometer.

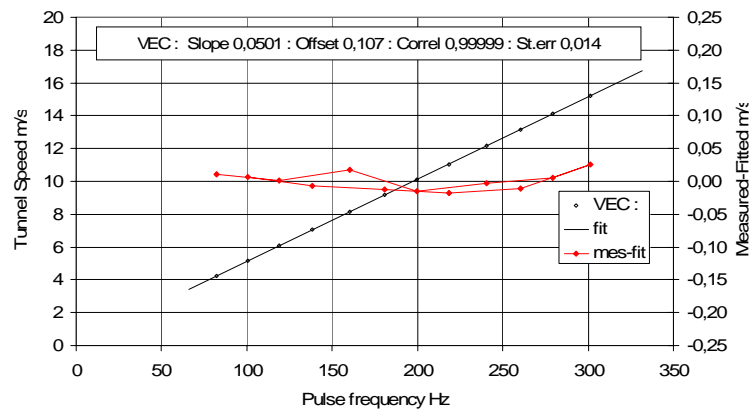


Figure 3-5 Linear regression results for the VEC cup anemometer.

3.1.2 Typical time traces from the calibrations

Figure 3-6 to Figure 3-10 present typical 30-second time traces of each cup anemometer and one of the four propellers. The traces are taken from the calibration points at 8 m/s wind speed. The graphs are included here to give the reader an impression of the magnitude of the so called “inherent turbulence” which has been found to be associated with most cup anemometers. As seen from the graphs the variations of the anemometer readings are significantly higher than the wind speed reading from the propeller.

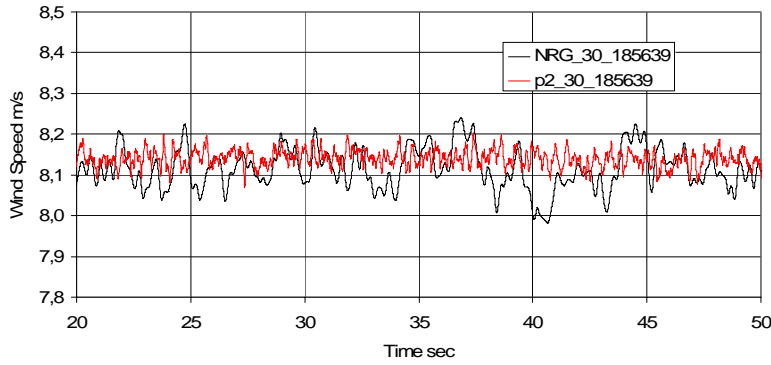


Figure 3-6 A typical 30-seconds time trace from calibration of the NRG cup anemometer (black curve) and one of the four propellers (red).

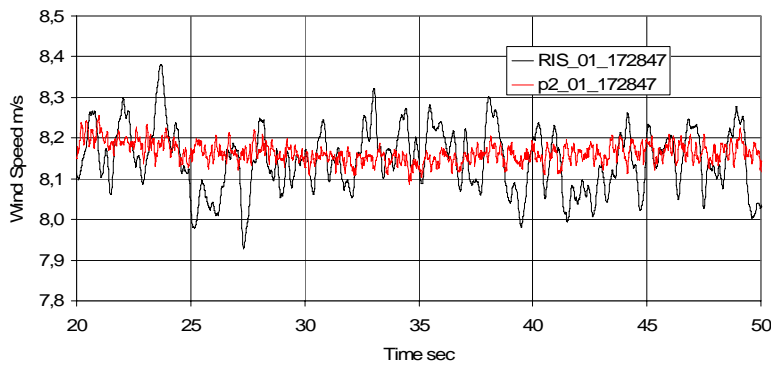


Figure 3-7 A typical 30-seconds time trace from calibration of the RIS cup anemometer (black curve) and one of the four propellers (red).

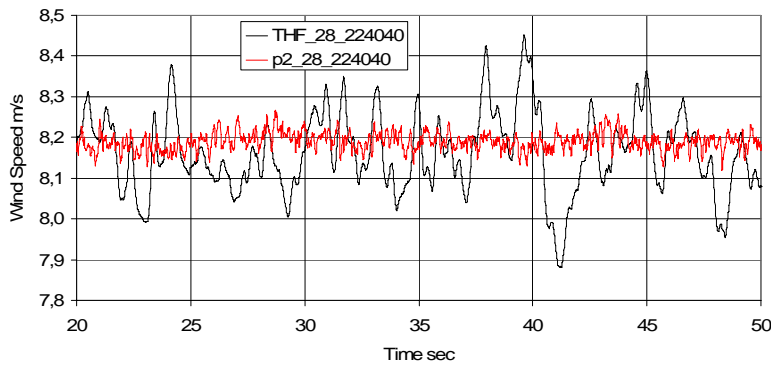


Figure 3-8 A typical 30-seconds time trace from calibration of the THF cup anemometer (black curve) and one of the four propellers (red).

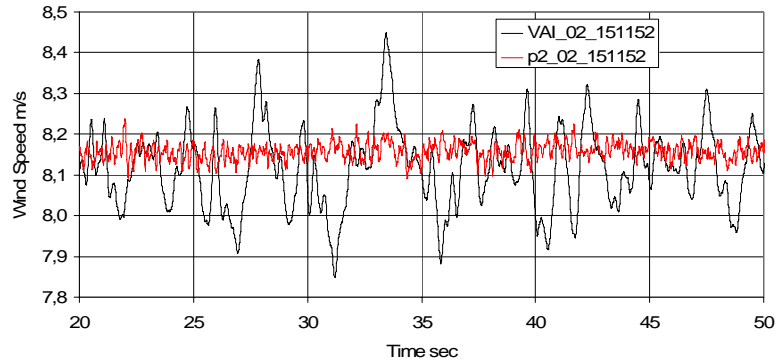


Figure 3-9 A typical 30-seconds time trace from calibration of the VAI cup anemometer (black curve) and one of the four propellers (red).

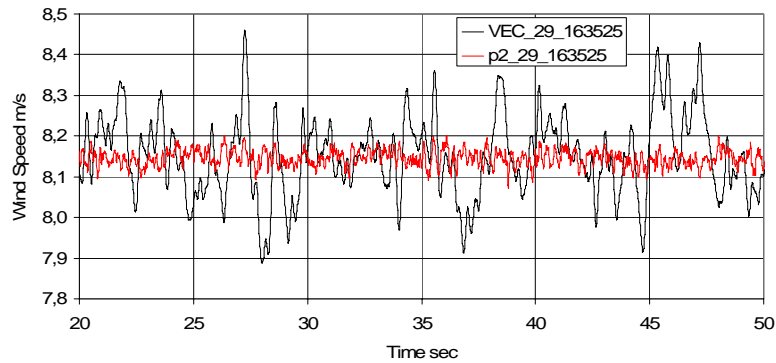


Figure 3-10 A typical 30-seconds time trace from calibration of the VEC cup anemometer (black curve) and one of the four propellers (red).

3.2 Angular response measurements by tilt tests at FOI

During the tilt tests in the LT5 wind tunnel at FOI the anemometer is slowly (approximately $2^\circ/\text{sec}$) tilted back and forth during 1050 seconds. The tilt angle and tunnel speed are continuously measured with 20Hz and the pulses from anemometer and the four propellers are sampled with a 100 kHz timer. The evaluation involves conversion from pulse frequencies to wind speed by using the transfer functions from the calibration. The data is sorted into 2° tilt bins and averaged. Tests are performed at wind speeds of 5, 8 (+8R) and 11m/s.

Figure 3-11 to Figure 3-15 presents results of the FOI tilt tests.

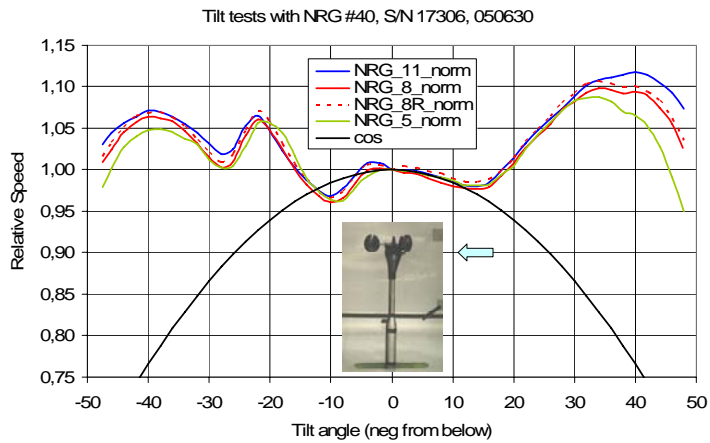


Figure 3-11 FOI tilt test measurements with the NRG anemometer.

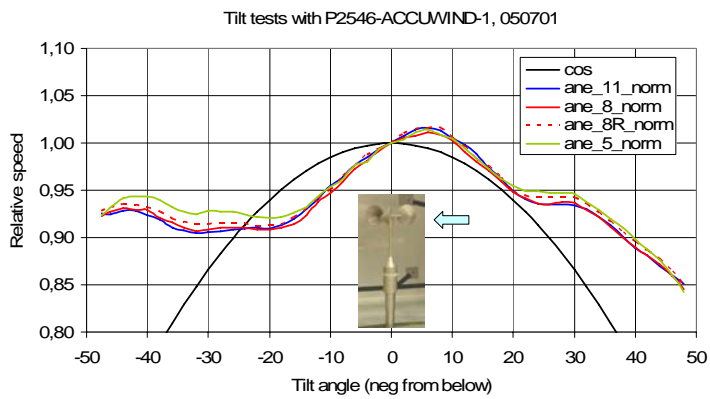


Figure 3-12 FOI tilt test measurements with the RIS anemometer.

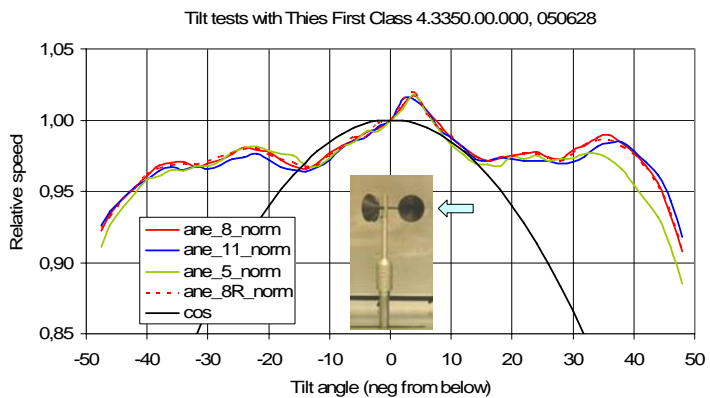


Figure 3-13 FOI tilt test measurements with the THF anemometer.

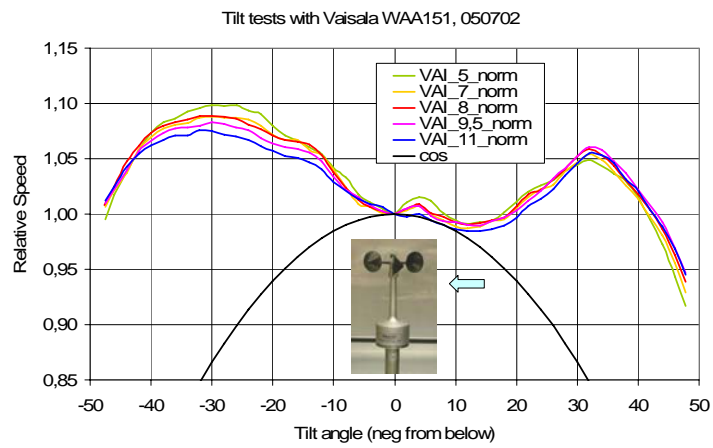


Figure 3-14 FOI tilt test measurements with the VAI anemometer.

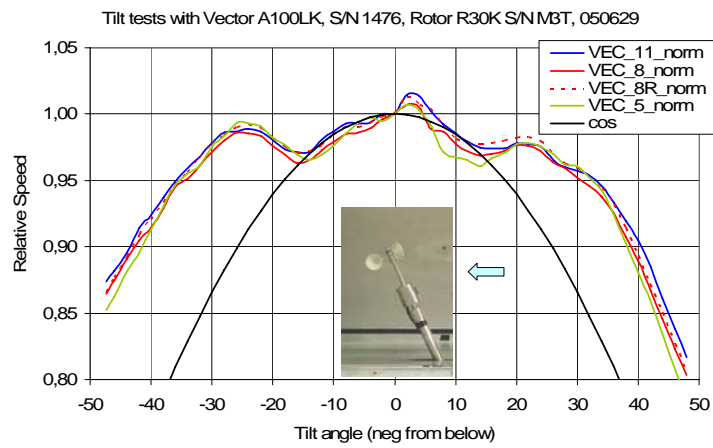


Figure 3-15 FOI tilt test measurements with the VEC anemometer.

3.3 Angular response measurements by tilt tests at DEWI

Figure 3-16 to Figure 3-20 presents results of the DEWI tilt tests.

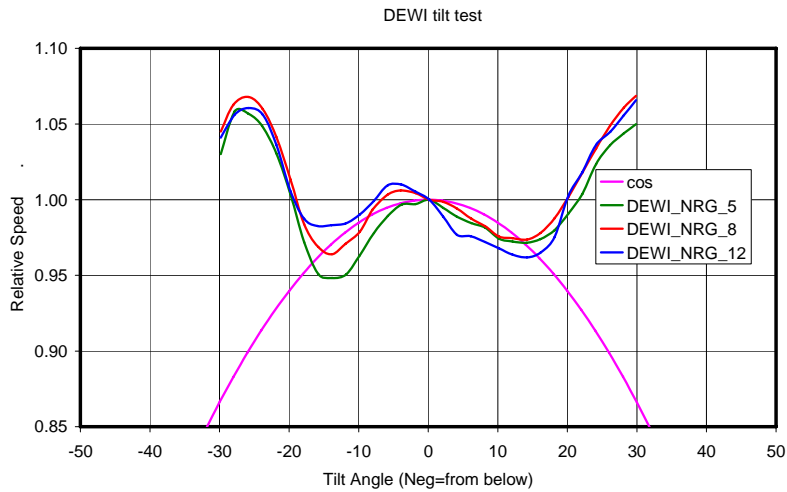


Figure 3-16 DEWI tilt test measurements with the NRG anemometer.

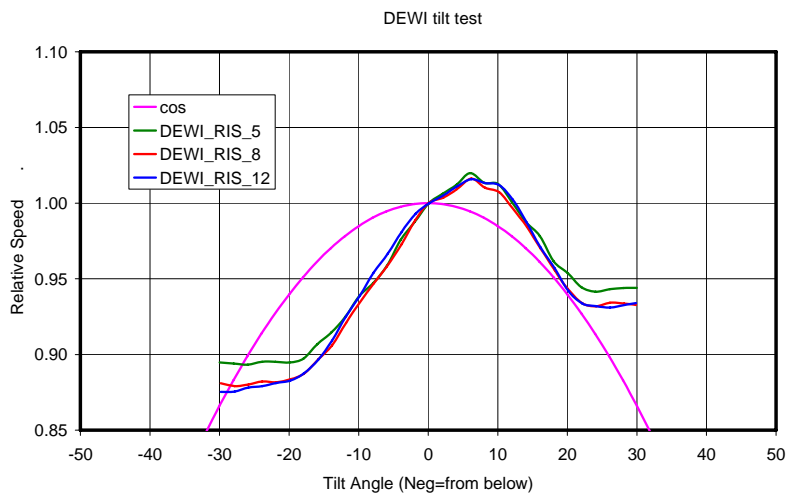


Figure 3-17 DEWI tilt test measurements with the RIS anemometer.

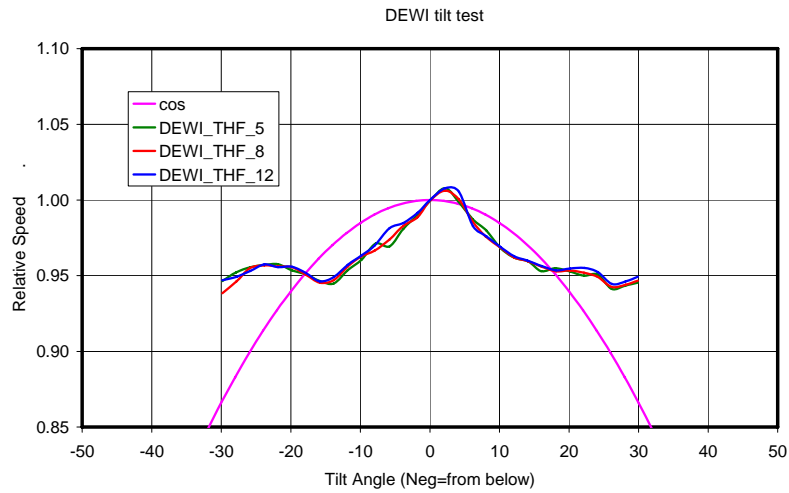


Figure 3-18 DEWI tilt test measurements with the THF anemometer.

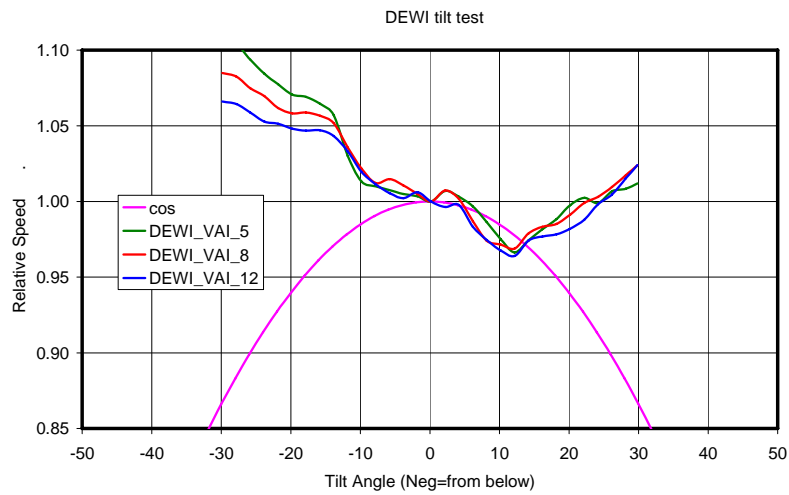


Figure 3-19 DEWI tilt test measurements with the VAI anemometer.

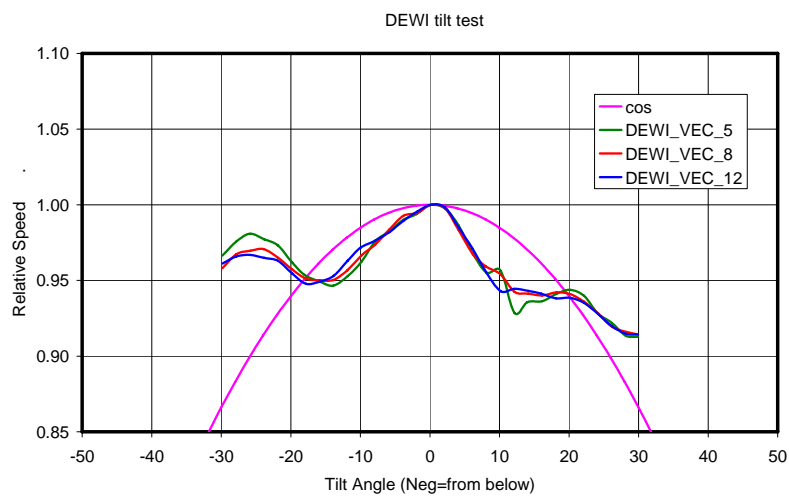


Figure 3-20 DEWI tilt test measurements with the VEC anemometer.

3.4 Torque coefficient curves from combined tilt and ramp-gust tests

This method to measure torque coefficient curves involves exposure of the tilted anemometer for wind gusts in a wind tunnel together with accurate measurements of the instantaneous wind speed and the rotational speed of the cup-anemometer. The torque-curve for each tilt angle (normalised torque coefficient versus speed ratio) is derived indirectly from the measured time traces.

The method includes one fitting action where the torque curve C_q for non inclined flow is matched with the calibration results. The fitting implies that a $\Delta\lambda$ is added to the actual speed ratio such that C_q becomes zero for the speed ratio derived from the calibration.

The graphs from Figure 3-21 to Figure 3-25 present the results from the evaluation of the tests. The legends in each graph give information of: tilt angle setting, time of measurement, number of pulses used to determine the speed of the anemometer, number of pulses used to determine the speed of the propellers and finally tooth wheel signature correction (1/0=yes/no)

The inclined flow torque coefficient curves are being used in simulations with the IFTC model.

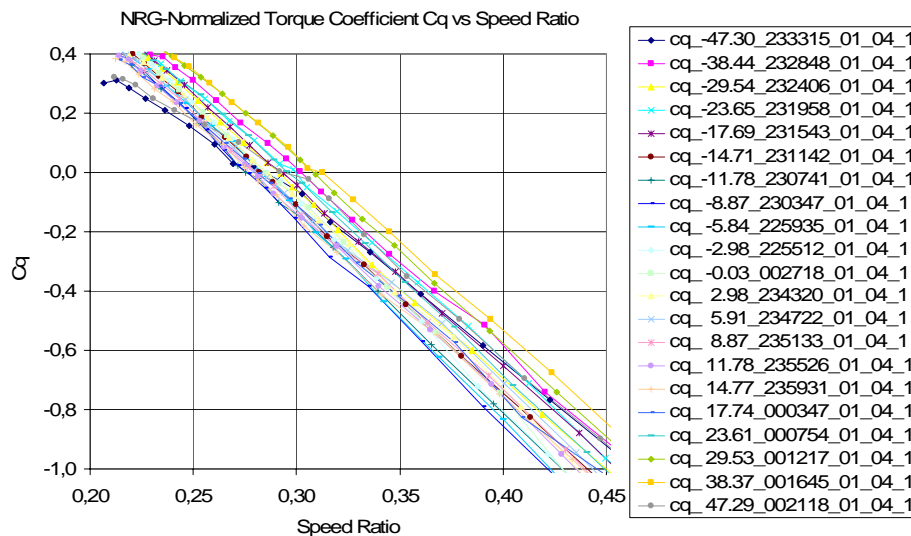


Figure 3-21 Derived torque coefficient curves (C_q versus speed ratio and tilt angle) for the NRG anemometer.

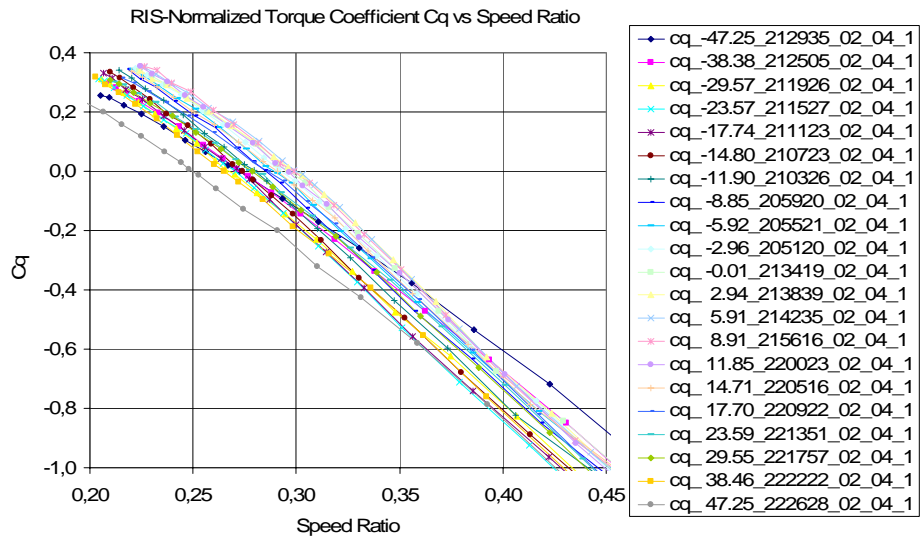


Figure 3-22 Derived torque coefficient curves (C_q versus speed ratio and tilt angle) for the RIS anemometer.

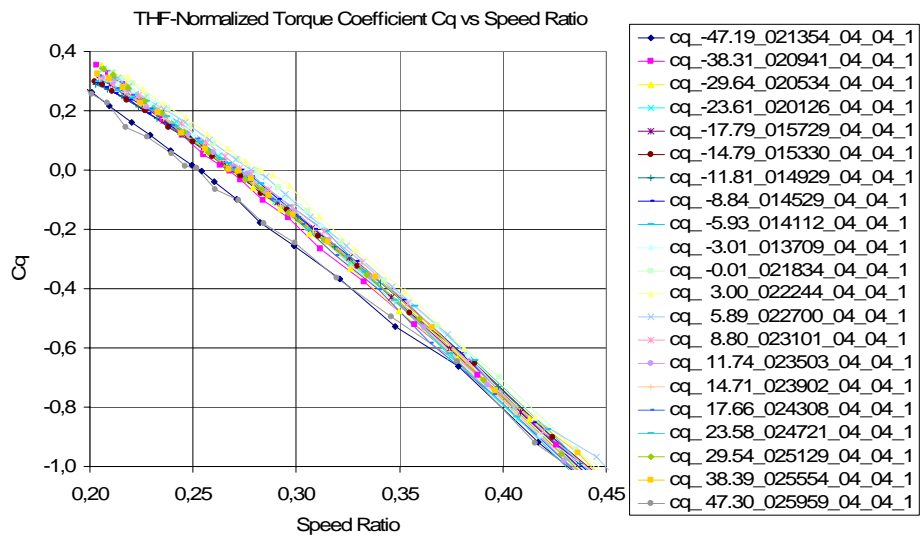


Figure 3-23 Derived torque coefficient curves (C_q versus speed ratio and tilt angle) for the THF anemometer.

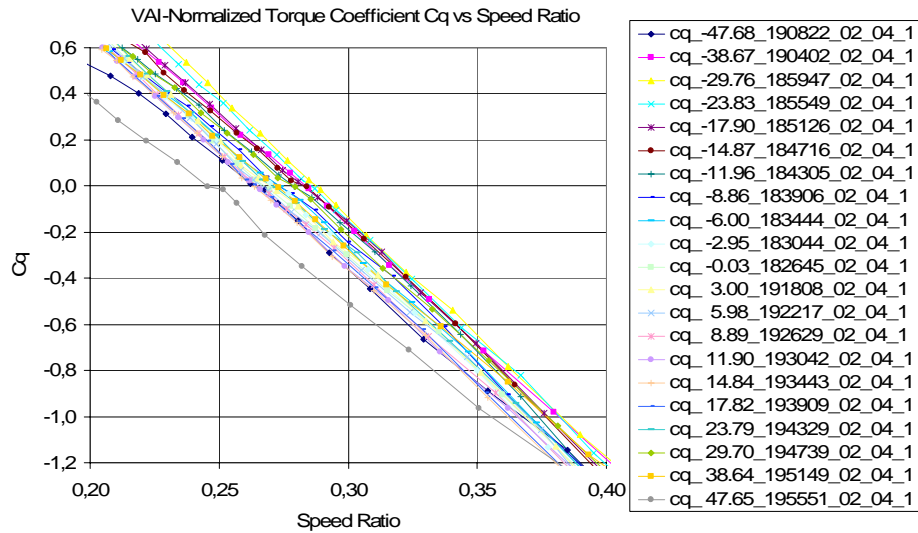


Figure 3-24 Derived torque coefficient curves (C_q versus speed ratio and tilt angle) for the VAI anemometer.

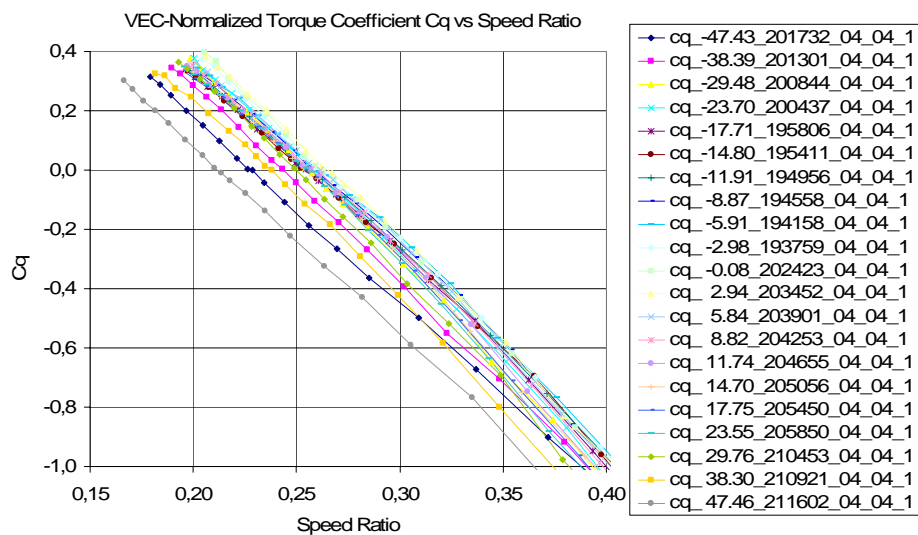


Figure 3-25 Derived torque coefficient curves (C_q versus speed ratio and tilt angle) for the VEC anemometer.

3.4.3 Torque coefficient curves for horizontal flow conditions.

The following graphs in Figure 3-26 to Figure 3-30 presents the torque coefficient curves for horizontal flow conditions only. These are the curves being used in the TRTC model simulations.

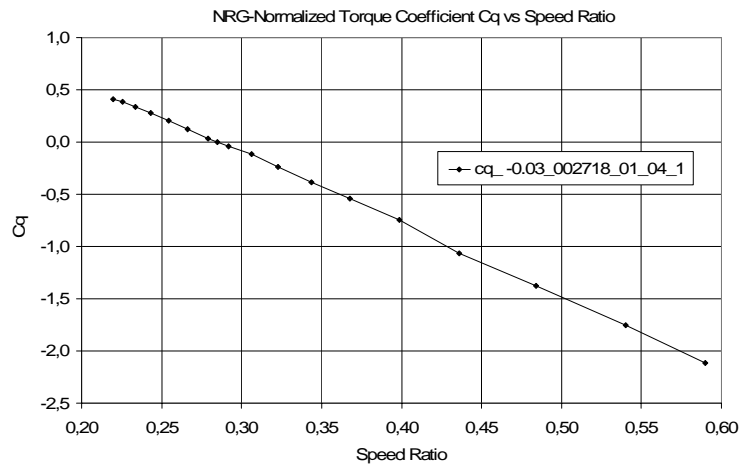


Figure 3-26 Derived torque coefficient curve (C_q versus speed ratio) for the NRG anemometer in non-tilted position.

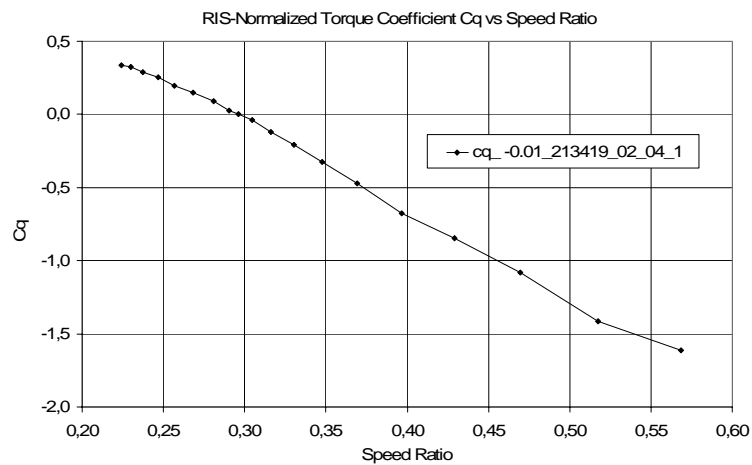


Figure 3-27 Derived torque coefficient curve (C_q versus speed ratio) for the RIS anemometer in non-tilted position.

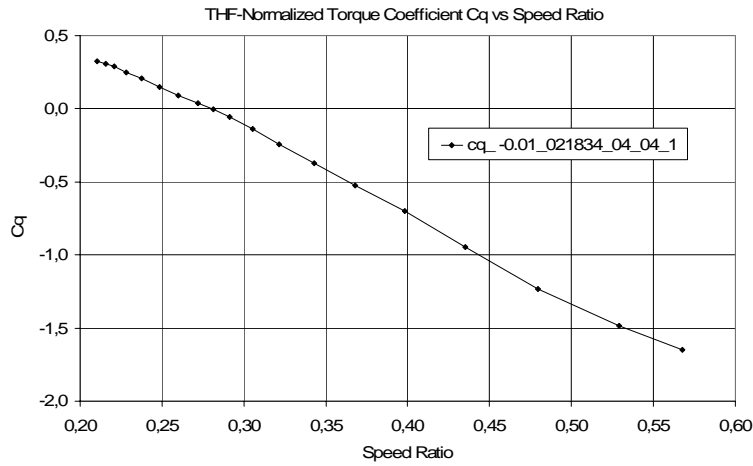


Figure 3-28 Derived torque coefficient curve (C_q versus speed ratio) for the THF anemometer in non-tilted position.

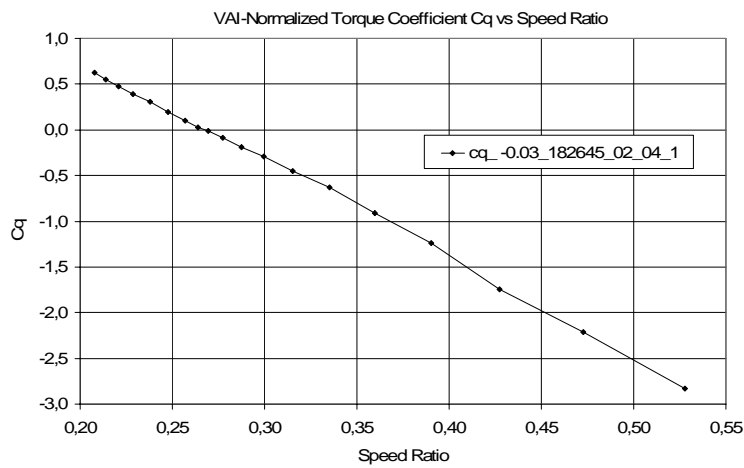


Figure 3-29 Derived torque coefficient curve (C_q versus speed ratio) for the VAI anemometer in non-tilted position.

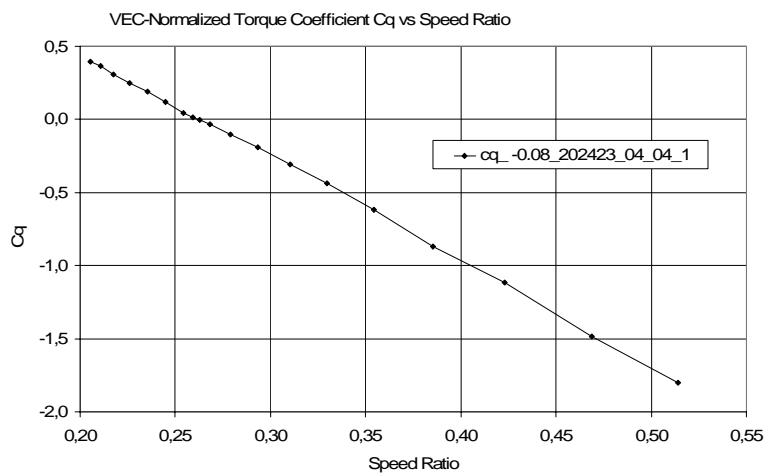


Figure 3-30 Derived torque coefficient curve (C_q versus speed ratio) for the VEC anemometer in non-tilted position.

3.4.4 Comparison of angular response from steady and dynamic measurements

One obvious comparison that can be made to the derived inclined flow torque coefficient curves is the interception points between each torque coefficient curve and the $C_q=0$ -line. After normalization of the speed ratios with the speed ratio for non-inclined flow an angular response curve arise, which indicate whether the angular responses, measured under dynamic tilted conditions, are similar to the angular response curve derived from the steady tilt tests. The five graphs from Figure 3-31 to Figure 3-35 present the comparison of angular responses.

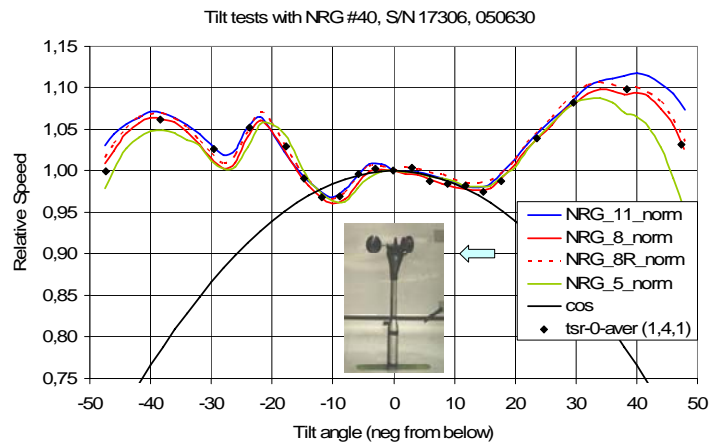


Figure 3-31 Comparison of angular response from steady and dynamic measurements on the NRG anemometer

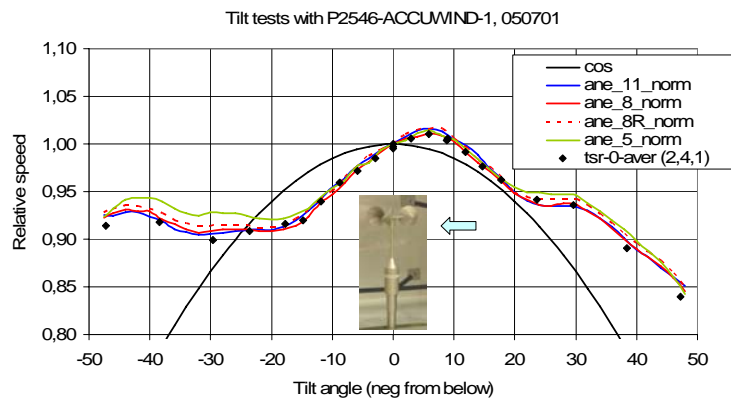


Figure 3-32 Comparison of angular response from steady and dynamic measurements on the RIS anemometer

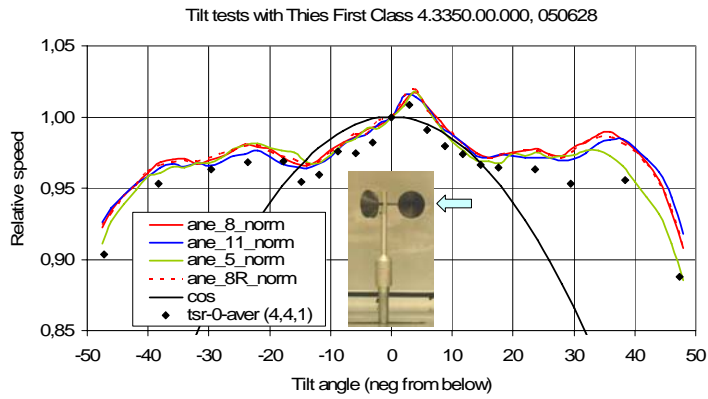


Figure 3-33 Comparison of angular response from steady and dynamic measurements on the THF anemometer

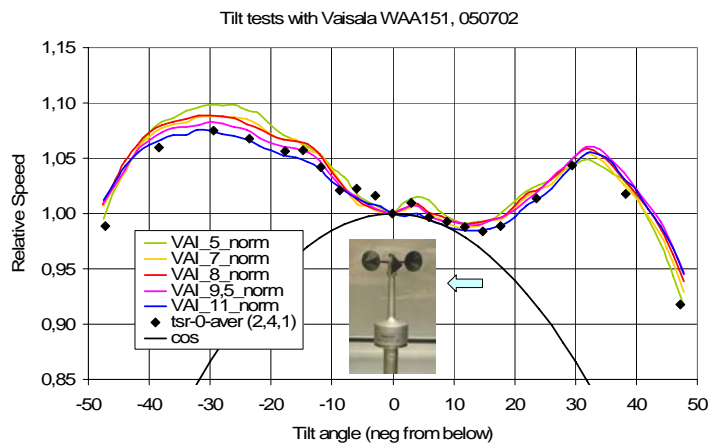


Figure 3-34 Comparison of angular response from steady and dynamic measurements on the VAI anemometer

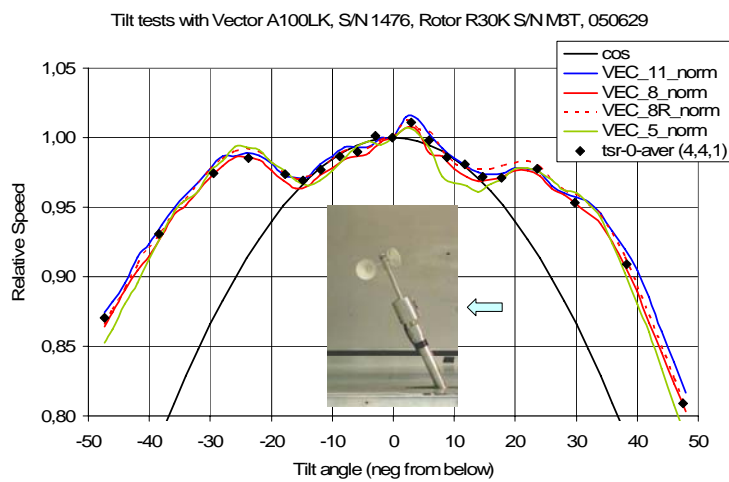


Figure 3-35 Comparison of angular response from steady and dynamic measurements on the VEC anemometer

3.5 Measurement of Rotor Inertia

The rotor inertia of each cup anemometer was measured by dismantling the rotor from the cup anemometer body, weighing the rotor and applying an oscillation inertia measurement procedure [1]. Shaft inertia was insignificant in most cases. For the NRG cup anemometer some body parts were included in the measurement, and an estimate of the inertia of this part was withdrawn. Results of inertia measurements are shown in Table 3-1.

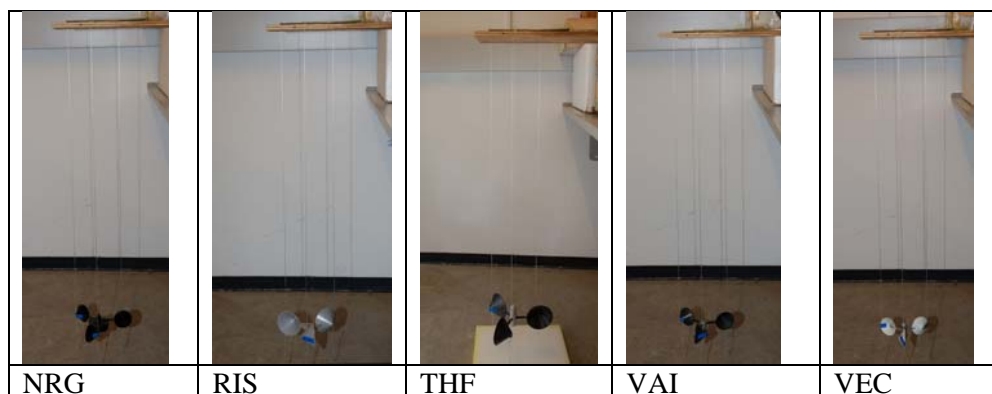


Figure 3-36 Oscillation tests for determination of rotor inertia according to the procedure in [1]

Table 3-1 Estimated rotor inertia according to oscillation test method [1]

Cup anem	NRG	RIS	THF	VAI	VEC
Rotor inertia (kgm ²)	1.01E-04	9.92E-05	2.89E-04	6.14E-05	4.40E-05

3.6 Measurement of Friction Characteristics

The friction in bearings was measured in climate chamber with a flywheel deceleration test, see [1]. Each rotor was dismantled from the cup anemometer and a flywheel with approximately the same weight as the rotor was mounted on the shaft. The flywheels on the cup anemometers are shown in Figure 3-37. At each temperature up to five runs were made on each cup anemometer.

The calculated friction from the deceleration runs are shown in Figure 3-38 to Figure 3-43. In the case of the NRG cup anemometer at 40°C the variations in friction was high. This was investigated separately, see [1]. In one case, RIS Figure 3-40, the friction tends to decrease at higher rotational speed. The reason for this is that in some cases the fitting of data to third order polynomial was made on rotational speeds that did not reach the full rotational speed range.

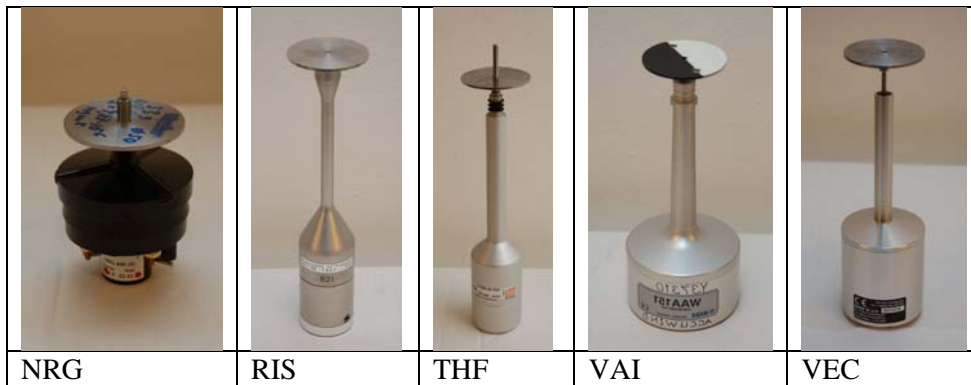


Figure 3-37 Flywheels mounted on cup anemometer shafts for flywheel deceleration tests in climate chamber according to the procedure in ref. 1.

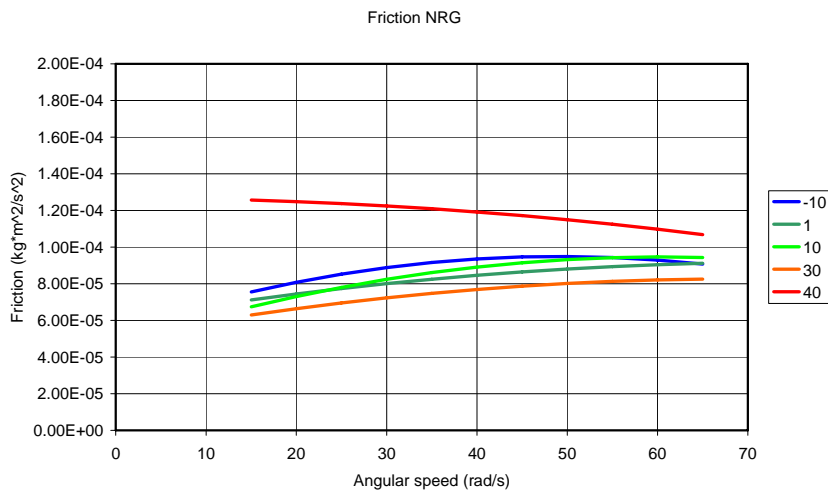


Figure 3-38 Friction of NRG cup anemometer measured in climate chamber by flywheel test

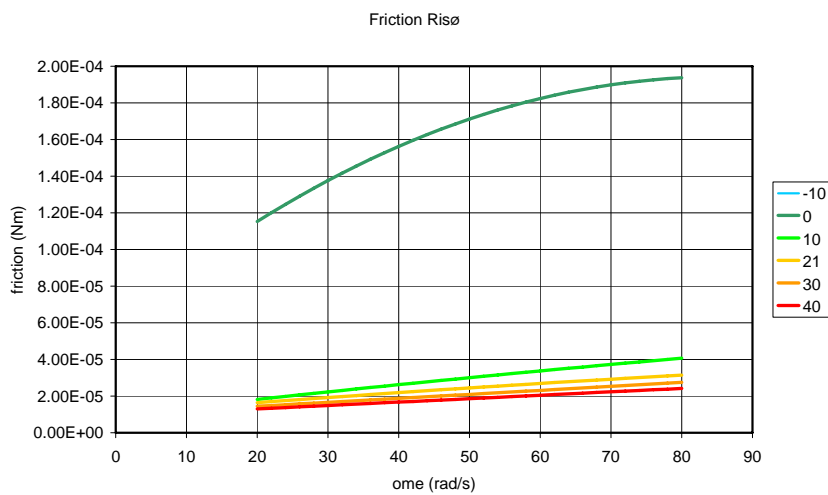


Figure 3-39 Friction of Risø cup anemometer measured in climate chamber by flywheel test

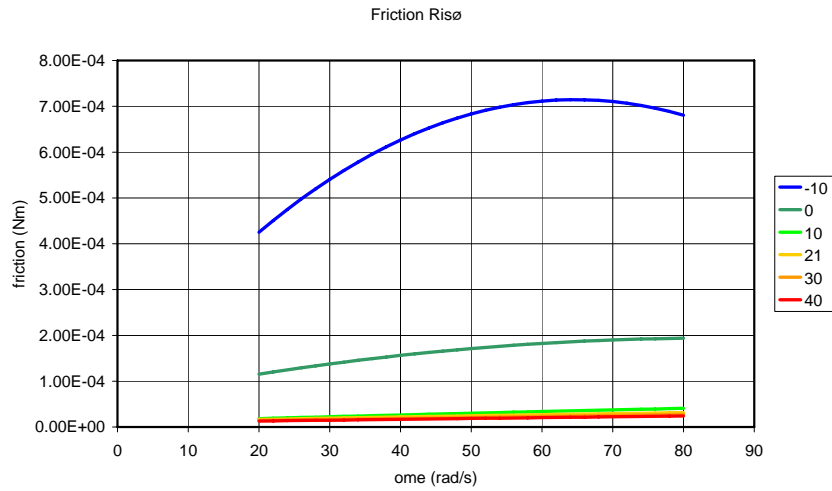


Figure 3-40 Friction of Risø cup anemometer measured in climate chamber by flywheel test

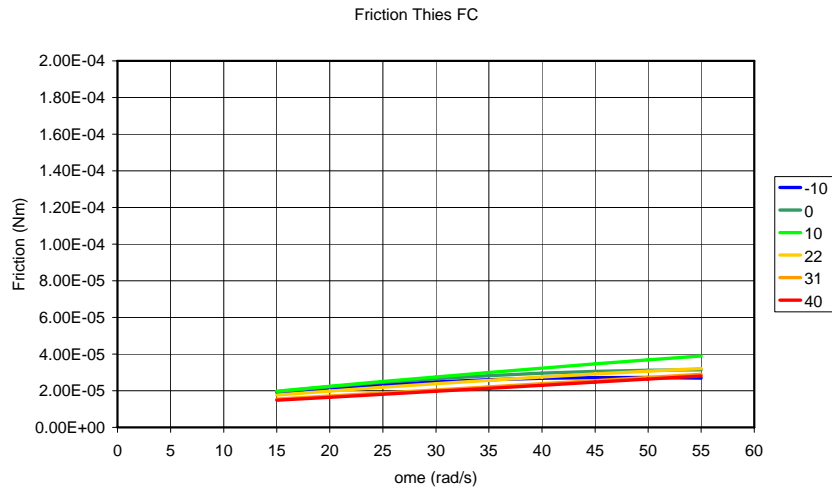


Figure 3-41 Friction of Thies FC cup anemometer measured in climate chamber by flywheel test

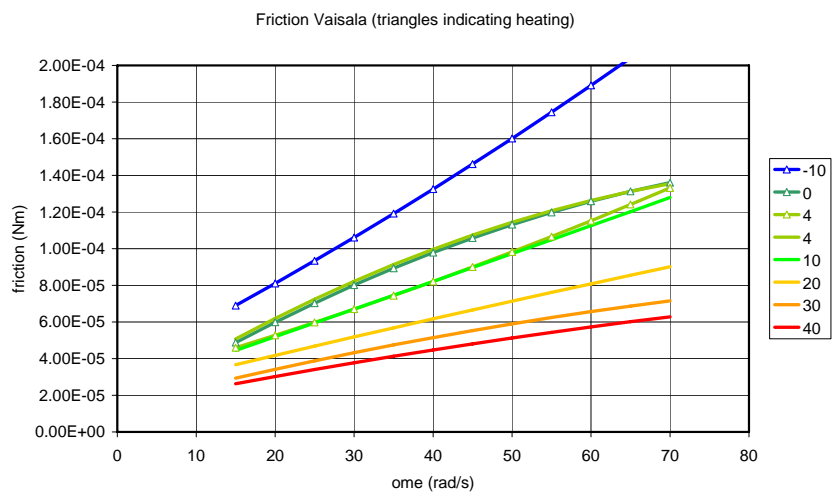


Figure 3-42 Friction of Vaisala cup anemometer measured in climate chamber by flywheel test

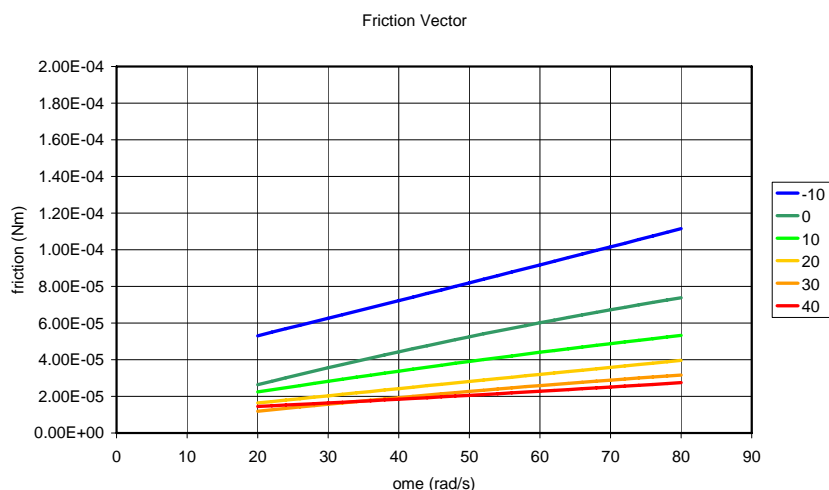


Figure 3-43 Friction of Vector cup anemometer measured in climate chamber by flywheel test

4 Classification

Classification of the five cup anemometers with data derived from wind tunnel and laboratory test is made according to annex I in the standard IEC61400-12-1, [3].

4.1 Classification Ranges

The classification according to the IEC standard on power performance measurements [3] divides the classification of cup anemometers into two classes, A and B. Table 4-1 show the required operational ranges of these two classes, including the turbulence models being used in the present evaluation.

From simulations of systematic deviations of the cup anemometers under the given ranges of operational conditions for a given class, a class index number is derived from the maximum of deviations ε_i for all wind configurations. The class index number is determined according to the formula:

$$k = 100 \cdot \max \left| \frac{\varepsilon_i}{U_i / 2 + 5 \text{ m/s}} \right|$$

Where

U_i is wind speed in bin i

ε_i is a systematic deviation within wind speed bin i

Table 4-1 Operational condition ranges of Class A and Class B category classification

	Class A Terrain meets requirements in annex B of standard		Class B Terrain does not meet requirements in annex B of standard	
	Min	Max	Min	Max
Wind speed range to cover [m/s]	4	16	4	16
Turbulence intensity	0,03	0,12+0,48/V	0,03	0,12+0,96/V
Turbulence structure $\sigma_u/\sigma_v/\sigma_w$	1/0,8/0,5 (non-isotropic turbulence) Kaimal wind spectrum with a longitudinal turbulence length scale of 350m		1/1/1 (isotropic turbulence) Von Karman wind spectrum with a longitudinal turbulence length scale of 170m	
Air temp. [°C]	0	40	-10	40
Air density [kg/m ³]	0,9	1,35	0,9	1,35
Average flow inclination angle [°]	-3	3	-15	15

The wind speed is in the IEC standard [3] defined as the horizontal wind speed:

$$U_{hor} = \sqrt{u^2 + v^2}$$

The deviations, calculated by the simulation models are based on 10min averaging:

$$U_{dev} = \sum_{10\min} U_{hor,measured} - \sum_{10\min} U_{hor}$$

The wind speed can alternatively be defined as a scalar vector wind speed:

$$U_{vec} = \sqrt{u^2 + v^2 + w^2}$$

The deviations are calculated as:

$$U_{dev} = \sum_{10\min} U_{vec,measured} - \sum_{10\min} U_{vec}$$

In this analysis the classification of the cup anemometers is made on the vector wind speed definition, as well as the horizontal wind speed, as required in [3].

4.2 Cup Anemometer Models and Fitting

The classification is made with the use of two different cup anemometer models, TRTC and IFTC. The two models are described in detail in [1].

The TRTC model makes use of static tilt tests for angular response measurements, torque coefficient curve measurements from horizontal flow static or dynamic tests, oscillation tests for rotor inertia measurements, and climate chamber bearing friction tests.

The IFTC makes use of inclined flow dynamic torque coefficient tests, while the model at present is not implemented to take account of bearing friction.

For both models a fitting is made of torque coefficient curves to fit the normal calibration curves. This is made because the tests have been made under different conditions at different times, and there are statistical variations which must be accounted

for. The fitting consist of inclusion of a delta speed ratio which ensures that simulation of the normal calibration is very precise.

4.3 Wind Generation Model

The turbulence model used to generate the 3D wind files for the calculations in this report is made by Jacob Mann [2], using either Kaimal spectra with longitudinal length scales of 350m or von Karman isotropic spectra with longitudinal length scales of 170m. Ten minute time series of 25Hz data are made for each calculation. The input data for the model are taken from the tables of operational ranges Table 4-1.

4.4 Classification with Inclined-Flow-Torque-Coefficient Model (IFTC)

The following chapters show the results of simulation of systematic deviations of the five cup anemometers with the IFTC model. The simulations show deviations for Class A and Class B categories, as well as for horizontal or vector wind speed definitions.

4.4.5 Classification of NRG cup anemometer

Figure 4-1 to Figure 4-4 presents simulated deviations with the IFTC model of the NRG cup anemometer.

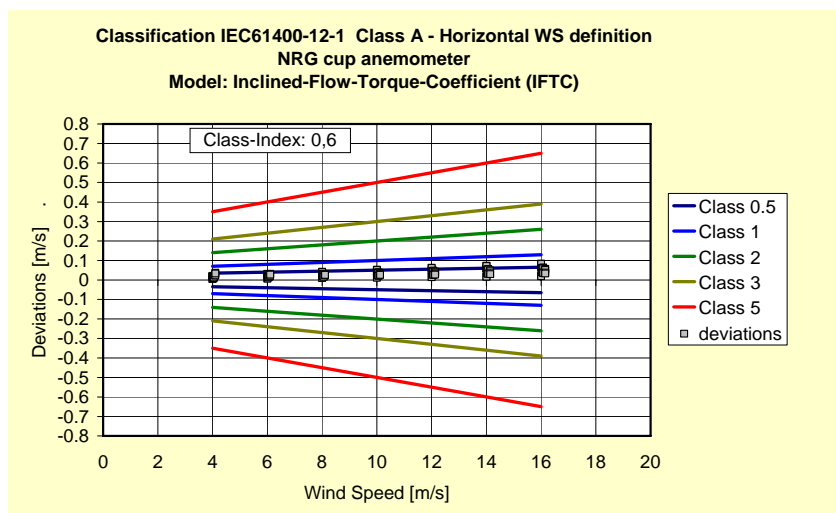


Figure 4-1 Classification of NRG cup anemometer with IFTC model for Class A – horizontal wind speed definition

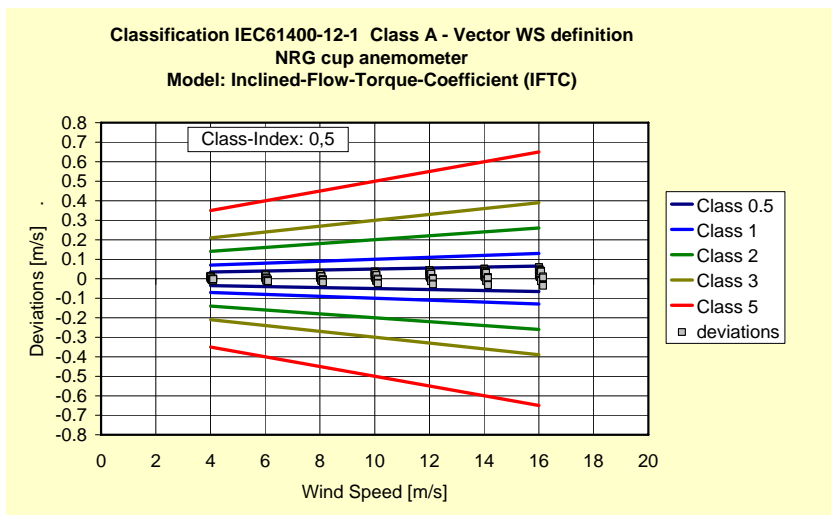


Figure 4-2 Classification of NRG cup anemometer with IFTC model for Class A – vector wind speed definition

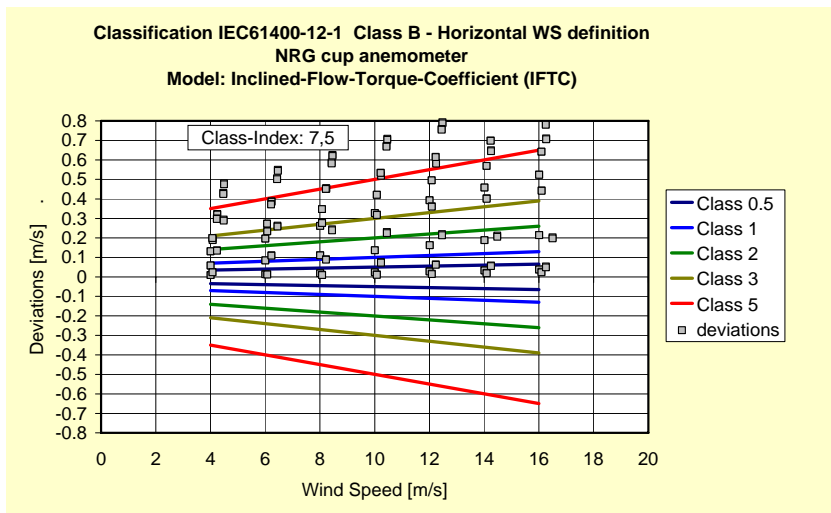


Figure 4-3 Classification of NRG cup anemometer with IFTC model for Class B – horizontal wind speed definition

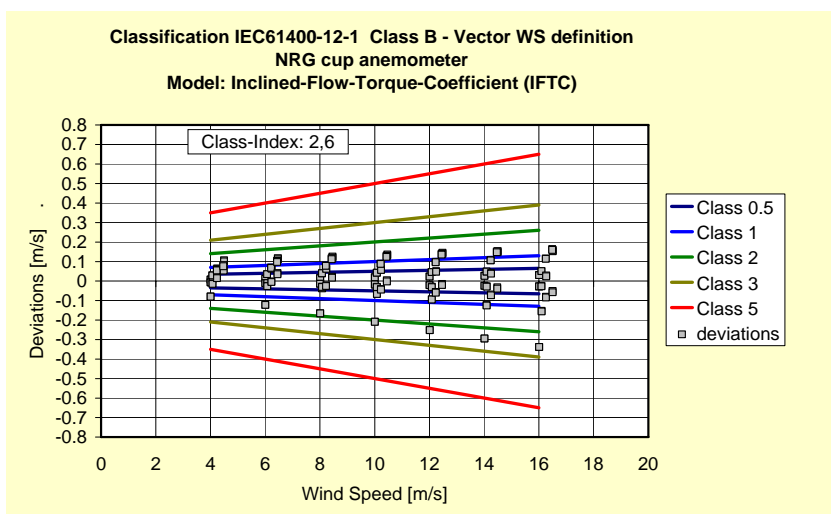


Figure 4-4 Classification of NRG cup anemometer with IFTC model for Class B – vector wind speed definition

4.4.6 Classification of Risø cup anemometer

Figure 4-5 to Figure 4-8 presents simulated deviations with the IFTC model of the Risø cup anemometer.

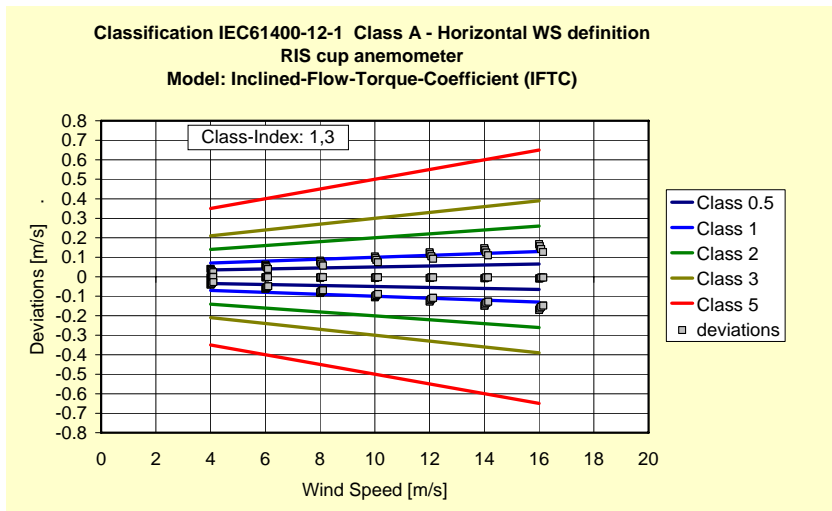


Figure 4-5 Classification of Risø cup anemometer with IFTC model for Class A – horizontal wind speed definition

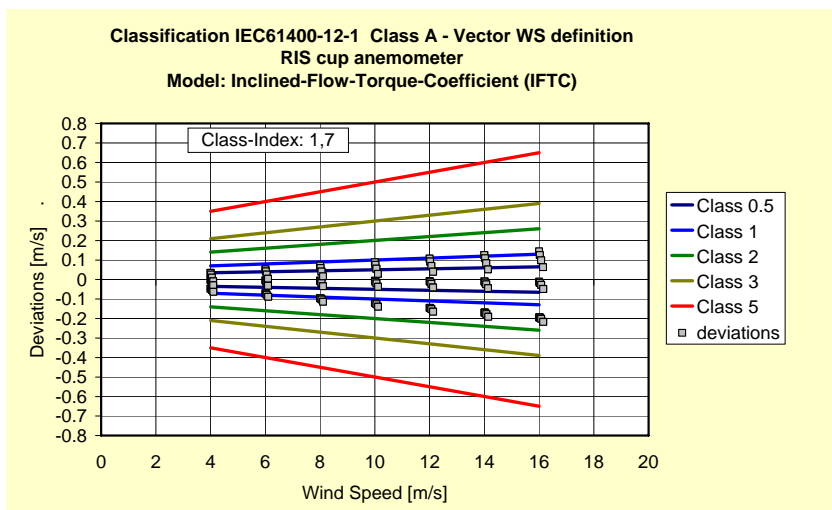


Figure 4-6 Classification of Risø cup anemometer with IFTC model for Class A – vector wind speed definition

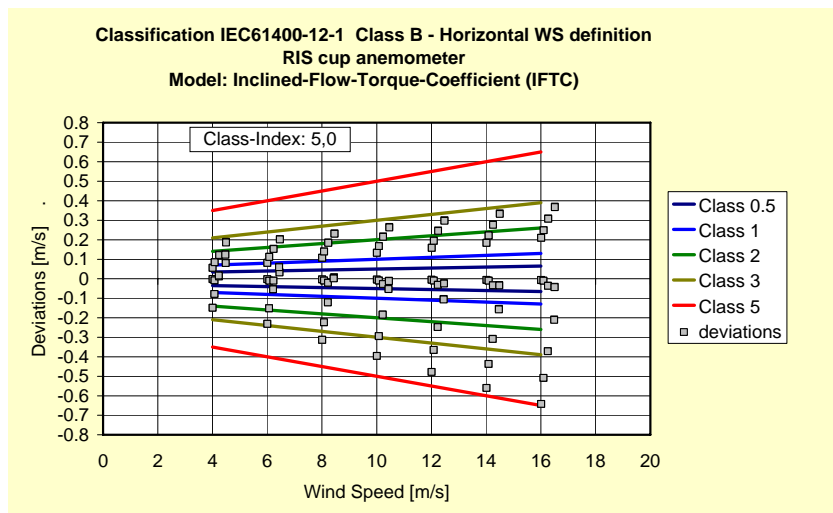


Figure 4-7 Classification of Risø cup anemometer with IFTC model for Class B – horizontal wind speed definition

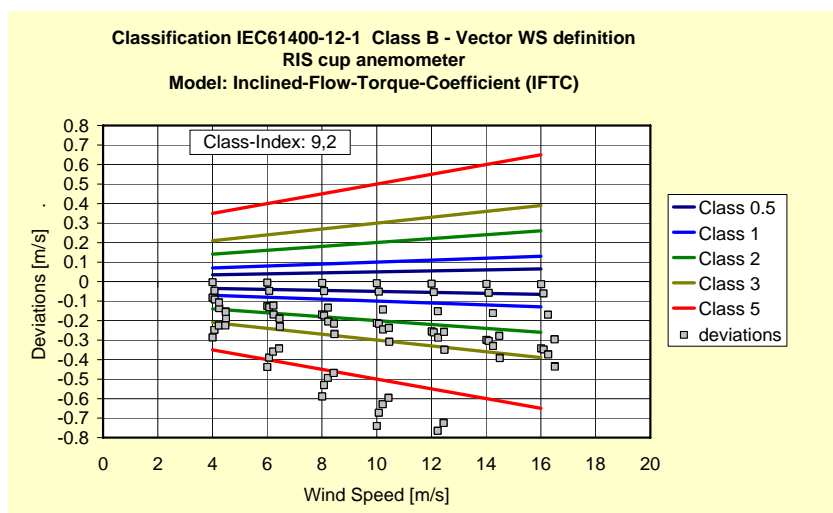


Figure 4-8 Classification of Risø cup anemometer with IFTC model for Class B – vector wind speed definition

4.4.7 Classification of Thies FC cup anemometer

Figure 4-9 to Figure 4-12 presents simulated deviations with the IFTC model of the Thies FC cup anemometer.

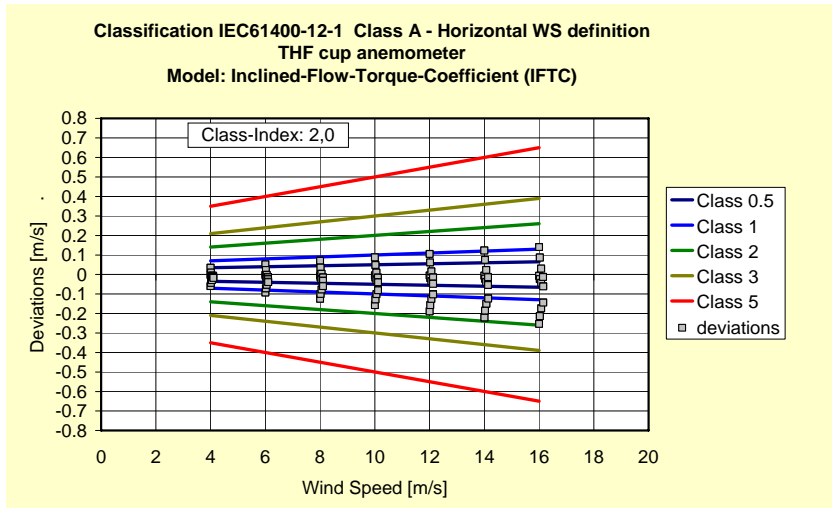


Figure 4-9 Classification of Thies FC cup anemometer with IFTC model for Class A – horizontal wind speed definition

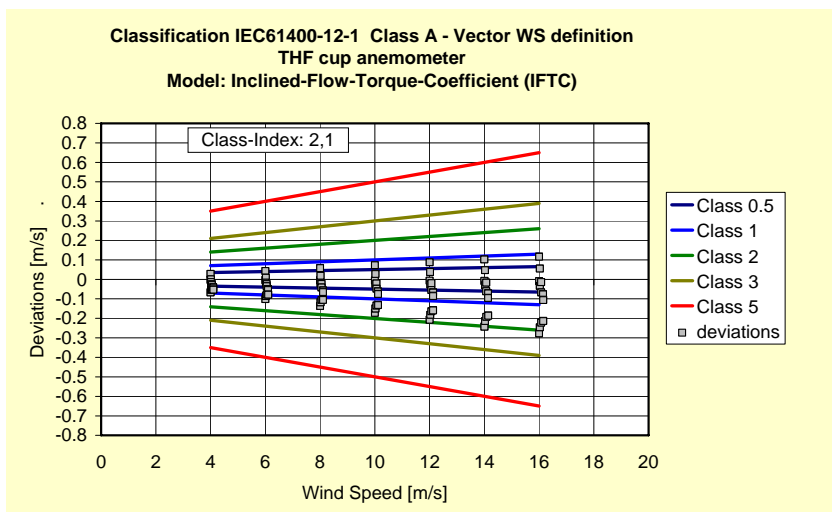


Figure 4-10 Classification of Thies FC cup anemometer with IFTC model for Class A – vector wind speed definition

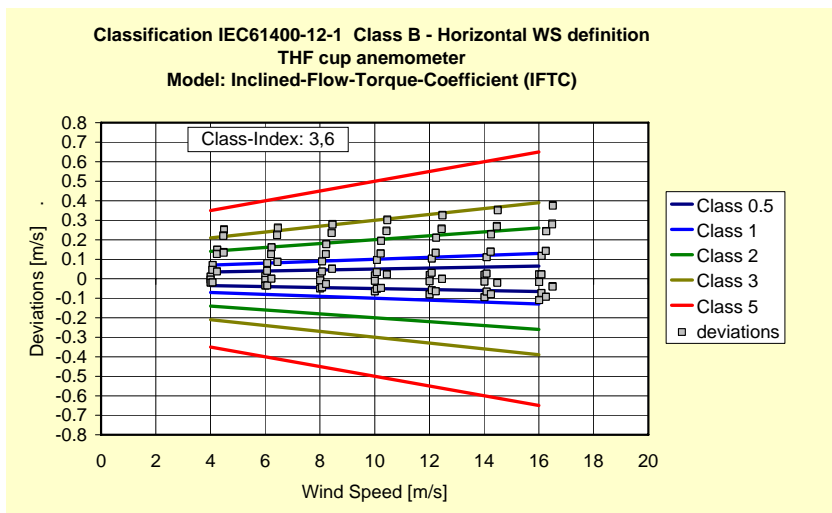


Figure 4-11 Classification of Thies FC cup anemometer with IFTC model for Class B – horizontal wind speed definition

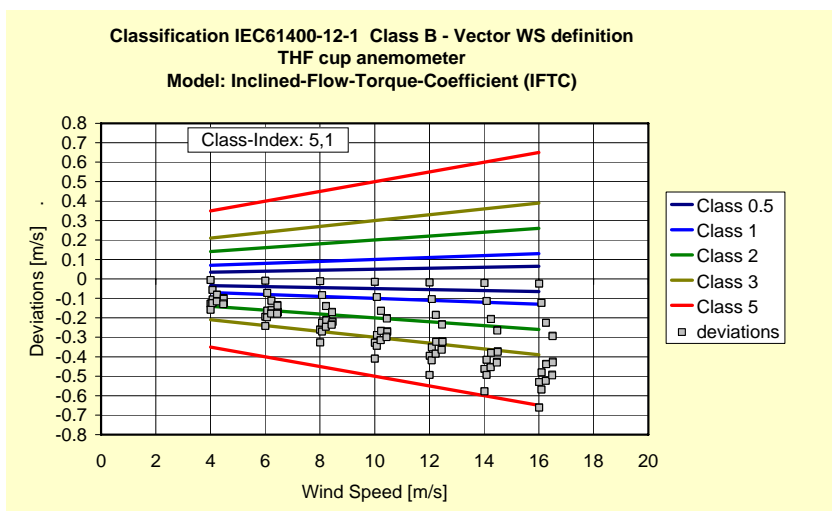


Figure 4-12 Classification of Thies FC cup anemometer with IFTC model for Class B – vector wind speed definition

4.4.8 Classification of Vaisala cup anemometer

Figure 4-13 to Figure 4-16 presents simulated deviations with the IFTC model of the Vaisala cup anemometer.

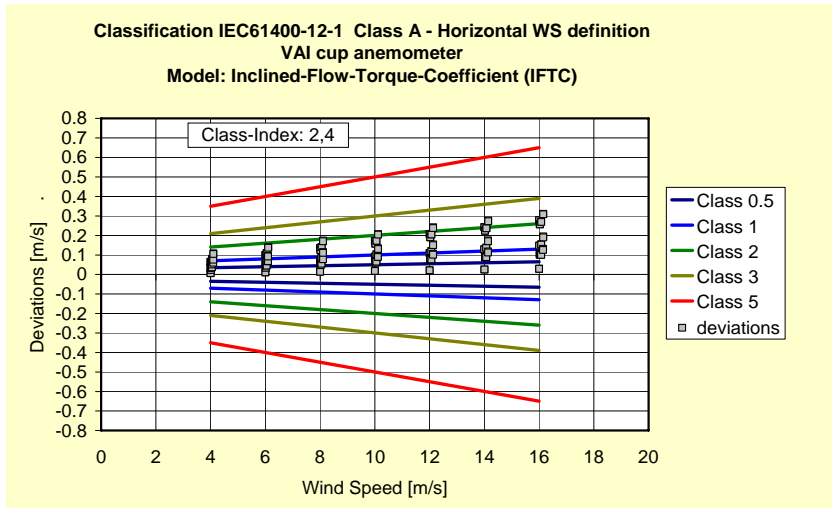


Figure 4-13 Classification of Vaisala cup anemometer with IFTC model for Class A – horizontal wind speed definition

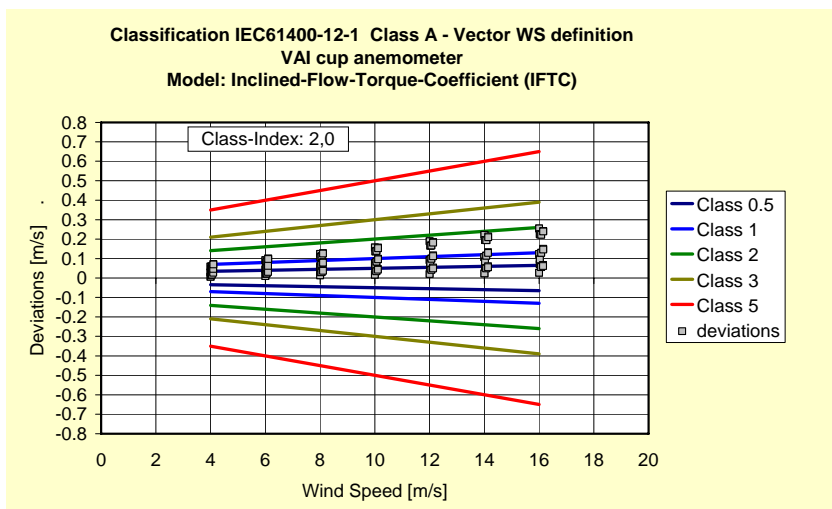


Figure 4-14 Classification of Vaisala cup anemometer with IFTC model for Class A – vector wind speed definition

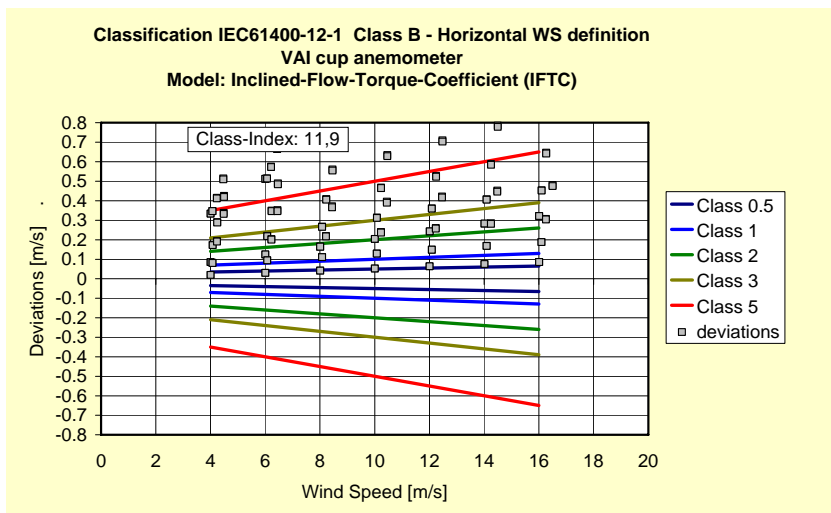


Figure 4-15 Classification of Vaisala cup anemometer with IFTC model for Class B – horizontal wind speed definition

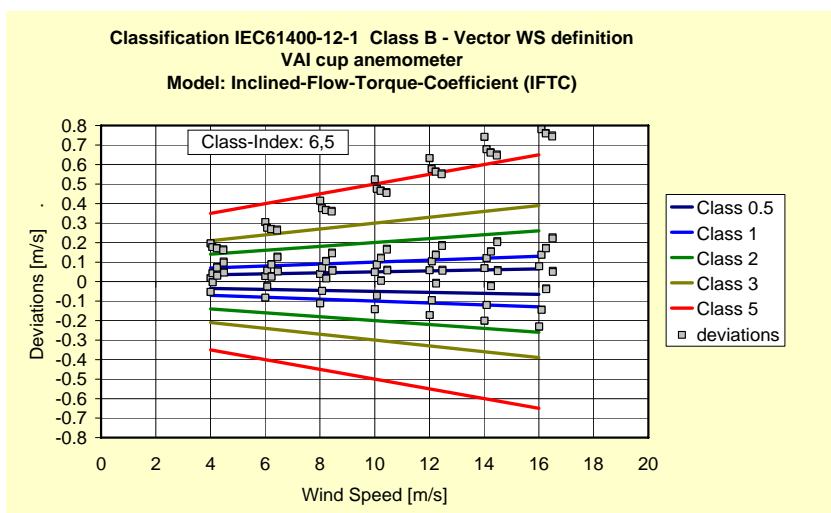


Figure 4-16 Classification of Vaisala cup anemometer with IFTC model for Class B – vector wind speed definition

4.4.9 Classification of Vector cup anemometer

Figure 4-17 to Figure 4-20 presents simulated deviations with the IFTC model of the Vector cup anemometer.

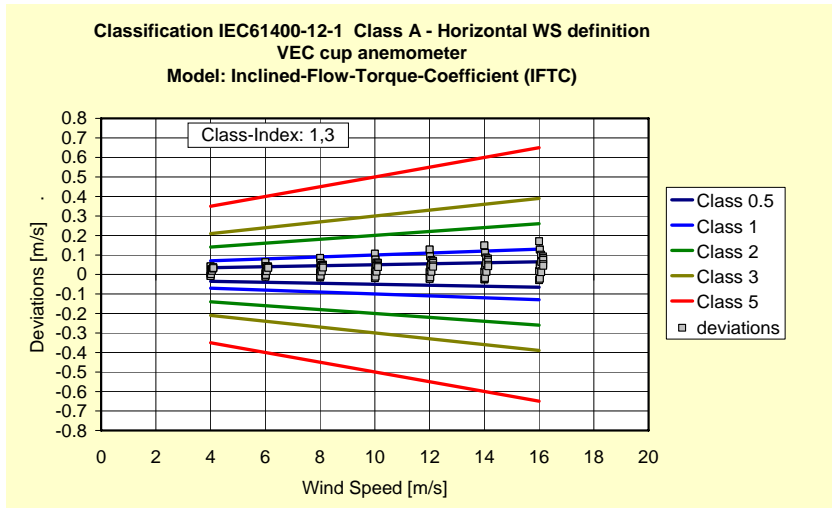


Figure 4-17 Classification of Vector cup anemometer with IFTC model for Class A – horizontal wind speed definition

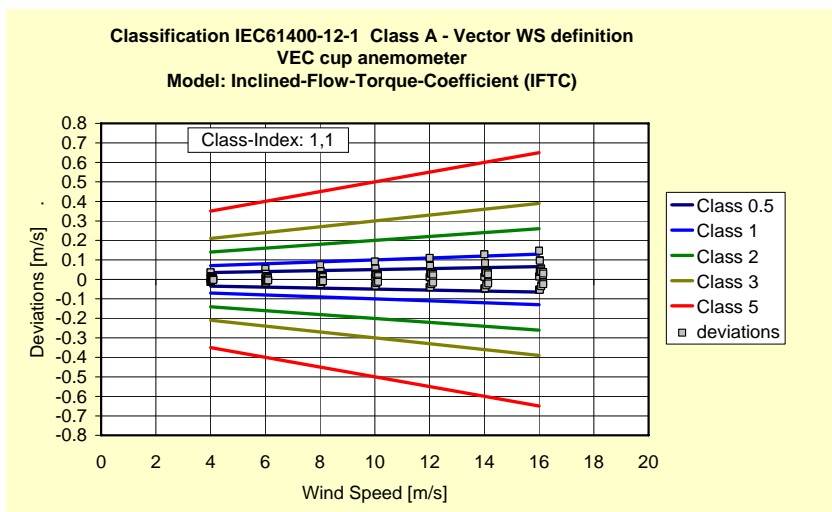


Figure 4-18 Classification of Vector cup anemometer with IFTC model for Class A – vector wind speed definition

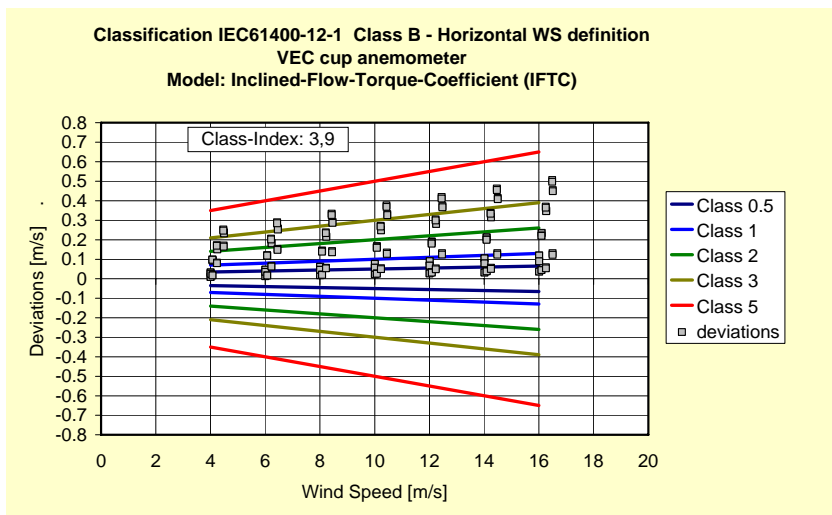


Figure 4-19 Classification of Vector cup anemometer with IFTC model for Class B – horizontal wind speed definition

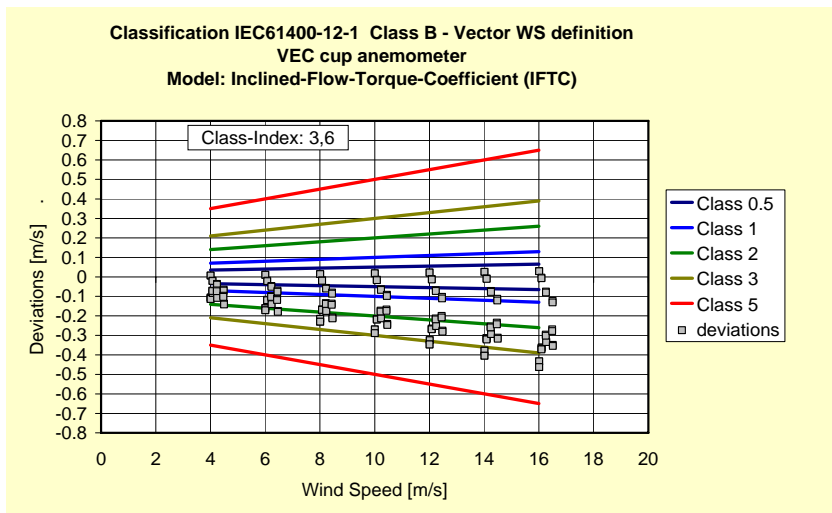


Figure 4-20 Classification of Vector cup anemometer with IFTC model for Class B – vector wind speed definition

4.5 Classification with Tilt-Response & Torque-Coefficient Model (TRTC)

The following chapters show the results of simulation of systematic deviations of the five cup anemometers with the TRTC model. The simulations show deviations for Class A and Class B categories, as well as for horizontal or vector wind speed definitions, and for angular response measurements made by either FOI or DEWI. The simulations include influence of friction.

4.5.10 Classification of NRG cup anemometer

Figure 4-21 to Figure 4-24 presents simulated deviations with the TRTC model of the NRG cup anemometer with FOI angular response measurements, and Figure 4-25 to Figure 4-28 presents simulated deviations with DEWI angular response measurements.

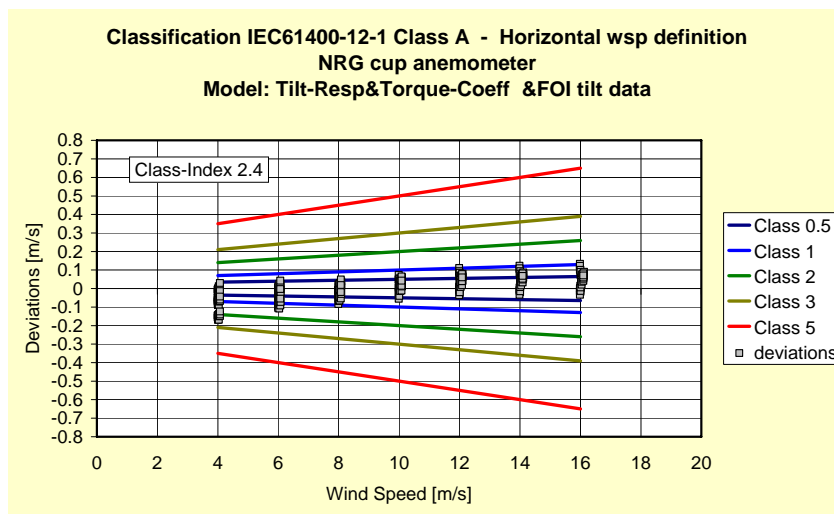


Figure 4-21 Classification of NRG cup anemometer with TRTC model for Class A – horizontal wind speed definition and FOI tilt data (note: friction variations are high for low wind speeds, see [1])

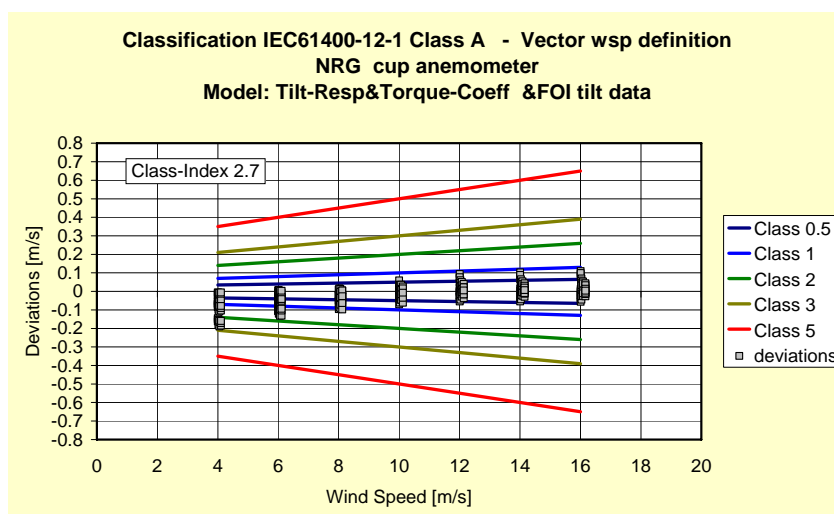


Figure 4-22 Classification of NRG cup anemometer with TRTC model for Class A – vector wind speed definition and FOI tilt data

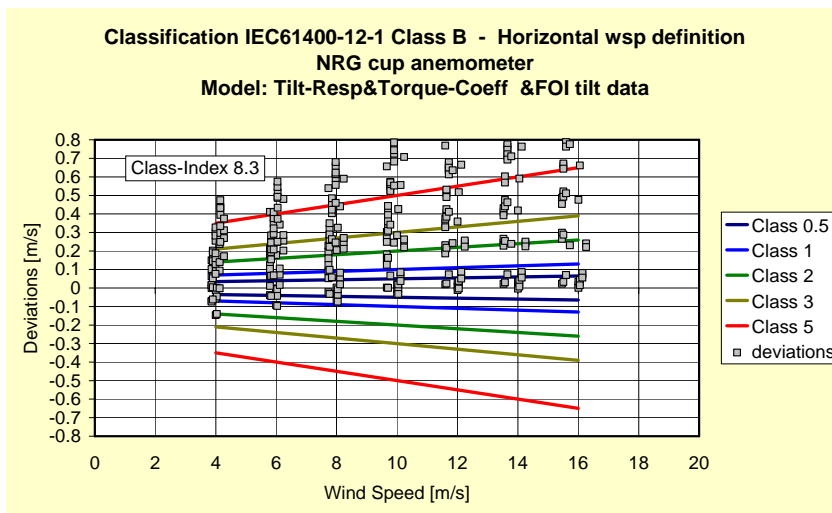


Figure 4-23 Classification of NRG cup anemometer with TRTC model for Class B – horizontal wind speed definition and FOI tilt data

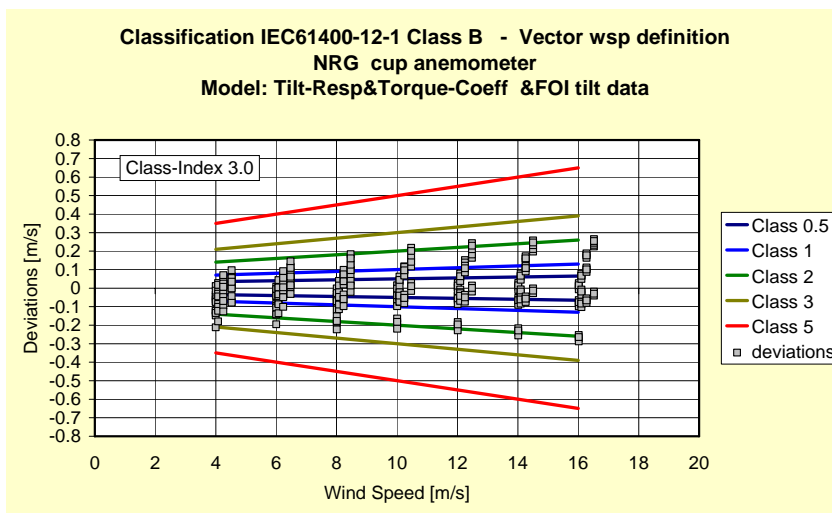


Figure 4-24 Classification of NRG cup anemometer with TRTC model for Class B – vector wind speed definition and FOI tilt data

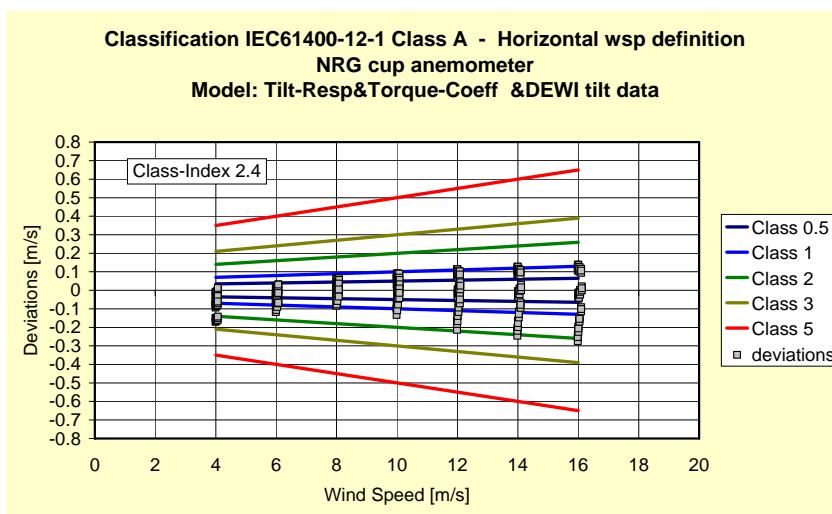


Figure 4-25 Classification of NRG cup anemometer with TRTC model for Class A – horizontal wind speed definition and DEWI tilt data

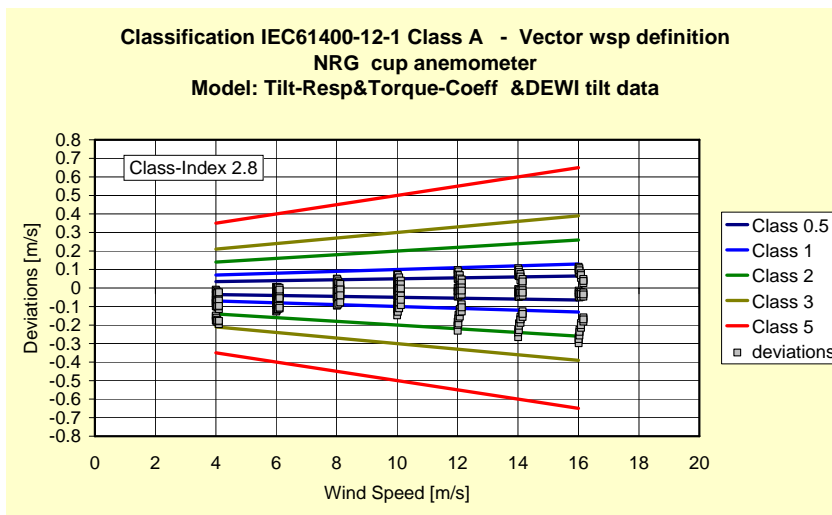


Figure 4-26 Classification of NRG cup anemometer with TRTC model for Class A – vector wind speed definition and DEWI tilt data

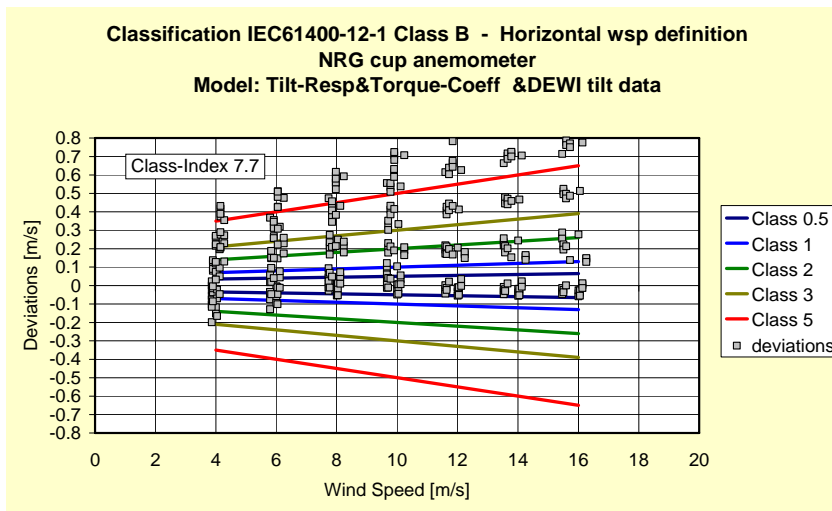


Figure 4-27 Classification of NRG cup anemometer with TRTC model for Class B – horizontal wind speed definition and DEWI tilt data

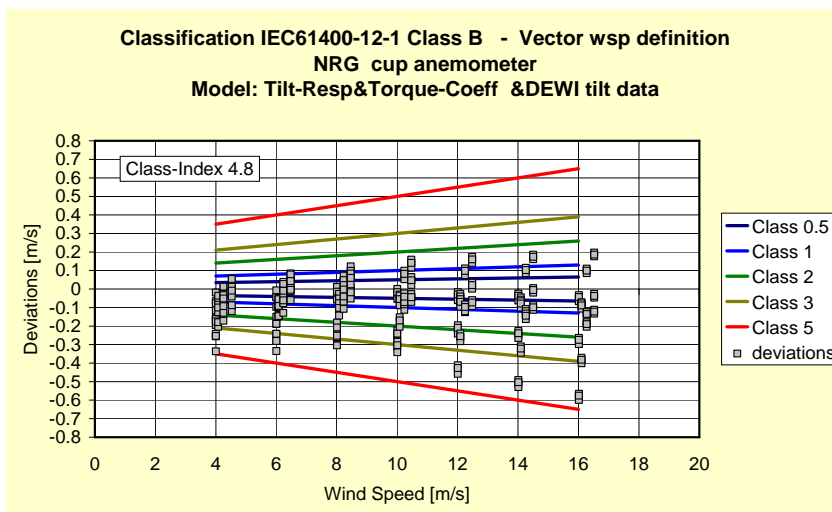


Figure 4-28 Classification of NRG cup anemometer with TRTC model for Class B – vector wind speed definition and DEWI tilt data

4.5.11 Classification of Risø cup anemometer

Figure 4-29 to Figure 4-32 presents simulated deviations with the TRTC model of the Risø cup anemometer with FOI angular response measurements, and Figure 4-33 to Figure 4-36 presents simulated deviations with DEWI angular response measurements.

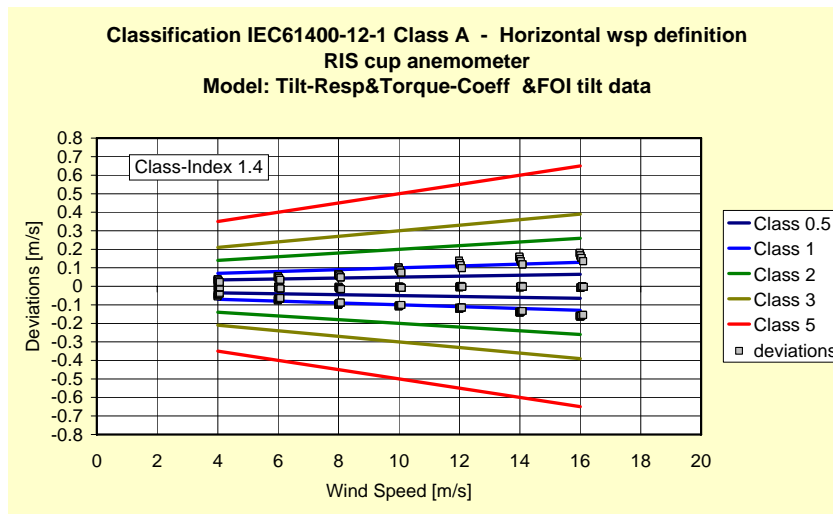


Figure 4-29 Classification of Risø cup anemometer with TRTC model for Class A – horizontal wind speed definition and FOI tilt data

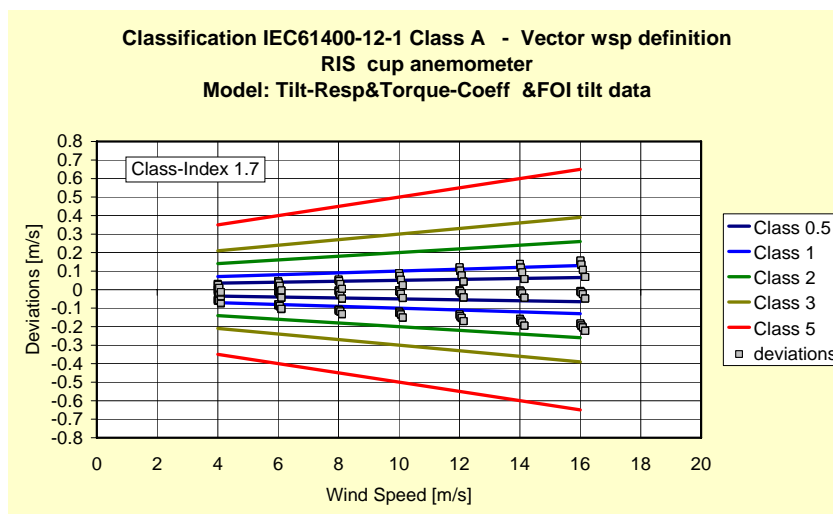


Figure 4-30 Classification of Risø cup anemometer with TRTC model for Class A – vector wind speed definition and FOI tilt data

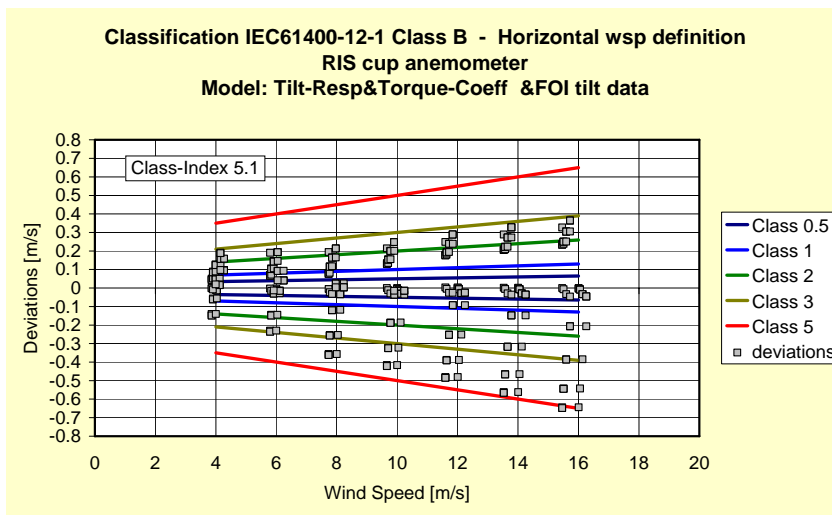


Figure 4-31 Classification of Risø cup anemometer with TRTC model for Class B – horizontal wind speed definition and FOI tilt data

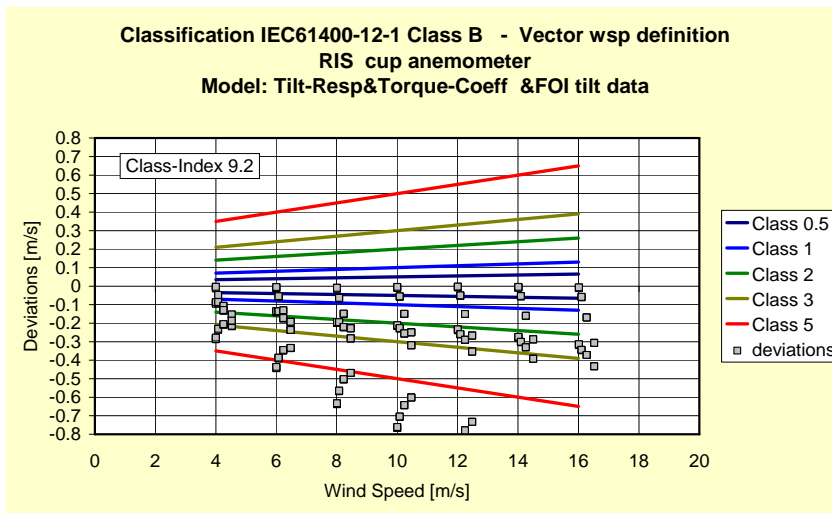


Figure 4-32 Classification of Risø cup anemometer with TRTC model for Class B – vector wind speed definition and FOI tilt data

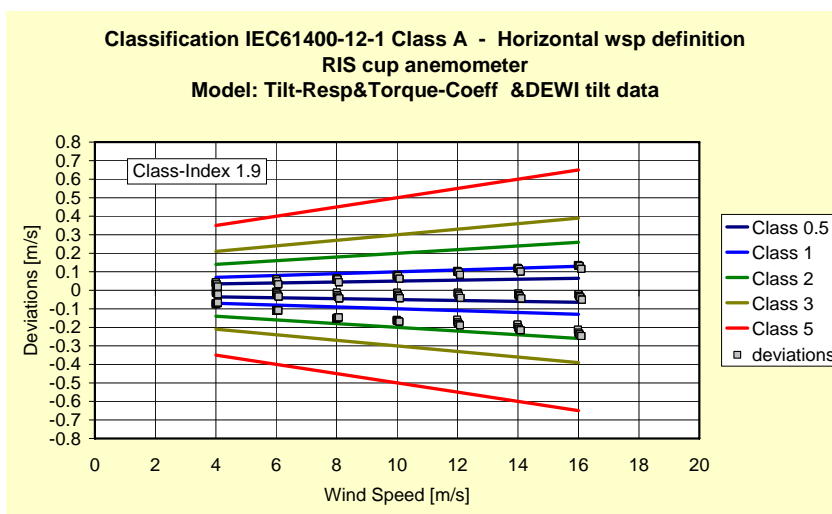


Figure 4-33 Classification of Risø cup anemometer with TRTC model for Class A – horizontal wind speed definition and DEWI tilt data

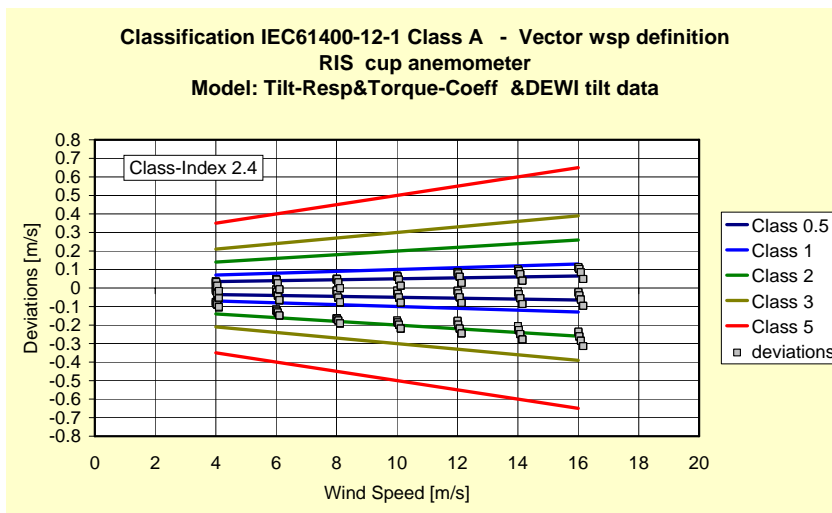


Figure 4-34 Classification of Risø cup anemometer with TRTC model for Class A – vector wind speed definition and DEWI tilt data

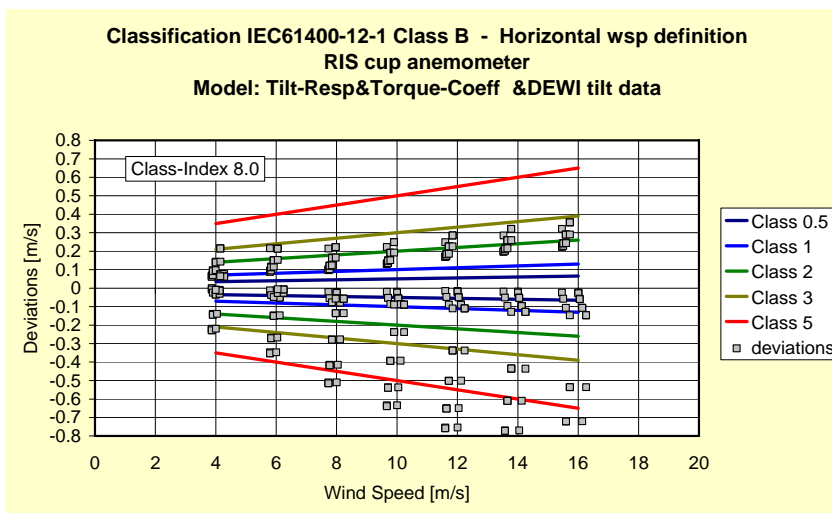


Figure 4-35 Classification of Risø cup anemometer with TRTC model for Class B – horizontal wind speed definition and DEWI tilt data

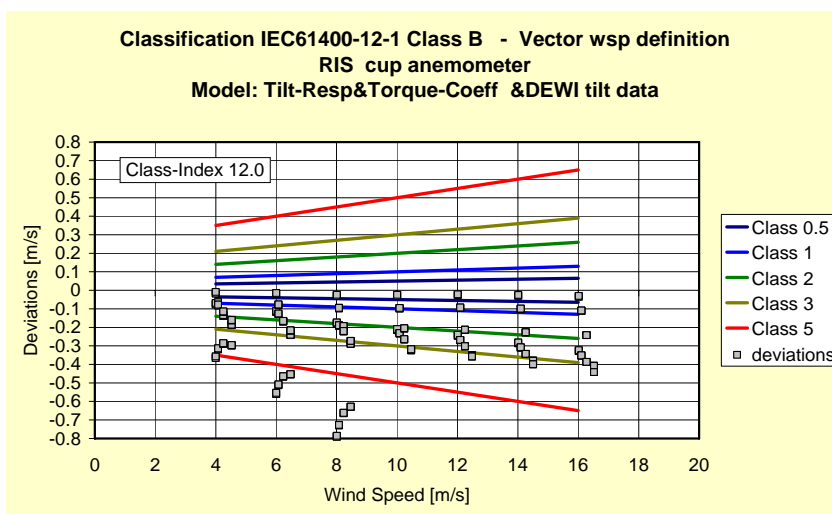


Figure 4-36 Classification of Risø cup anemometer with TRTC model for Class B – vector wind speed definition and DEWI tilt data

4.5.12 Classification of Thies FC cup anemometer

Figure 4-37 to Figure 4-40 presents simulated deviations with the TRTC model of the Thies FC cup anemometer with FOI angular response measurements, and Figure 4-41 to Figure 4-44 presents simulated deviations with DEWI angular response measurements.

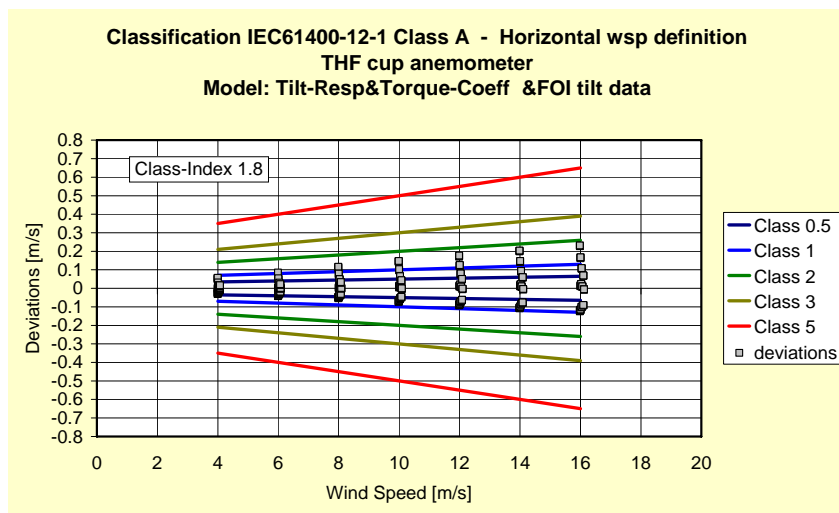


Figure 4-37 Classification of Thies FC cup anemometer with TRTC model for Class A – horizontal wind speed definition and FOI tilt data

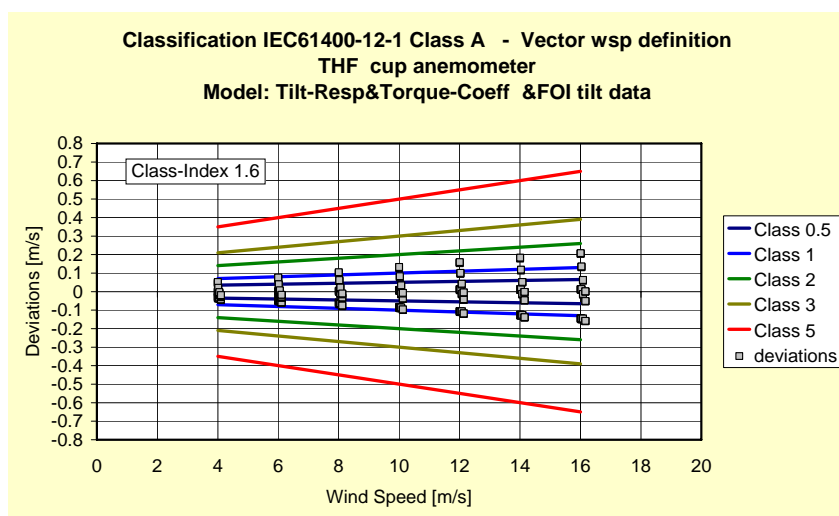


Figure 4-38 Classification of Thies FC cup anemometer with TRTC model for Class A – vector wind speed definition and FOI tilt data

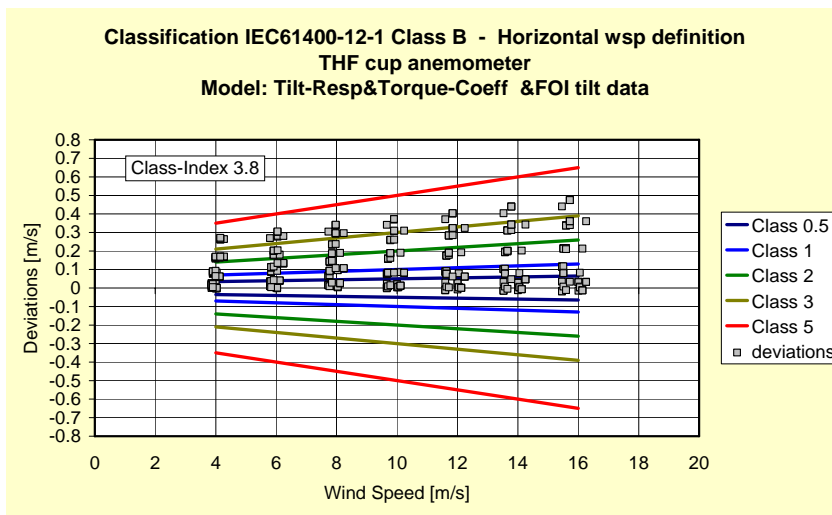


Figure 4-39 Classification of Thies FC cup anemometer with TRTC model for Class B – horizontal wind speed definition and FOI tilt data

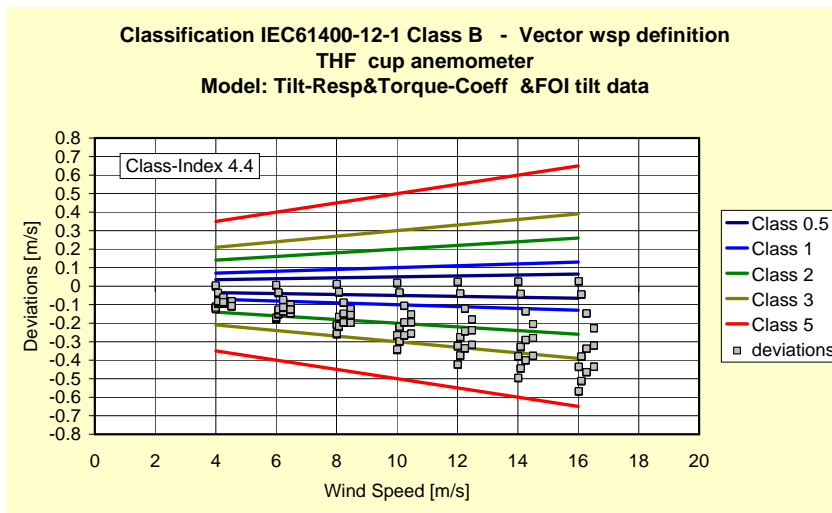


Figure 4-40 Classification of Thies FC cup anemometer with TRTC model for Class B – vector wind speed definition and FOI tilt data

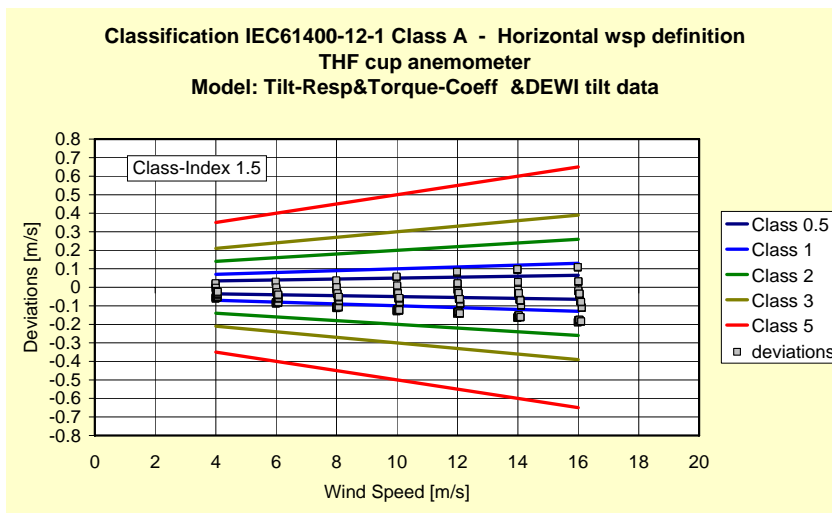


Figure 4-41 Classification of Thies FC cup anemometer with TRTC model for Class A – horizontal wind speed definition and DEWI tilt data

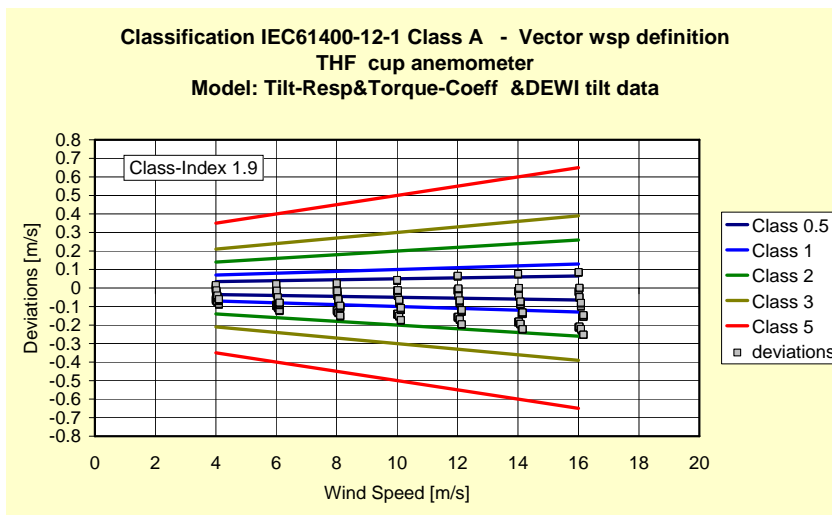


Figure 4-42 Classification of Thies FC cup anemometer with TRTC model for Class A – vector wind speed definition and DEWI tilt data

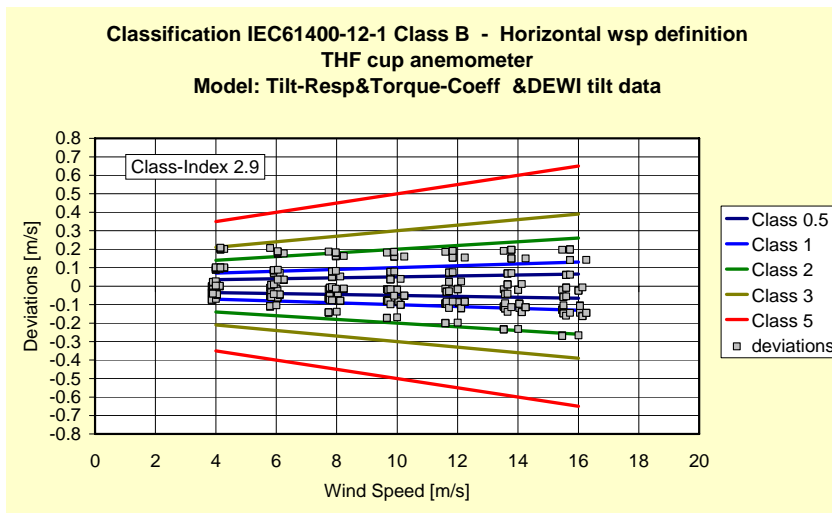


Figure 4-43 Classification of Thies FC cup anemometer with TRTC model for Class B – horizontal wind speed definition and DEWI tilt data

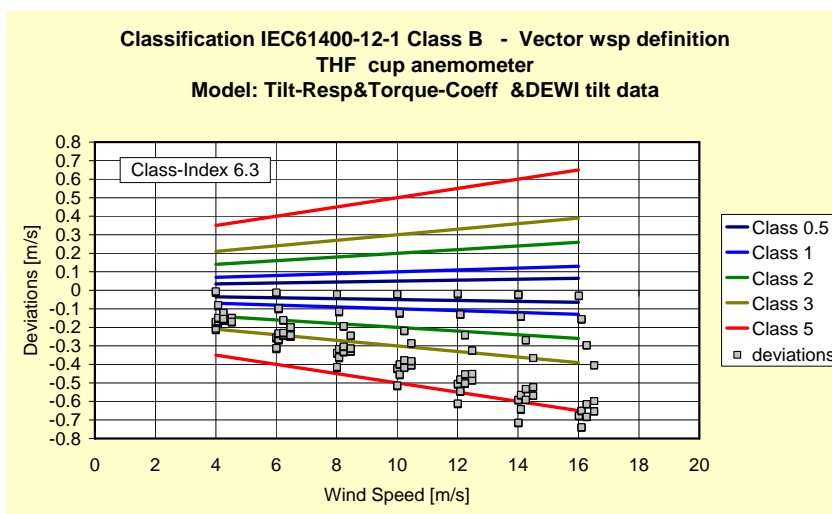


Figure 4-44 Classification of Thies FC cup anemometer with TRTC model for Class B – vector wind speed definition and DEWI tilt data

4.5.13 Classification of Vaisala cup anemometer

Figure 4-45 to Figure 4-48 presents simulated deviations with the TRTC model of the Vaisala cup anemometer with FOI angular response measurements, and Figure 4-49 to Figure 4-52 presents simulated deviations with DEWI angular response measurements.

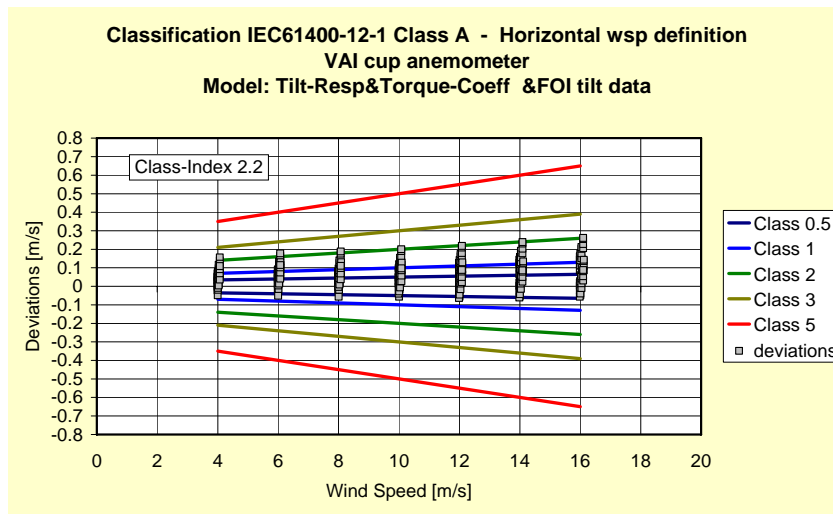


Figure 4-45 Classification of Vaisala cup anemometer with TRTC model for Class A – horizontal wind speed definition and FOI tilt data

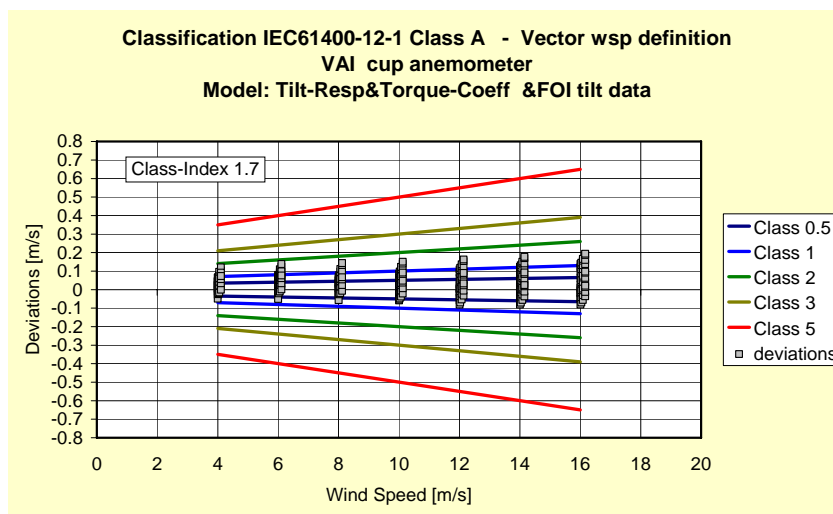


Figure 4-46 Classification of Vaisala cup anemometer with TRTC model for Class A – vector wind speed definition and FOI tilt data

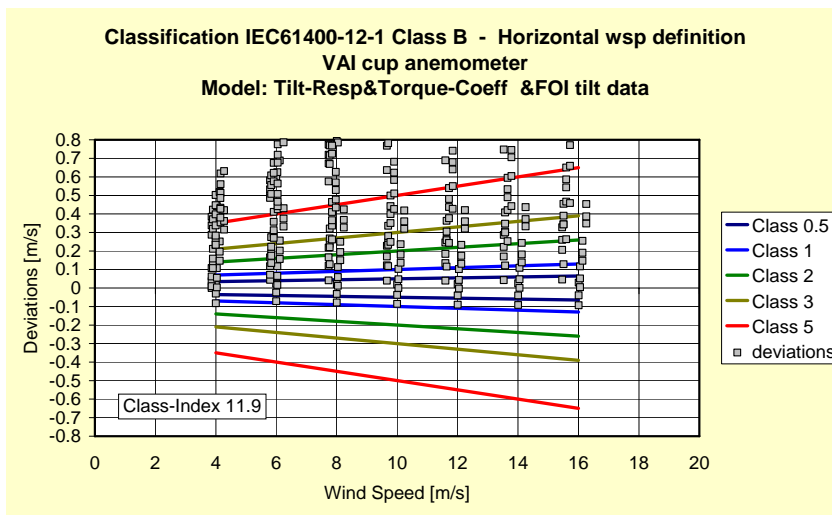


Figure 4-47 Classification of Vaisala cup anemometer with TRTC model for Class B – horizontal wind speed definition and FOI tilt data

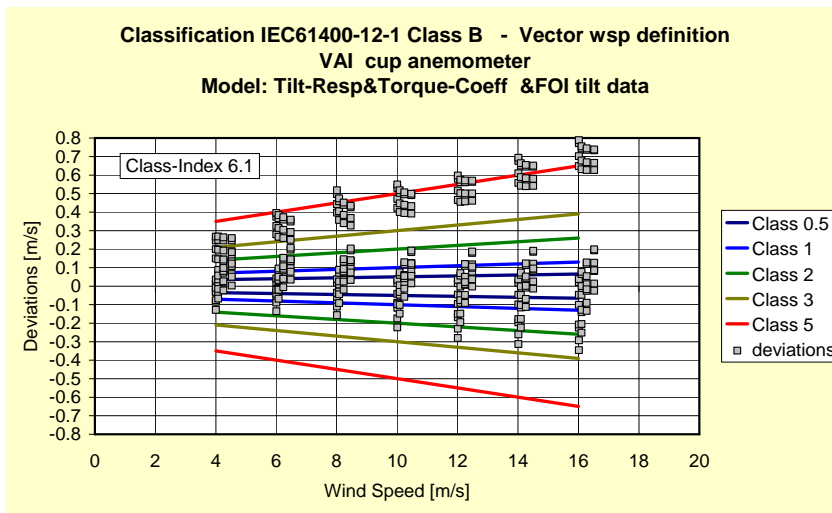


Figure 4-48 Classification of Vaisala cup anemometer with TRTC model for Class B – vector wind speed definition and FOI tilt data

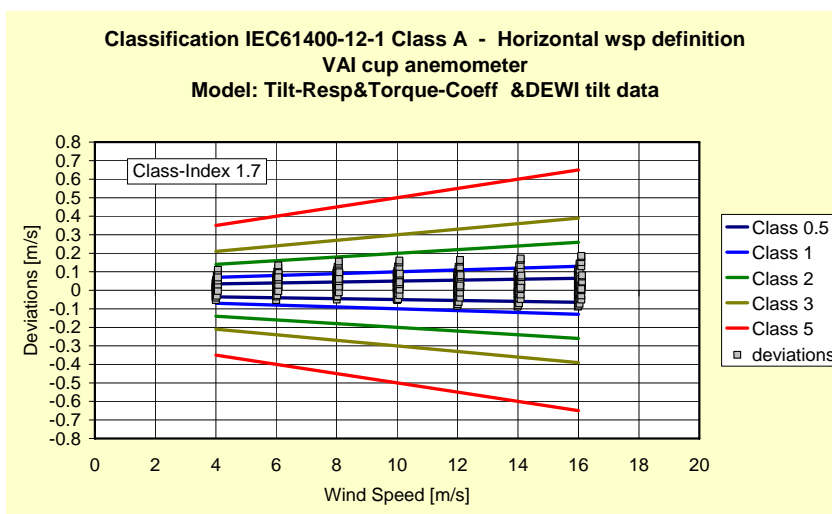


Figure 4-49 Classification of Vaisala cup anemometer with TRTC model for Class A – horizontal wind speed definition and DEWI tilt data

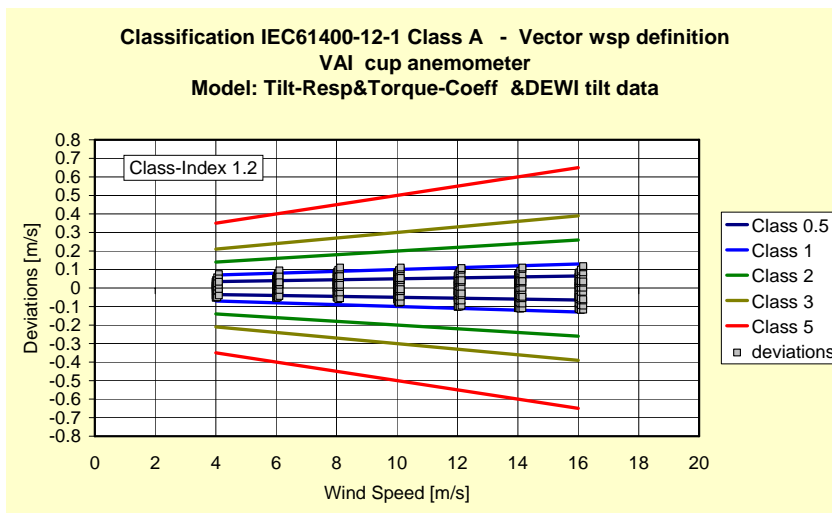


Figure 4-50 Classification of Vaisala cup anemometer with TRTC model for Class A – vector wind speed definition and DEWI tilt data

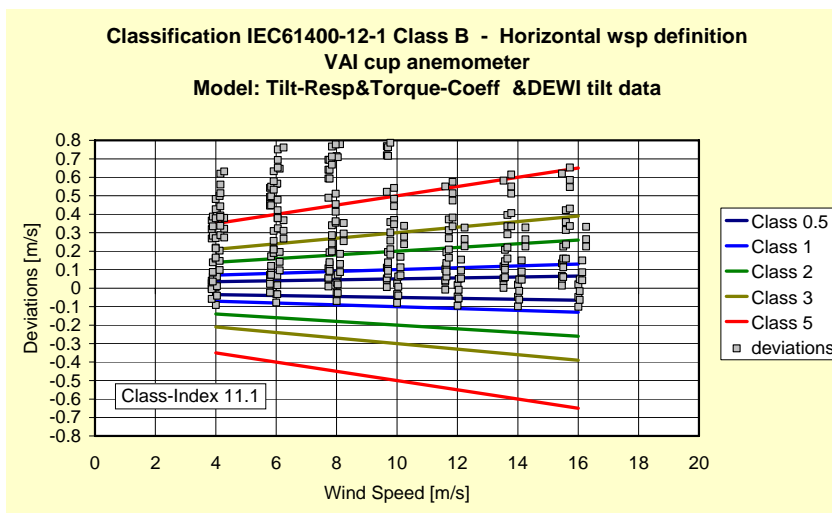


Figure 4-51 Classification of Vaisala cup anemometer with TRTC model for Class B – horizontal wind speed definition and DEWI tilt data

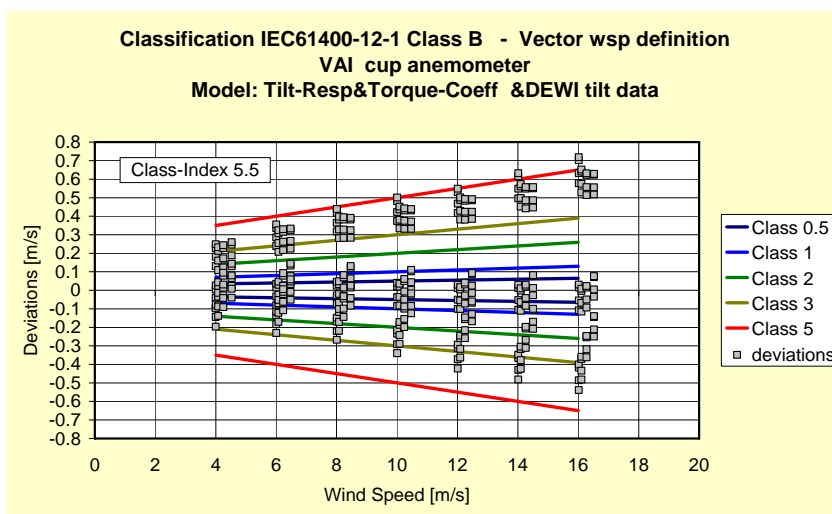


Figure 4-52 Classification of Vaisala cup anemometer with TRTC model for Class B – vector wind speed definition and DEWI tilt data

4.5.14 Classification of Vector cup anemometer

Figure 4-53 to Figure 4-56 presents simulated deviations with the TRTC model of the Vector cup anemometer with FOI angular response measurements, and Figure 4-57 to Figure 4-60 presents simulated deviations with DEWI angular response measurements.

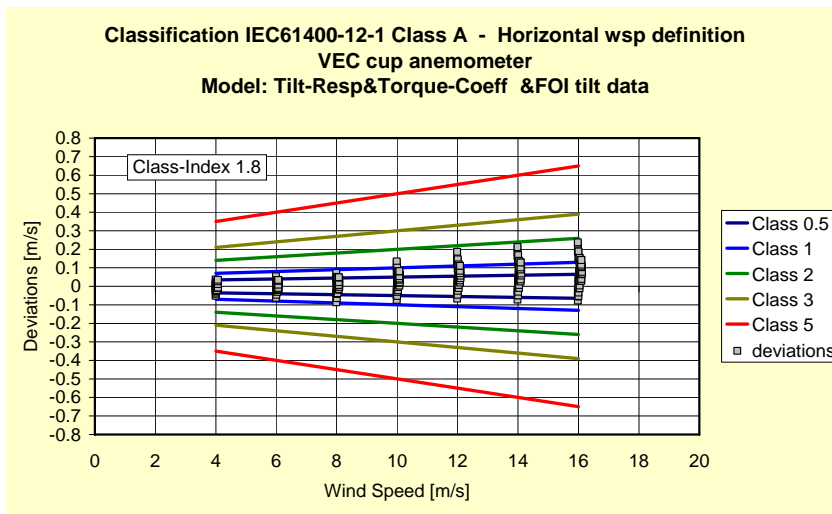


Figure 4-53 Classification of Vector cup anemometer with TRTC model for Class A – horizontal wind speed definition and FOI tilt data

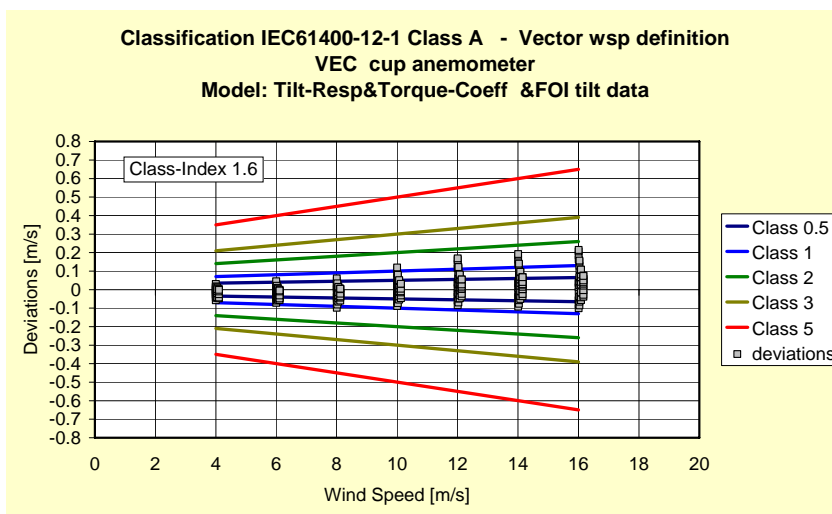


Figure 4-54 Classification of Vector cup anemometer with TRTC model for Class A – vector wind speed definition and FOI tilt data

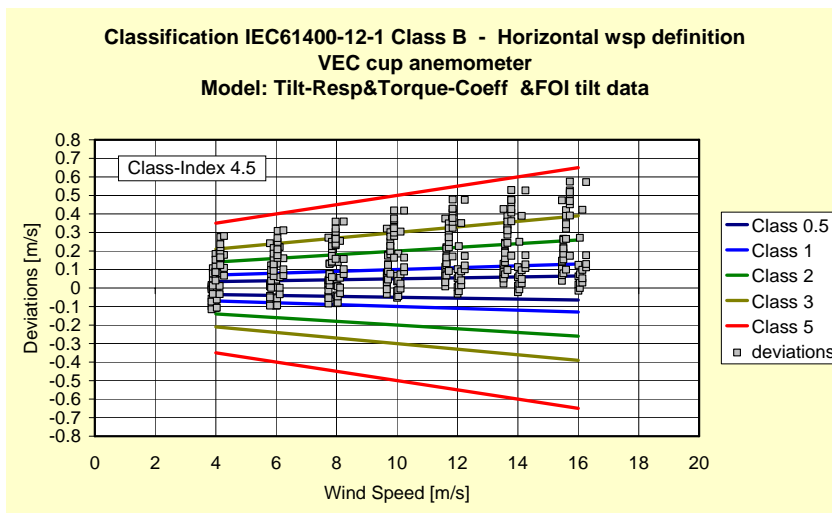


Figure 4-55 Classification of Vector cup anemometer with TRTC model for Class B – horizontal wind speed definition and FOI tilt data

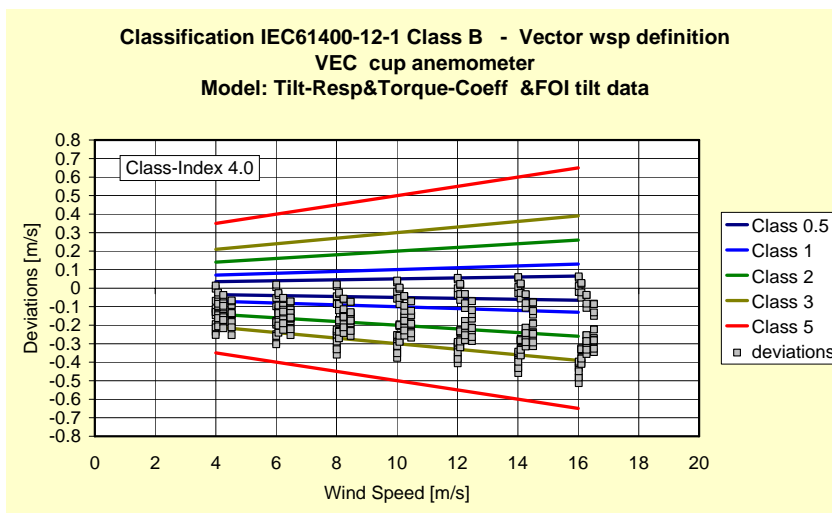


Figure 4-56 Classification of Vector cup anemometer with TRTC model for Class B – vector wind speed definition and FOI tilt data

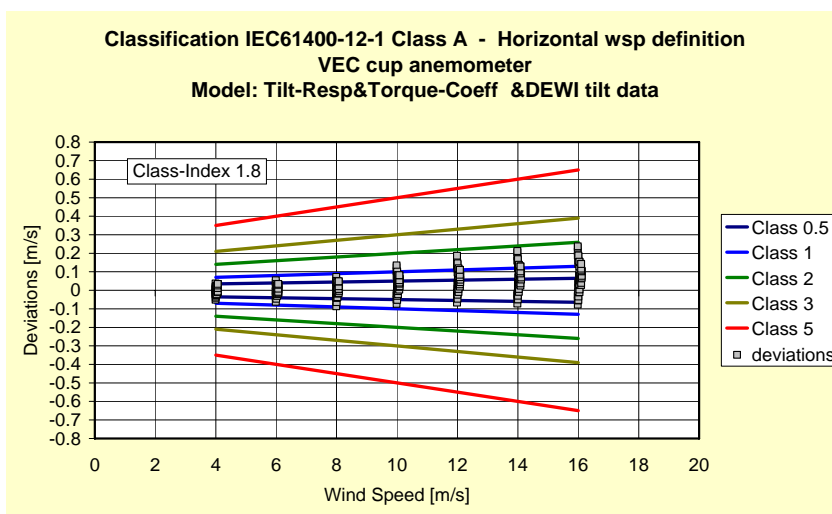


Figure 4-57 Classification of Vector cup anemometer with TRTC model for Class A – horizontal wind speed definition and DEWI tilt data

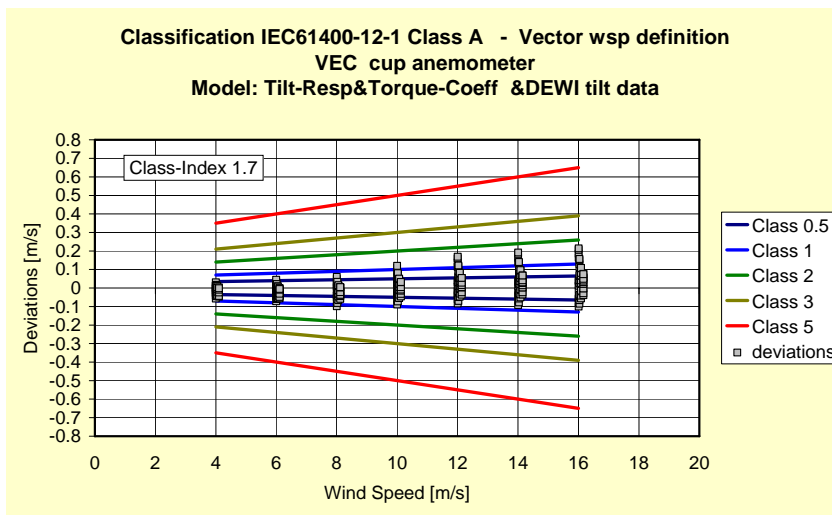


Figure 4-58 Classification of Vector cup anemometer with TRTC model for Class A – vector wind speed definition and DEWI tilt data

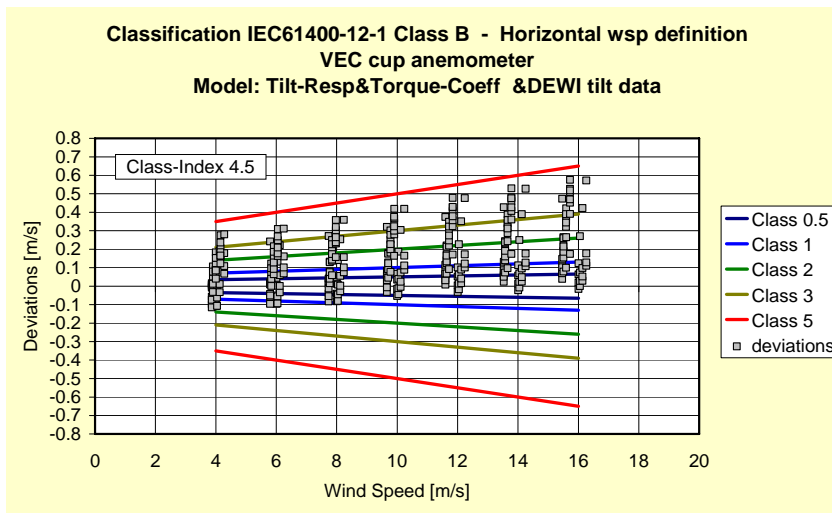


Figure 4-59 Classification of Vector cup anemometer with TRTC model for Class B – horizontal wind speed definition and DEWI tilt data

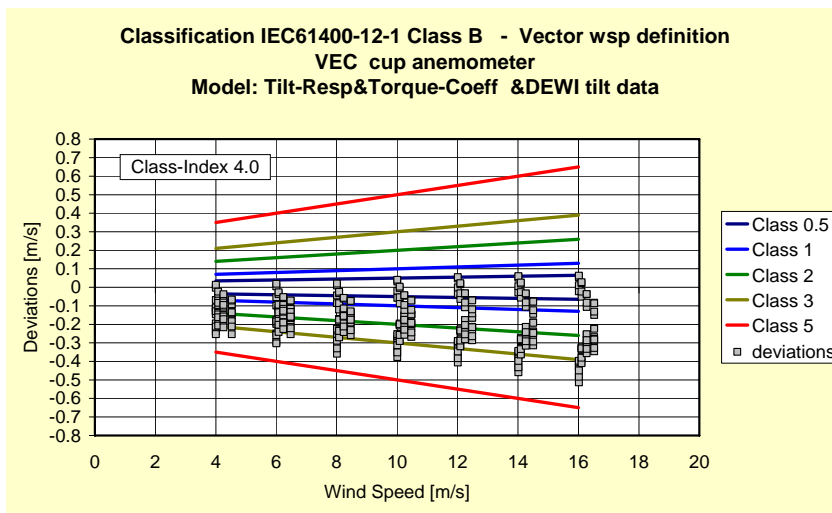


Figure 4-60 Classification of Vector cup anemometer with TRTC model for Class B – vector wind speed definition and DEWI tilt data

4.6 Classification with Tilt-Response & Torque-Coefficient Model (TRTC) without friction

The following chapters show the results of simulation of systematic deviations of the five cup anemometers with the TRTC model without influence of friction. Otherwise, all conditions are the same as in the former chapter.

4.6.15 Classification of NRG cup anemometer without influence of friction

Figure 4-61 to Figure 4-64 presents simulated deviations with the TRTC model of the NRG cup anemometer without influence of friction, and with FOI angular response measurements. Figure 4-65 to Figure 4-68 presents simulated deviations with DEWI angular response measurements.

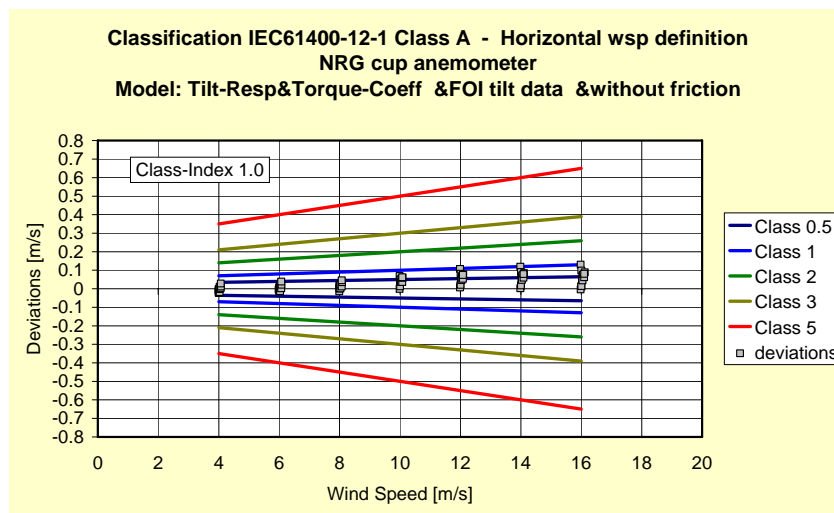


Figure 4-61 Classification of NRG cup anemometer with TRTC model for Class A – horizontal wind speed definition and FOI tilt data without influence of friction

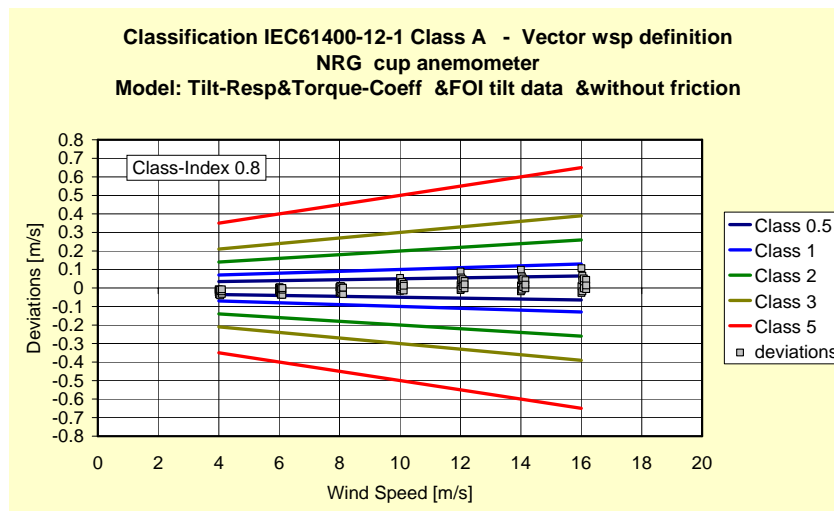


Figure 4-62 Classification of NRG cup anemometer with TRTC model for Class A – vector wind speed definition and FOI tilt data without influence of friction

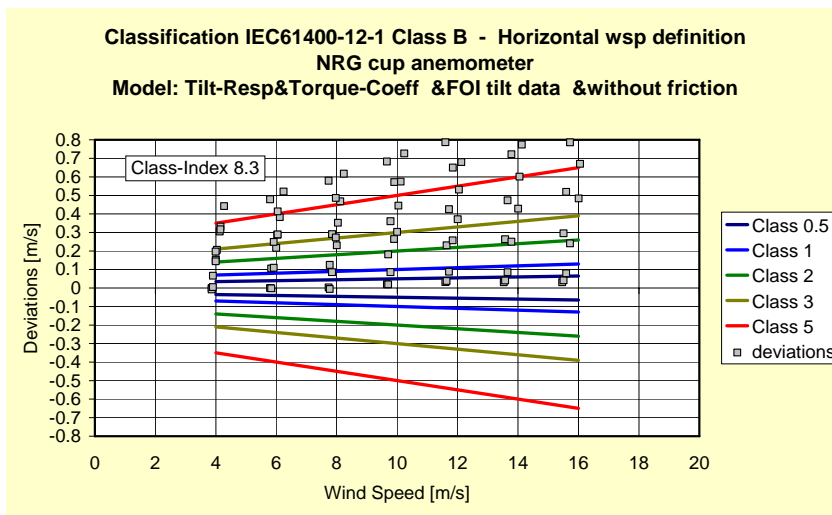


Figure 4-63 Classification of NRG cup anemometer with TRTC model for Class B – horizontal wind speed definition and FOI tilt data without influence of friction

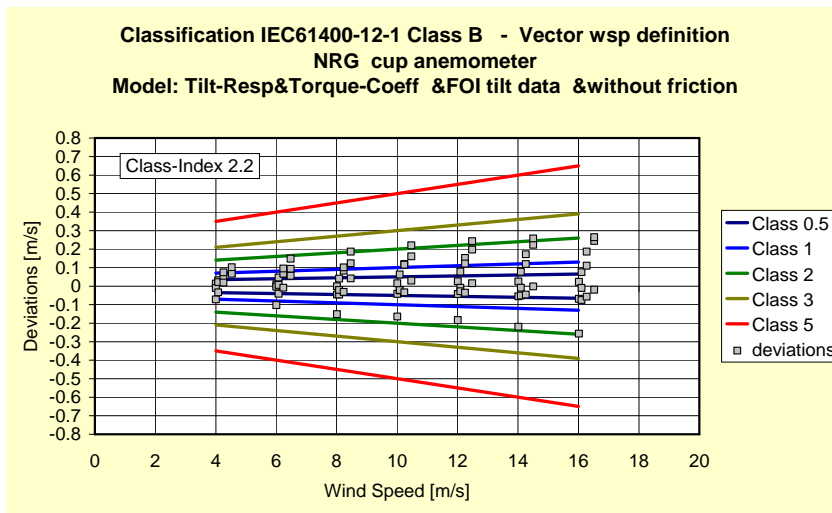


Figure 4-64 Classification of NRG cup anemometer with TRTC model for Class B – vector wind speed definition and FOI tilt data without influence of friction

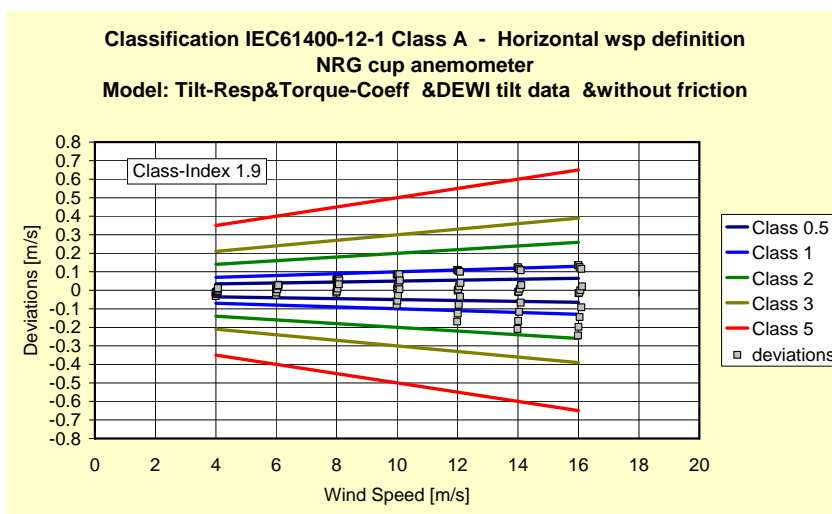


Figure 4-65 Classification of NRG cup anemometer with TRTC model for Class A – horizontal wind speed definition and DEWI tilt data without influence of friction

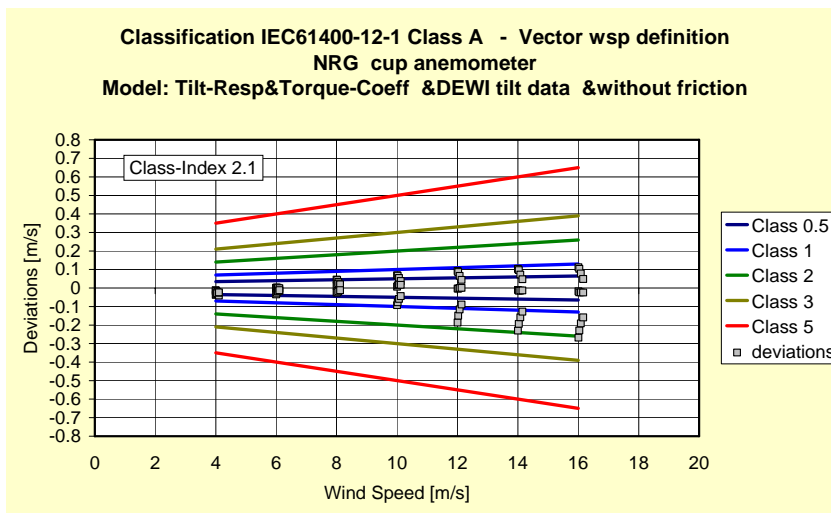


Figure 4-66 Classification of NRG cup anemometer with TRTC model for Class A – vector wind speed definition and DEWI tilt data without influence of friction

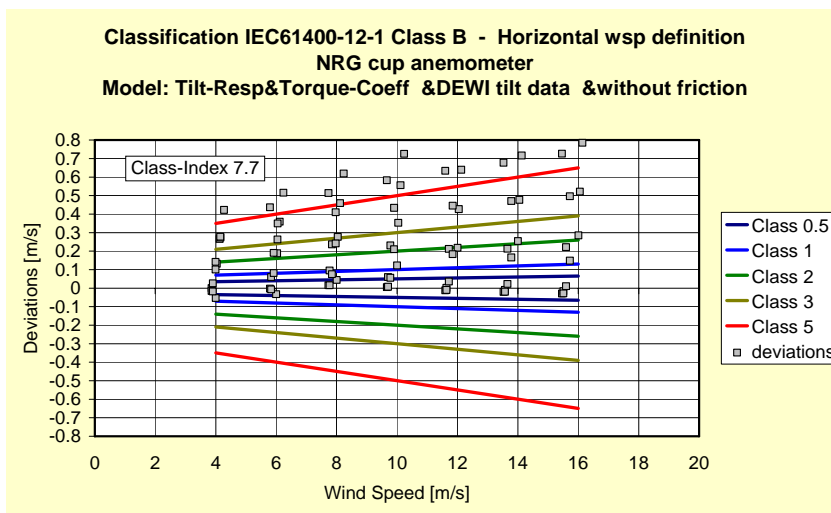


Figure 4-67 Classification of NRG cup anemometer with TRTC model for Class B – horizontal wind speed definition and DEWI tilt data without influence of friction

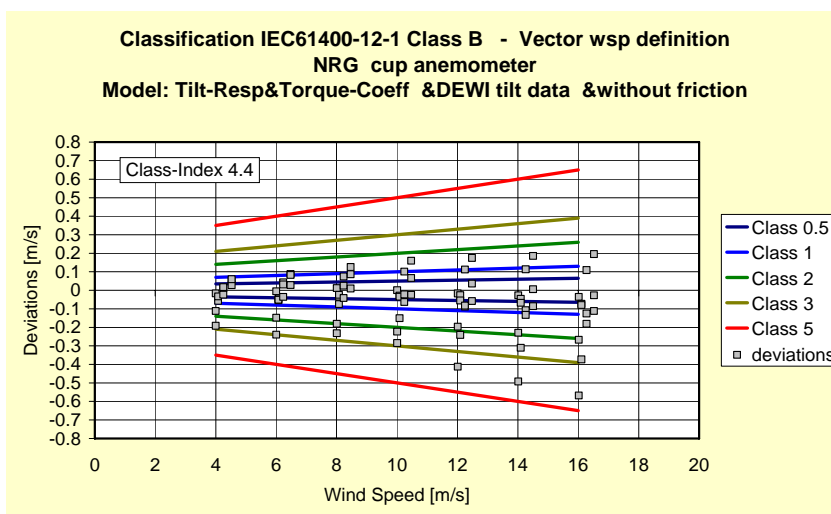


Figure 4-68 Classification of NRG cup anemometer with TRTC model for Class B – vector wind speed definition and DEWI tilt data without influence of friction

4.6.16 Classification of Risø cup anemometer without influence of friction

Figure 4-69 to Figure 4-72 presents simulated deviations with the TRTC model of the Risø cup anemometer without influence of friction and with FOI angular response measurements. Figure 4-73 to Figure 4-76 presents simulated deviations with DEWI angular response measurements.

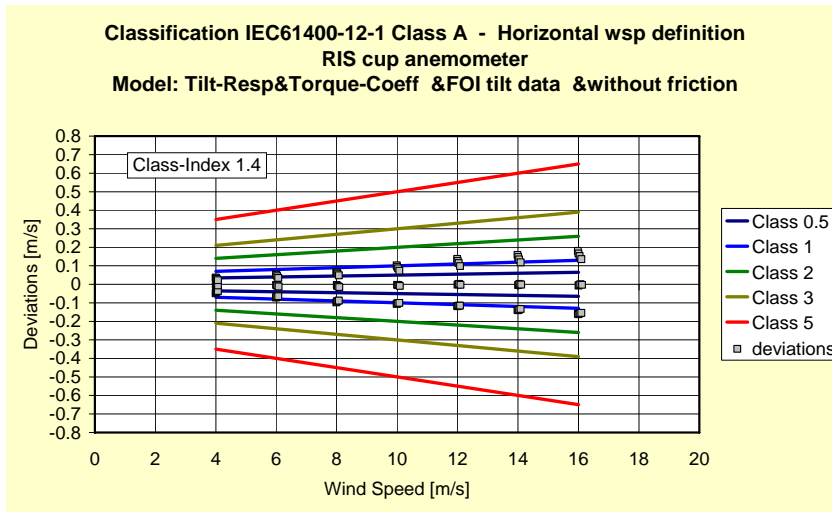


Figure 4-69 Classification of Risø cup anemometer with TRTC model for Class A – horizontal wind speed definition and FOI tilt data without influence of friction

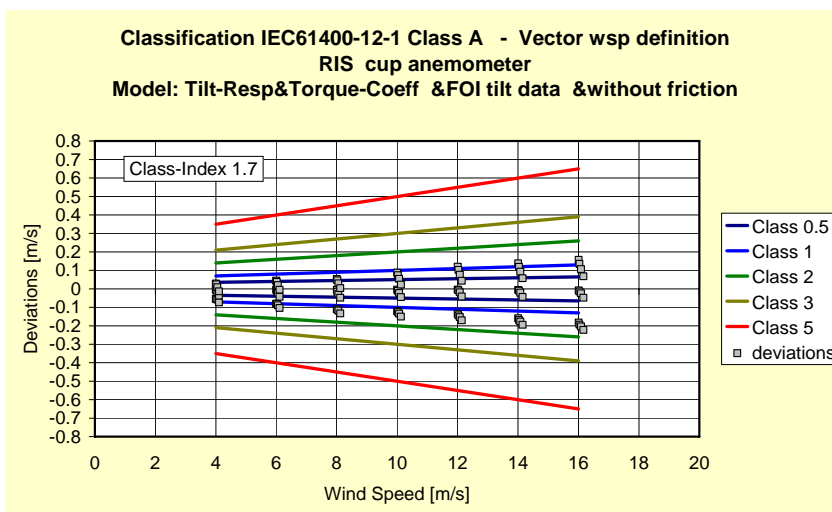


Figure 4-70 Classification of Risø cup anemometer with TRTC model for Class A – vector wind speed definition and FOI tilt data without influence of friction

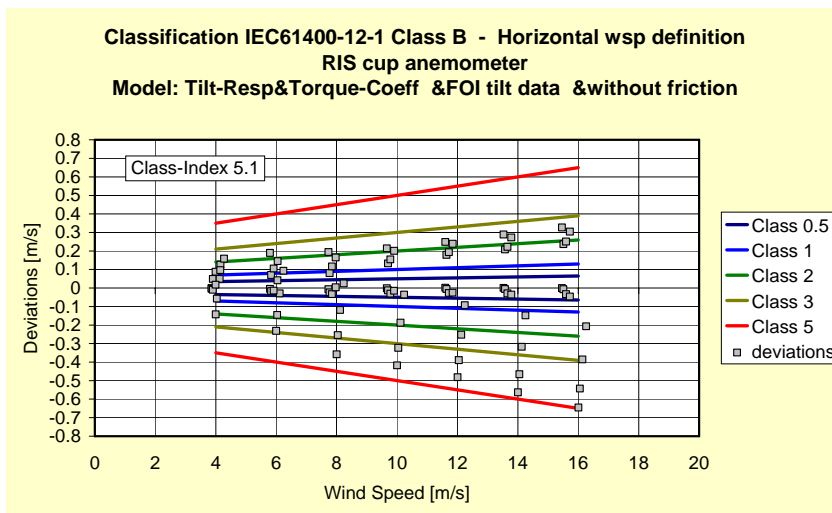


Figure 4-71 Classification of Risø cup anemometer with TRTC model for Class B – horizontal wind speed definition and FOI tilt data without influence of friction

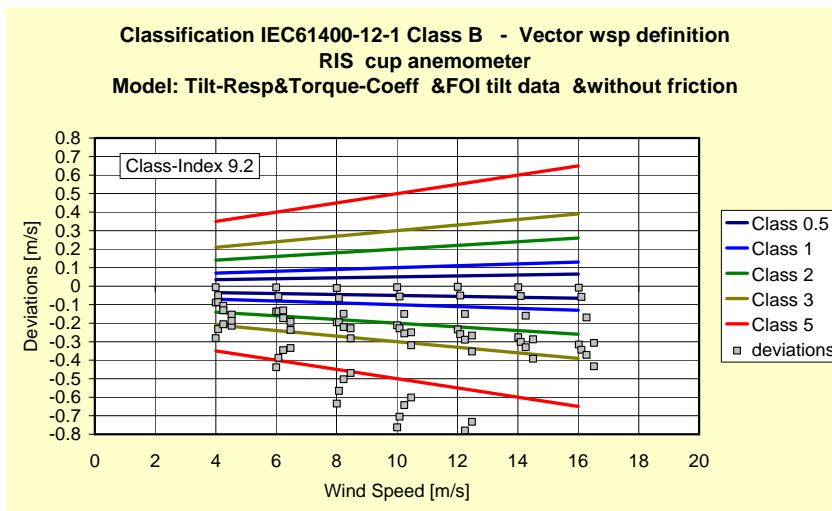


Figure 4-72 Classification of Risø cup anemometer with TRTC model for Class B – vector wind speed definition and FOI tilt data without influence of friction

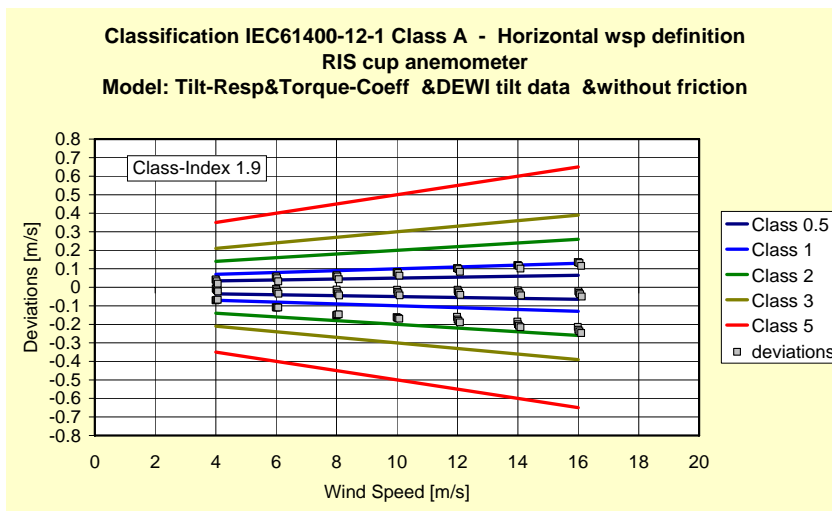


Figure 4-73 Classification of Risø cup anemometer with TRTC model for Class A – horizontal wind speed definition and DEWI tilt data without influence of friction

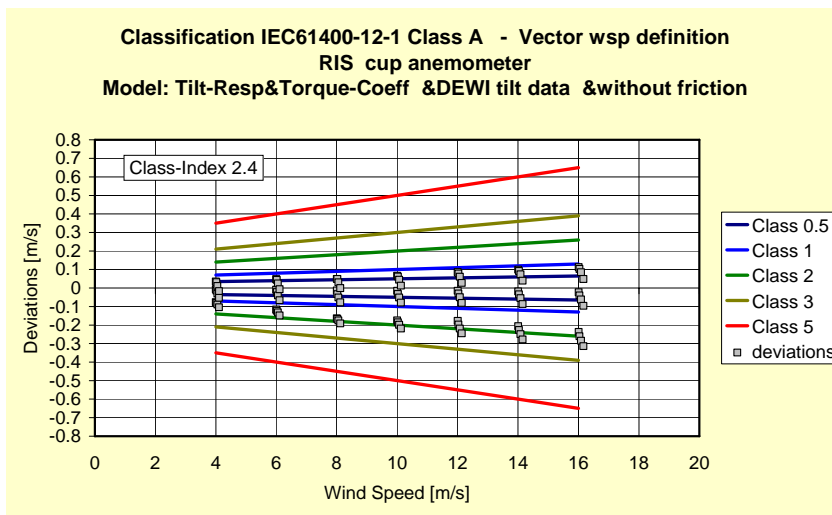


Figure 4-74 Classification of Risø cup anemometer with TRTC model for Class A – vector wind speed definition and DEWI tilt data without influence of friction

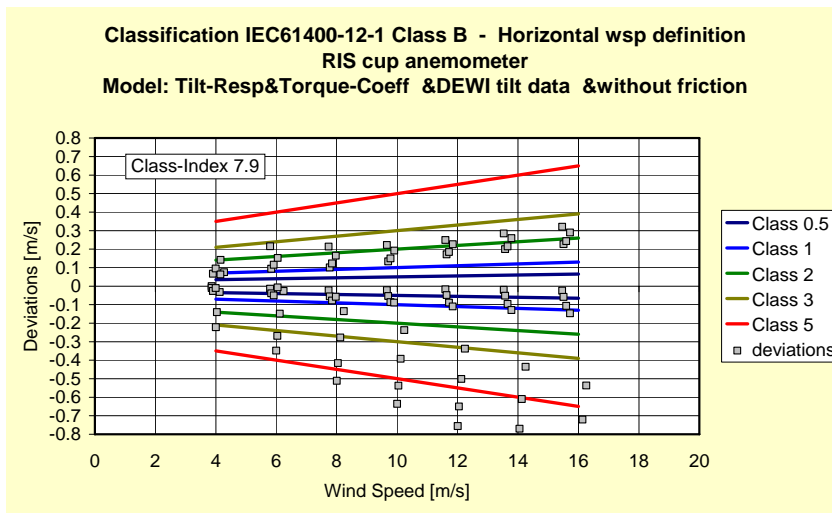


Figure 4-75 Classification of Risø cup anemometer with TRTC model for Class B – horizontal wind speed definition and DEWI tilt data without influence of friction

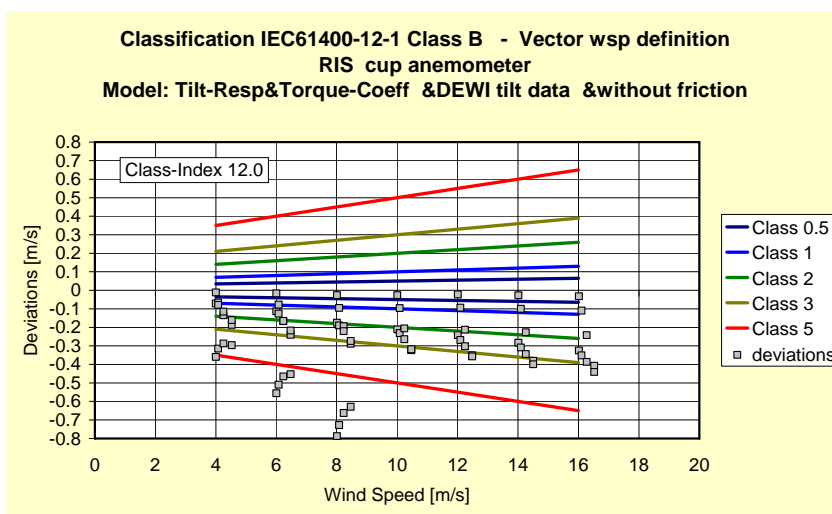


Figure 4-76 Classification of Risø cup anemometer with TRTC model for Class B – vector wind speed definition and DEWI tilt data without influence of friction

4.6.17 Classification of Thies FC cup anemometer without influence of friction

Figure 4-77 to Figure 4-80 presents simulated deviations with the TRTC model of the Thies FC cup anemometer without influence of friction and with FOI angular response measurements. Figure 4-81 to Figure 4-84 presents simulated deviations with DEWI angular response measurements.

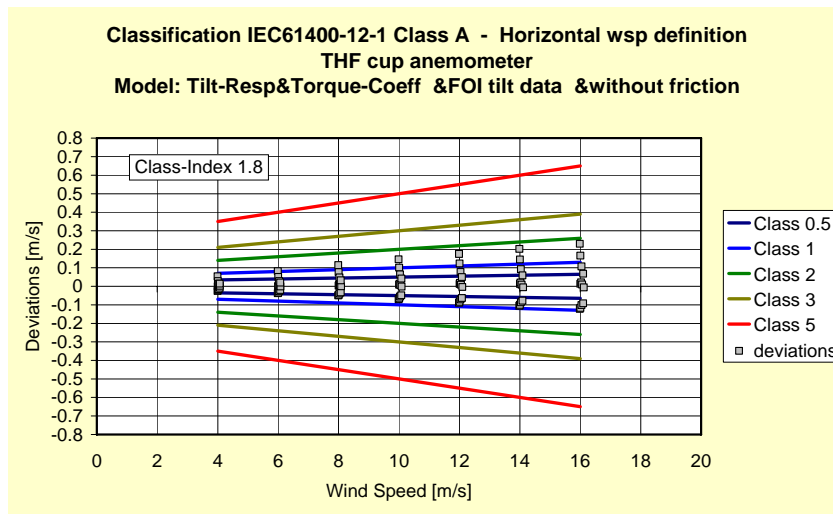


Figure 4-77 Classification of Thies FC cup anemometer with TRTC model for Class A – horizontal wind speed definition and FOI tilt data without influence of friction

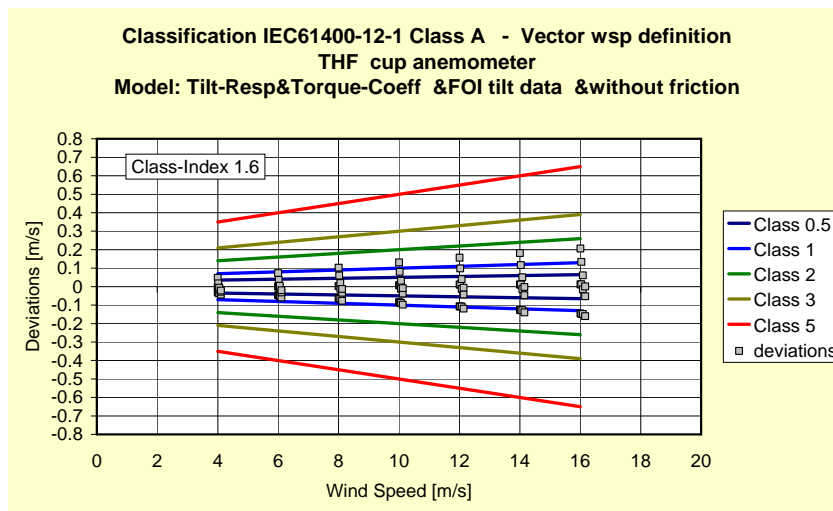


Figure 4-78 Classification of Thies FC cup anemometer with TRTC model for Class A – vector wind speed definition and FOI tilt data without influence of friction

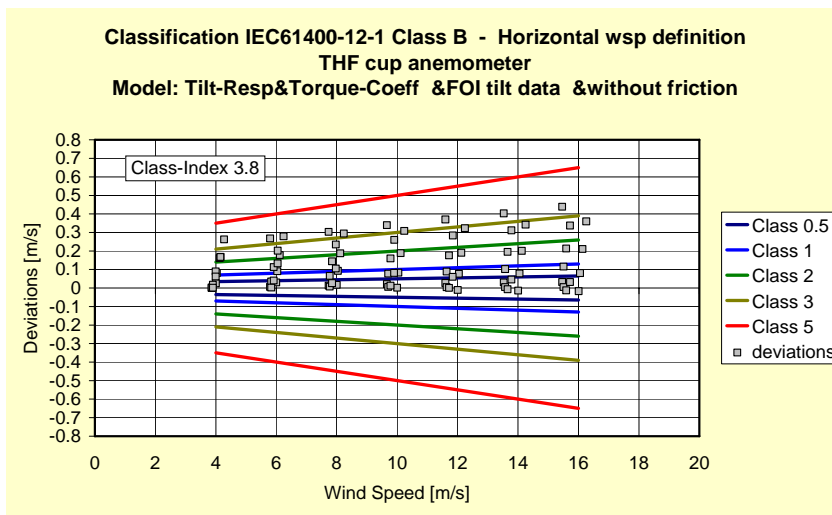


Figure 4-79 Classification of Thies FC cup anemometer with TRTC model Class B – horizontal wind speed definition and FOI tilt data without influence of friction

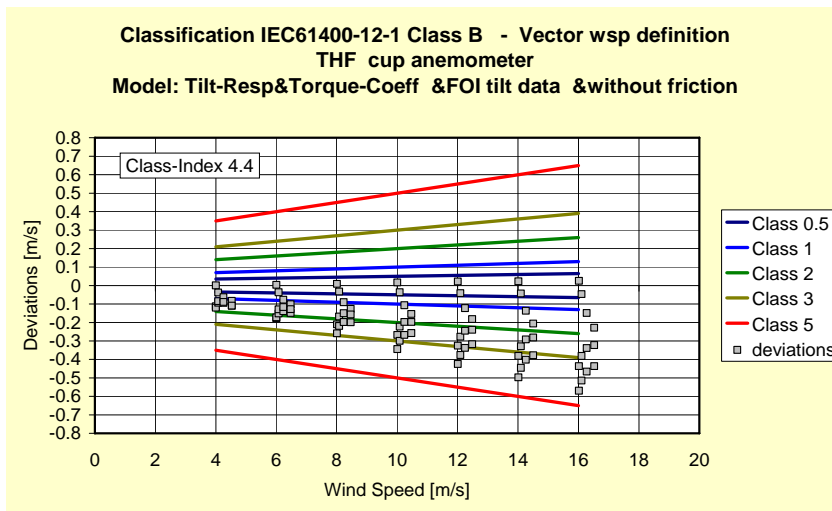


Figure 4-80 Classification of Thies FC cup anemometer with TRTC model Class B – vector wind speed definition and FOI tilt data without influence of friction

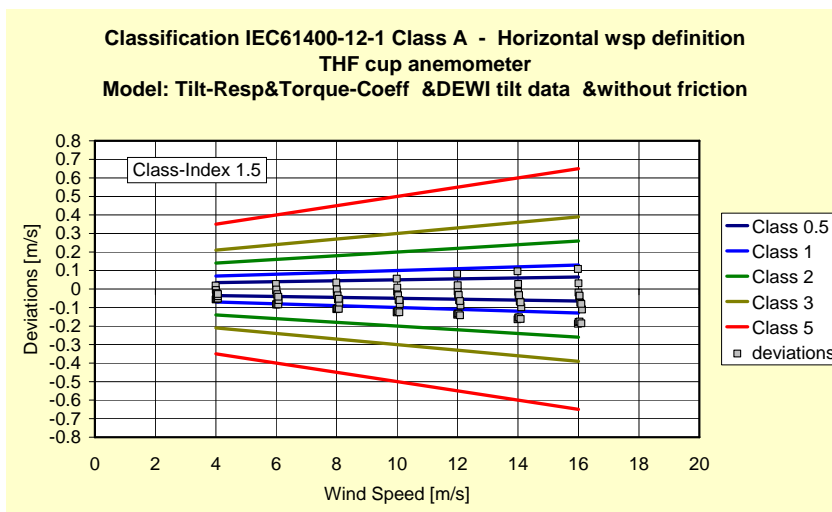


Figure 4-81 Classification of Thies FC cup anemometer with TRTC model Class A – horizontal wind speed definition and DEWI tilt data without influence of friction

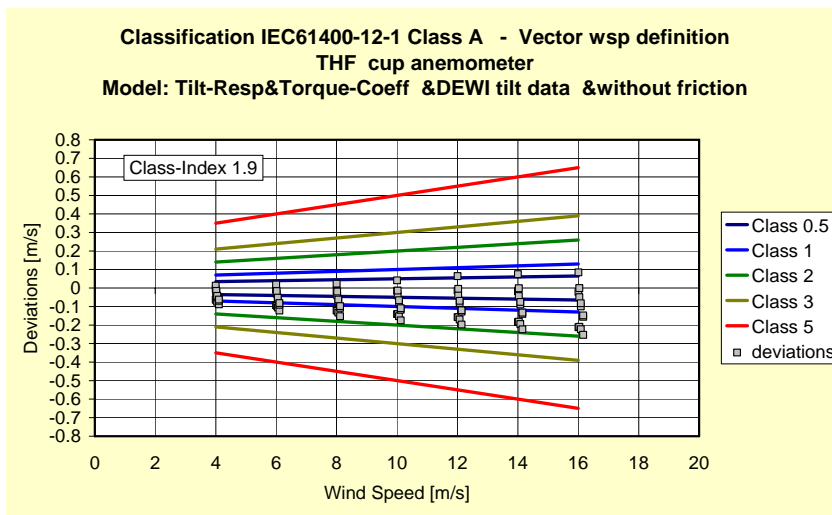


Figure 4-82 Classification of Thies FC cup anemometer with TRTC model Class A – vector wind speed definition and DEWI tilt data without influence of friction

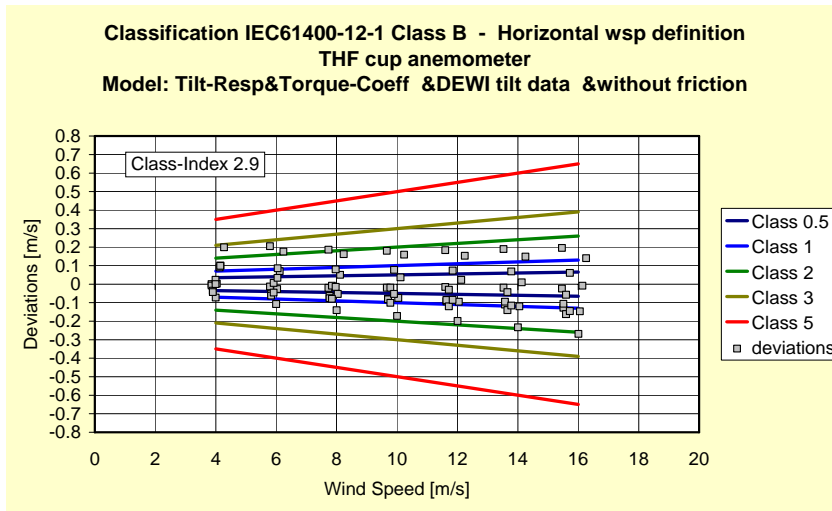


Figure 4-83 Classification of Thies FC cup anemometer with TRTC model Class B – horizontal wind speed definition and DEWI tilt data without influence of friction

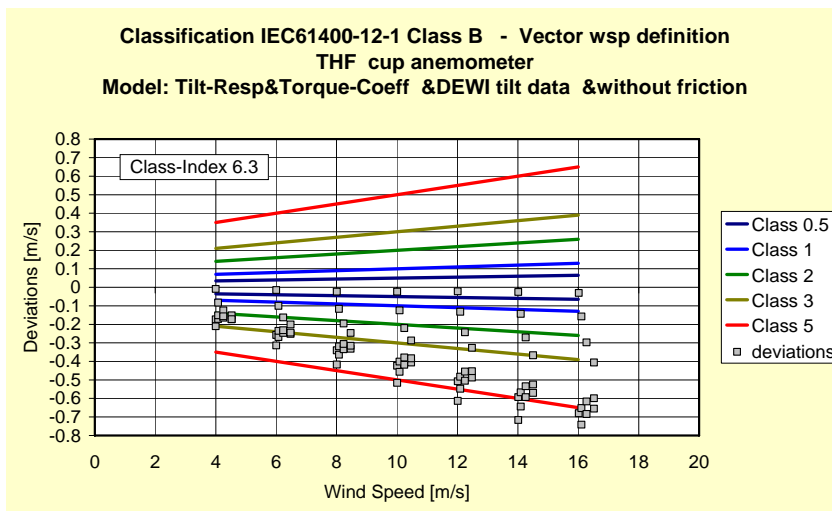


Figure 4-84 Classification of Thies FC cup anemometer with TRTC model Class B – vector wind speed definition and DEWI tilt data without influence of friction

4.6.18 Classification of Vaisala cup anemometer without influence of friction

Figure 4-85 to Figure 4-88 presents simulated deviations with the TRTC model of the Vaisala cup anemometer without influence of friction and with FOI angular response measurements. Figure 4-89 to Figure 4-92 presents simulated deviations with DEWI angular response measurements.

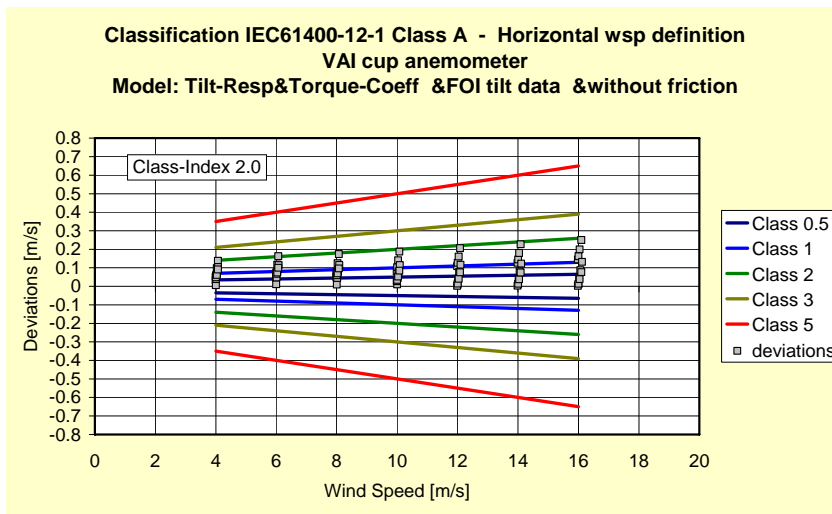


Figure 4-85 Classification of Vaisala cup anemometer with TRTC model for Class A – horizontal wind speed definition and FOI tilt data without influence of friction

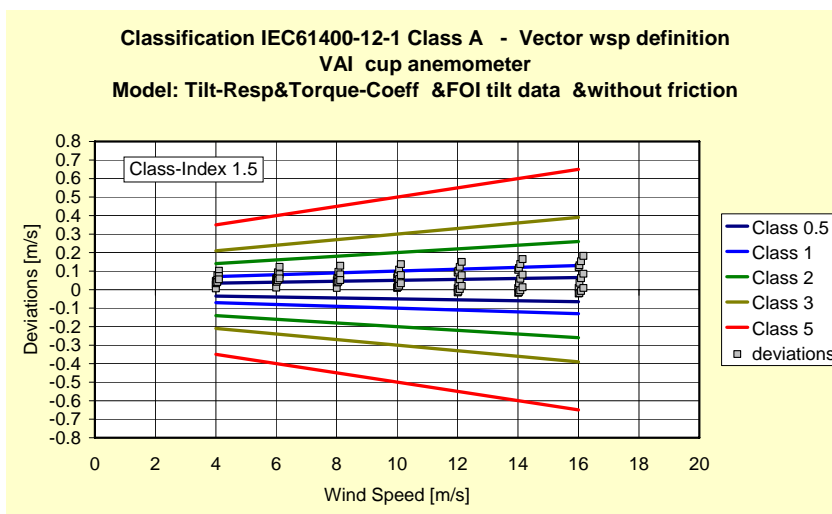


Figure 4-86 Classification of Vaisala cup anemometer with TRTC model for Class A – vector wind speed definition and FOI tilt data without influence of friction

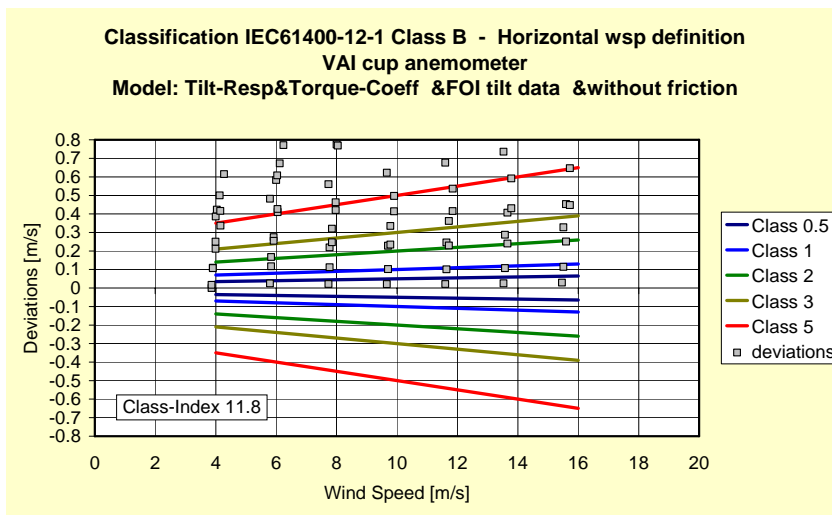


Figure 4-87 Classification of Vaisala cup anemometer with TRTC model for Class B – horizontal wind speed definition and FOI tilt data without influence of friction

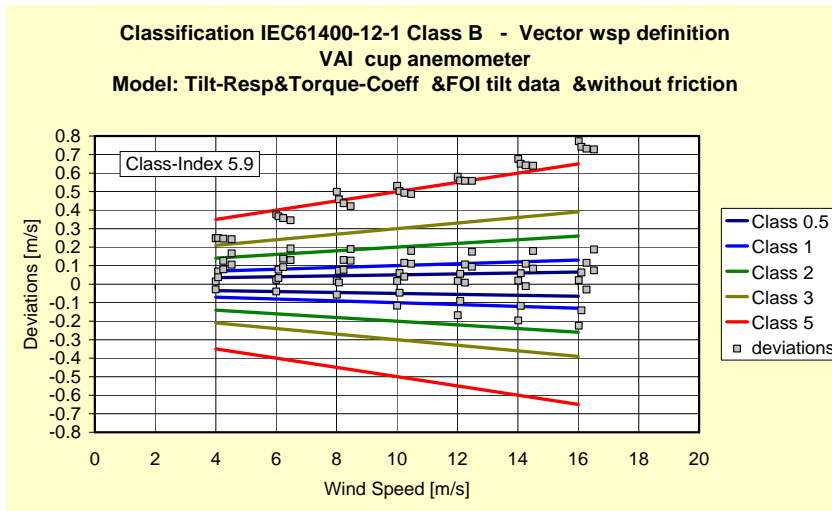


Figure 4-88 Classification of Vaisala cup anemometer with TRTC model for Class B – vector wind speed definition and FOI tilt data without influence of friction

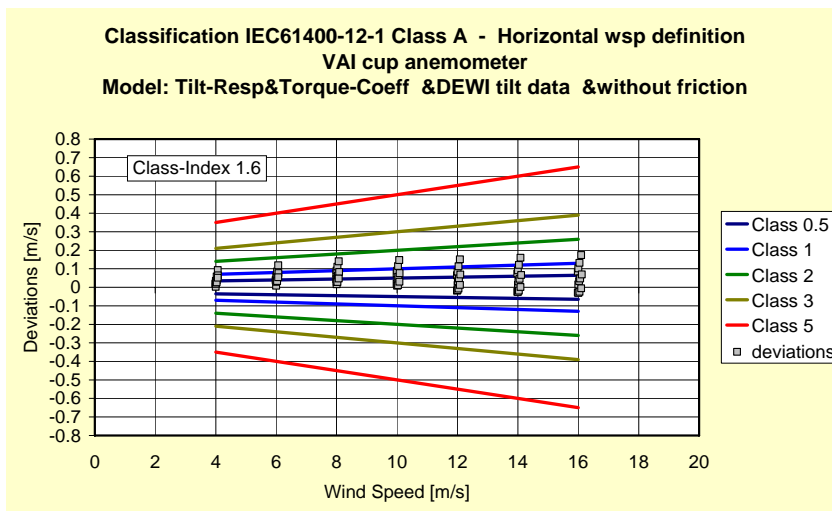


Figure 4-89 Classification of Vaisala cup anemometer with TRTC model for Class A – horizontal wind speed definition and DEWI tilt data without influence of friction

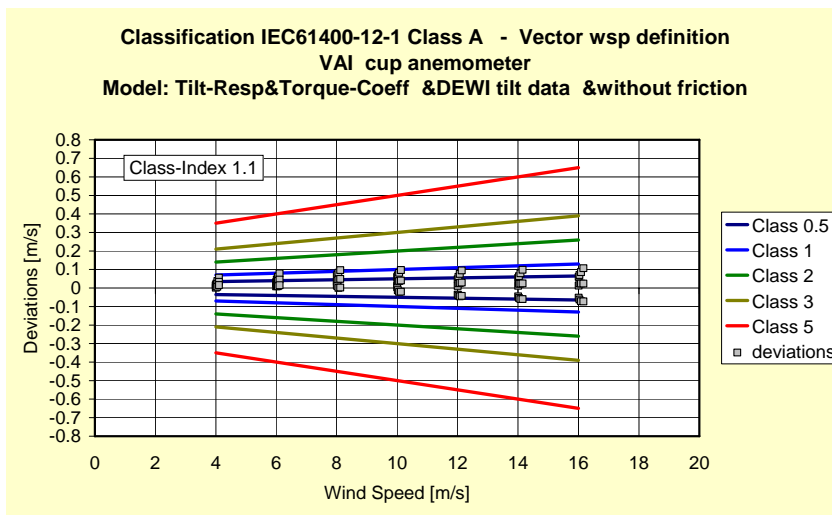


Figure 4-90 Classification of Vaisala cup anemometer with TRTC model for Class A – vector wind speed definition and DEWI tilt data without influence of friction

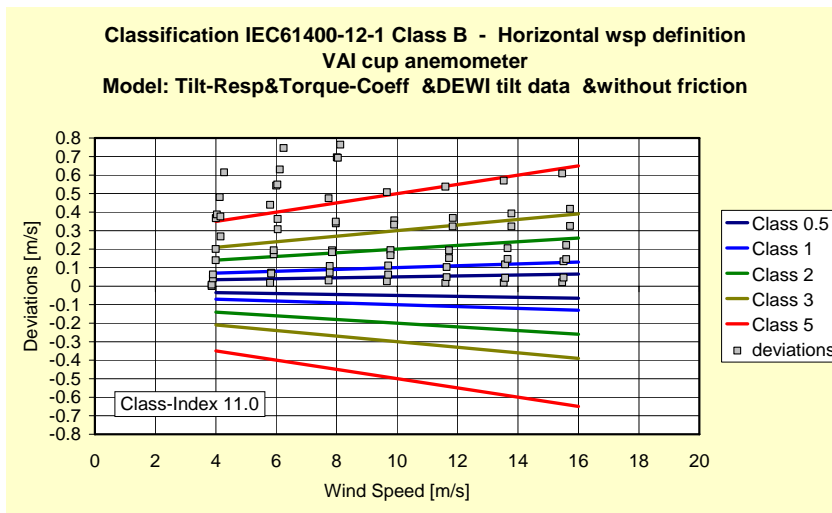


Figure 4-91 Classification of Vaisala cup anemometer with TRTC model for Class B – horizontal wind speed definition and DEWI tilt data without influence of friction

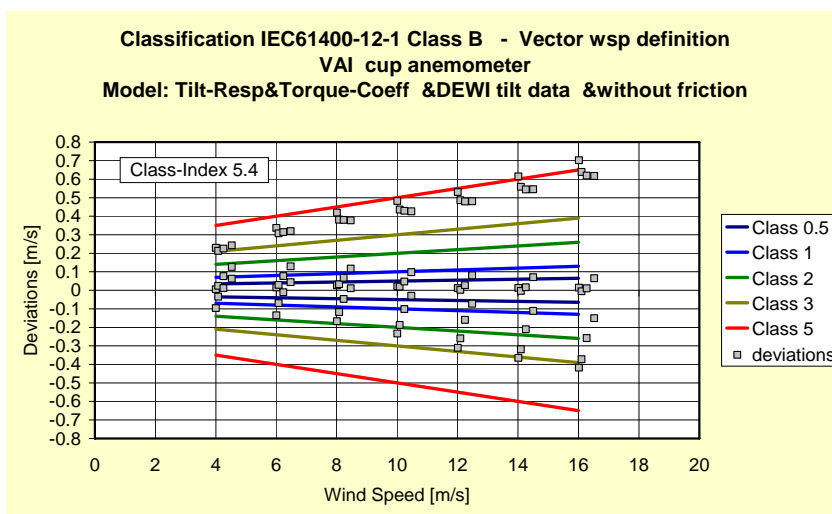


Figure 4-92 Classification of Vaisala cup anemometer with TRTC model for Class B – vector wind speed definition and DEWI tilt data without influence of friction

4.6.19 Classification of Vector cup anemometer without influence of friction

Figure 4-93 to Figure 4-96 presents simulated deviations with the TRTC model of the Vector cup anemometer without influence of friction and with FOI angular response measurements. Figure 4-97 to Figure 4-100 presents simulated deviations with DEWI angular response measurements.

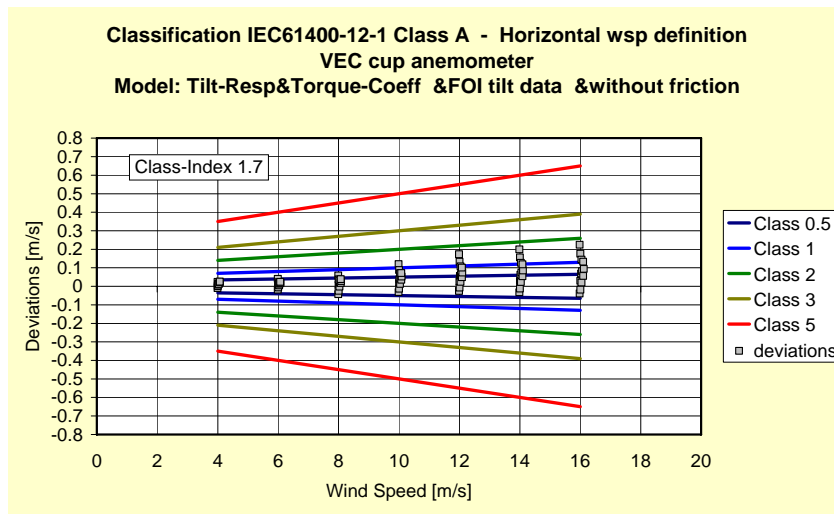


Figure 4-93 Classification of Vector cup anemometer with TRTC model for Class A – horizontal wind speed definition and FOI tilt data without influence of friction

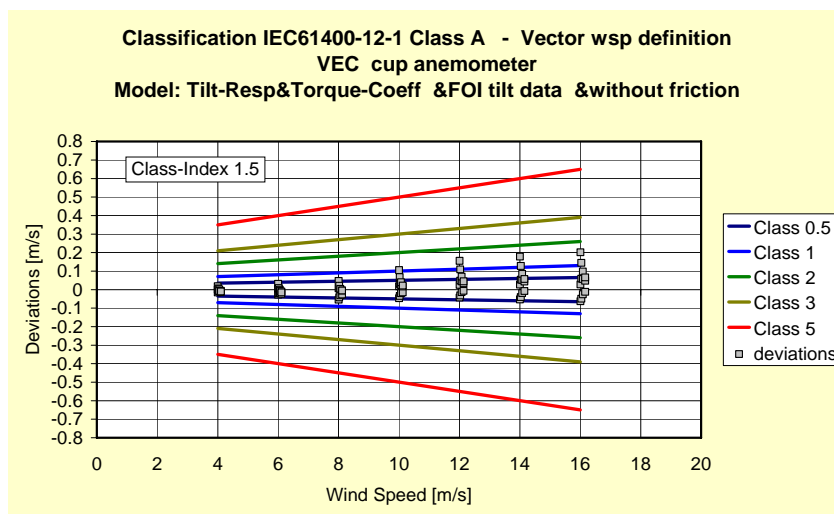


Figure 4-94 Classification of Vector cup anemometer with TRTC model for Class A – vector wind speed definition and FOI tilt data without influence of friction

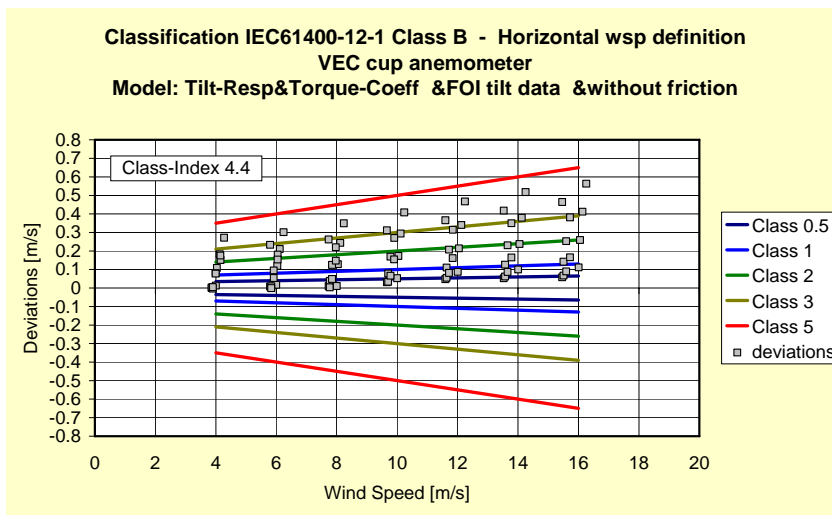


Figure 4-95 Classification of Vector cup anemometer with TRTC model for Class B – horizontal wind speed definition and FOI tilt data without influence of friction

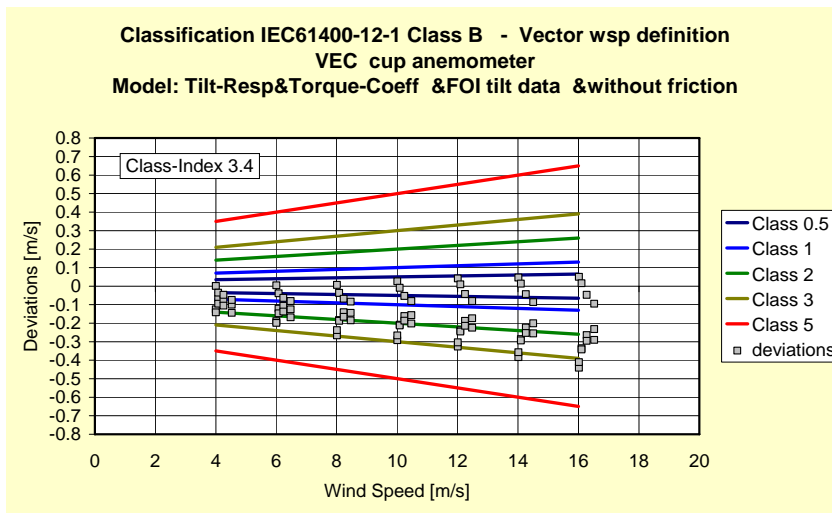


Figure 4-96 Classification of Vector cup anemometer with TRTC model for Class B – vector wind speed definition and FOI tilt data without influence of friction

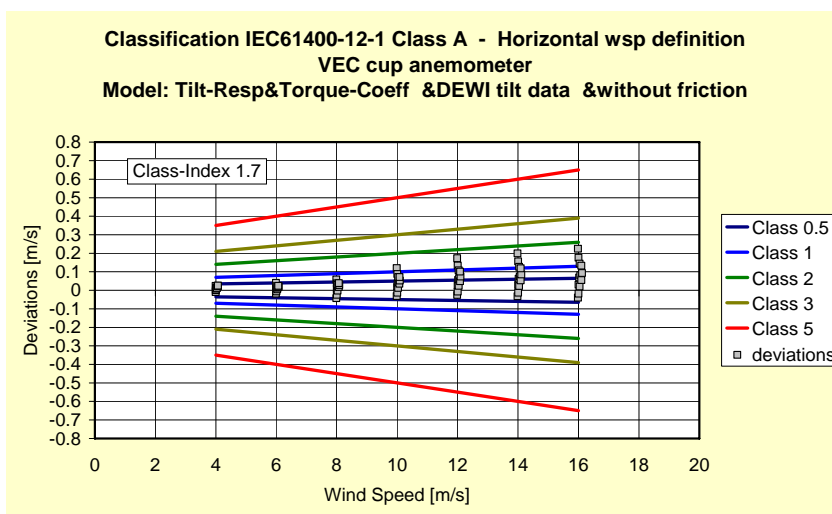


Figure 4-97 Classification of Vector cup anemometer with TRTC model for Class A – horizontal wind speed definition and DEWI tilt data without influence of friction

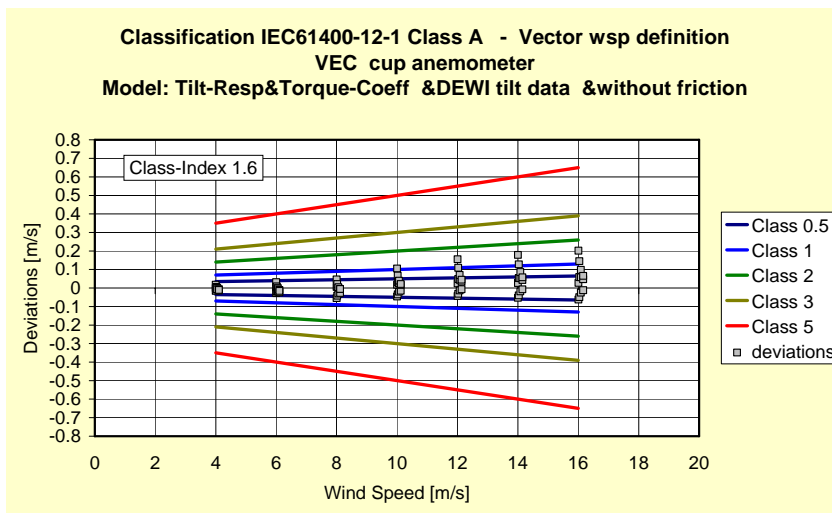


Figure 4-98 Classification of Vector cup anemometer with TRTC model for Class A – vector wind speed definition and DEWI tilt data without influence of friction

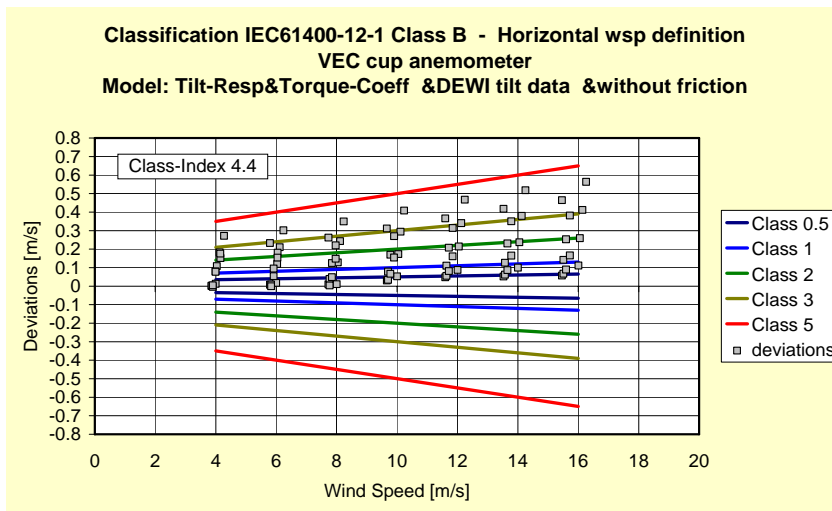


Figure 4-99 Classification of Vector cup anemometer with TRTC model for Class B – horizontal wind speed definition and DEWI tilt data without influence of friction

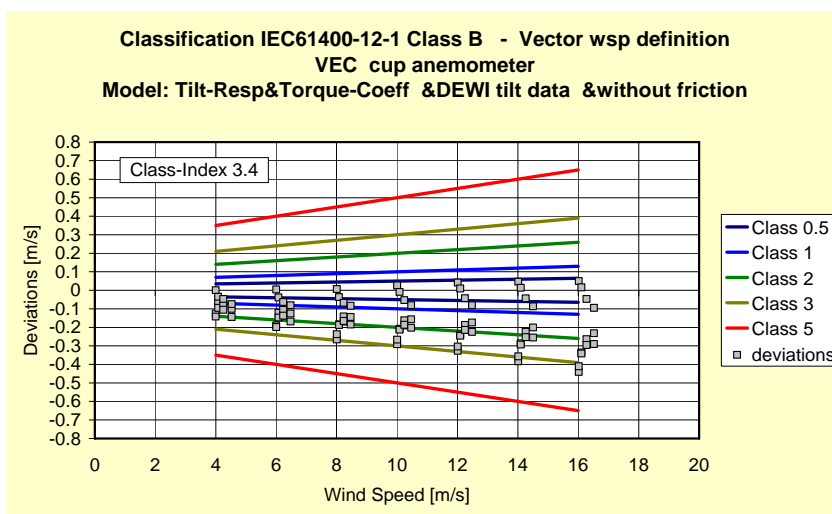


Figure 4-100 Classification of Vector cup anemometer with TRTC model for Class B – vector wind speed definition and DEWI tilt data without influence of friction

4.7 Comparison of Data

Table 4-2 to Table 4-6 summarize the classification indices by the use of the two cup anemometer models IFTC and TRTC.

Table 4-2 Classification of five cup anemometers according to IEC51400-12-1 using the IFTC model (without influence of friction)

Classification IEC61400-12-1 Model: Inclined-Flow-Torque-Coefficient (IFTC)				
	Horizontal wsp definition		Vector wsp definition	
Cup anemometer	Class A	Class B	Class A	Class B
NRG max 40	0.6	7.5	0.5	2.6
Risø P2546	1.3	5.0	1.7	9.2
Thies FC	2.0	3.6	2.1	5.1
Vaisala WAA151	2.4	11.9	2.0	6.6
Vector L100	1.3	4.0	1.1	3.6

Table 4-3 Classification of five cup anemometers according to IEC51400-12-1 using the TRTC model with FOI tilt data and with influence of friction

Classification IEC61400-12-1 Model: TRTC +FOI tilt response +with friction				
	Horizontal wsp definition		Vector wsp definition	
Cup anemometer	Class A	Class B	Class A	Class B
NRG max 40	2.4	8.3	2.7	3.0
Risø P2546	1.4	5.1	1.7	9.2
Thies FC	1.8	3.8	1.6	4.4
Vaisala WAA151	2.2	11.9	1.7	6.1
Vector L100	1.8	4.5	1.6	4.0

Table 4-4 Classification of five cup anemometers according to IEC51400-12-1 using the TRTC model with FOI tilt data and without influence of friction

Classification IEC61400-12-1 Model: TRTC +FOI tilt response +without friction				
	Horizontal wsp definition		Vector wsp definition	
Cup anemometer	Class A	Class B	Class A	Class B
NRG max 40	1.0	8.3	0.8	2.2
Risø P2546	1.4	5.1	1.7	9.2
Thies FC	1.8	3.8	1.6	4.4
Vaisala WAA151	2.0	11.8	1.5	5.9
Vector L100	1.7	4.4	1.5	3.4

Table 4-5 Classification of five cup anemometers according to IEC51400-12-1 using the TRTC model with DEWI tilt data and with influence of friction

Classification IEC61400-12-1				
Model: TRTC +DEWI tilt response +with friction				
	Horizontal wsp definition		Vector wsp definition	
Cup anemometer	Class A	Class B	Class A	Class B
NRG max 40	2.4	7.7	2.8	4.8
Risø P2546	1.9	8.0	2.4	12.0
Thies FC	1.5	2.9	1.9	6.3
Vaisala WAA151	1.7	11.1	1.2	5.5
Vector L100	1.8	4.5	1.7	4.0

Table 4-6 Classification of five cup anemometers according to IEC51400-12-1 using the TRTC model with DEWI tilt data and without influence of friction

Classification IEC61400-12-1				
Model: TRTC +DEWI tilt response +without friction				
	Horizontal wsp definition		Vector wsp definition	
Cup anemometer	Class A	Class B	Class A	Class B
NRG max 40	1.9	7.7	2.1	4.4
Risø P2546	1.9	7.9	2.4	12.0
Thies FC	1.5	2.9	1.9	6.3
Vaisala WAA151	1.6	11.0	1.1	5.4
Vector L100	1.7	4.4	1.6	3.4

Comparison regarding torque coefficient data

Torque coefficient data are varied in the simulations with use of the IFTC model, Table 4-2, and the TRTC model without friction, Table 4-4. Comparing only the FOI data, it is seen that for horizontal wind speed definition the IFTC model predicts lower class indices. For NRG, VAI and VEC the difference in Class A is 0.4, while for THF it is 0.2 and for RIS only 0.1. For Class B the difference is 0.8 for NRG, 0.4 for VEC, 0.2 for THF and 0.1 for RIS and VAI.

Comparison regarding angular response variations

Angular response data are varied in the simulations with the TRTC model using data from FOI or DEWI tilt tests. Looking at the data that includes influence of friction, shown in Table 4-3 and Table 4-5, and for horizontal wind speed definition, it is seen that the class indices changes individually for each cup anemometer. Same class indices are seen for the VEC anemometer and for NRG Class A, while for the RIS the class index increases with 0.5 for Class A and 2.9 for Class B going from FOI to DEWI tilt data. The THF goes down with 0.3 for Class A and 0.9 for Class B. The VAI goes down with 0.5 for Class A and 0.8 for Class B.

Comparison regarding friction

Simulations with the TRTC model with or without inclusion of friction are shown in Table 4-3 and Table 4-4 for FOI angular response data. It is seen that influence of friction does not seem to change the class indices of the Risø and Thies FC cup anemometers. The VAI and VEC cup anemometer changes 0.1-0.2 when friction influ-

ence is included, and the NRG changes 0.4-0.5. It should be noted, though, that the friction measured on the NRG varies quite a bit 40°C, and this explains the difference, see [1].

5 Conclusions

Five cup anemometers have been assessed and analysed for torque characteristics, angular response characteristics and friction. The measured characteristics have been fitted to two different cup anemometer models, the IFTC and TRTC models, which are presented in detail in [1]. Model calculations were used to simulate responses of free field operational conditions and to determine systematic deviations from normal calibration data. The results are shown in graphs of systematic deviations, according to classification of cup anemometer, annex I and J of the IEC standard on power performance measurements [3].

The results of the classification according to the horizontal wind speed definition of the NRG cup anemometer in Class A was 0.6-2.4, and in Class B 7.5-8.3. Classification of the Risø cup anemometer in Class A was 1.3-1.9, and in Class B 5.0-8.0. Classification of the Thies FC in Class A was 1.5-1.8, and in Class B 2.9-3.8. Classification of the Vaisala cup anemometer in Class A was 1.6-2.4, and in Class B 11.0-11.9. Classification of the Vector cup anemometer in Class A was 1.3-1.8, and in Class B 4.0-4.5.

6 References

- [1] Pedersen, T.F, Dahlberg, J-Å, “ACCUWIND – Methods for Classification of Cup Anemometers”, Risø-R-1555(EN), May 2006
- [2] Mann J “Wind field simulation”, Probabilistic Engineering Mechanics 13(4): 269-282, Oct 1998
- [3] IEC 61400-12-1, first edition 2005-12, Wind turbines – Part 12-1: “Power performance measurements of electricity producing wind turbines”
- [4] Dahlberg, J.-Å., Gustavsson, J., Ronsten, G., Pedersen, T.F., Paulsen, U.S., Westermann, D., “Development of a Standardised Cup Anemometer suited to Wind Energy Applications”, Contract JOR3-CT98-0263, Publishable Final Report; June 2001

Author: Troels Friis Pedersen (Risø), Jan-Åke Dahlberg (FOI), Peter Busche (DEWI)
Title: ACCUWIND - Classification of Five Cup Anemometers According to IEC61400-12-1
Department: Wind Energy Department

Abstract (max. 2000 char.):

The characteristics of five cup anemometers were investigated in detail, and data are presented in figures and tables. The characteristics include: normal wind tunnel calibrations; angular response measurements at 5, 8 and 11m/s; torque coefficient curve measurements from combined tilt and ramp-gust tests, torque coefficient curve measurements for non-tilted conditions; rotor inertia measurements and measurements of friction of bearings at temperatures -10°C to 40°C. The characteristics are fitted to two different time domain cup anemometer models, and simulations of the cup anemometers are made with artificial wind generators to make classifications according to annex I and J of the standard IEC 61400-12-1 on power performance measurements. Results of classification are shown in graphs of systematic deviations and class index tables.

Risø-R-1556(EN)
May 2006

ISSN 0106-2840
ISBN 87-550-3516-7

Contract no.:

Group's own reg. no.:

Sponsorship:

Cover :

Pages: 70
Tables: 8
References: 4

Risø National Laboratory
Information Service Department
P.O.Box 49
DK-4000 Roskilde
Denmark
Telephone +45 46774004
bibl@risoe.dk
Fax +45 46774013
www.risoe.dk

Risø's research is aimed at solving concrete problems in the society.

Research targets are set through continuous dialogue with business, the political system and researchers.

The effects of our research are sustainable energy supply and new technology for the health sector.